



Weakly supervised anomaly detection for resonant new physics in the dijet final state using proton–proton collisions at $\sqrt{s} = 13$ TeV with the ATLAS detector

The ATLAS Collaboration

An anomaly detection search for narrow-width resonances beyond the Standard Model that decay into a pair of jets is presented. The search is based on 139 fb^{-1} of proton–proton collisions at $\sqrt{s} = 13$ TeV recorded during 2015–2018 with the ATLAS detector at the Large Hadron Collider. The analysis is optimized without a particular signal model and aims to be sensitive to a broad range of new physics. It uses two different machine learning strategies to estimate the background in different signal regions. In each region, a weakly supervised classifier is trained to distinguish this background estimate from data. The analysis focuses on events with high transverse momentum jets reconstructed as large-radius jets. The mass and substructure of these jets are used as inputs to the classifiers. After a classifier-based selection, the distribution of the invariant mass of the two jets is used to search for potential local excesses. The model-independent results of both the anomaly detection methods show no signs of significant local excesses. In addition to model-independent results, a representative set of signal models is injected into the data, and the sensitivity of the methods to these scenarios is reported.

Contents

1	Introduction	2
2	ATLAS detector	4
3	Data and simulated event samples	5
4	Event reconstruction and selection	6
5	Analysis method	7
5.1	Definition of signal and background regions	8
5.2	Background estimate	9
5.3	Classification of a potential signal	10
5.4	Inference framework	11
5.5	Validation	13
6	Results	14
6.1	Signal enhancement	15
6.2	Exclusion limits	15
7	Conclusions	18
	Appendix	21
A	Analysis implementation	21
B	Test data samples	21
B.1	LARGE $ \Delta Y $ test data sample	21
B.2	MONTE CARLO test data sample	22
B.3	DOWN-UP-SAMPLING test data sample	22
C	Validation	23

1 Introduction

From the existence of dark matter to the matter-antimatter asymmetry, there are compelling motivations to search for particles beyond the Standard Model (BSM). However, there are too many possibilities to search for all models individually. Anomaly detection (AD) has emerged as an alternative approach to dedicated searches, capable of broad sensitivity to complement the deep sensitivity of targeted approaches. Machine learning has catalyzed the development of new methods, with the ability to holistically explore high-dimensional spaces [1–3]. Two broad classes of AD methods have emerged: *weakly supervised AD* which uses weakly supervised machine learning to distinguish a target data sample from a reference data sample [4]; and *unsupervised AD* which uses unsupervised machine learning to identify events that are rare [5]. This study explores the former, searching for a narrow resonance in dijet events from proton–proton (pp) collisions at $\sqrt{s} = 13$ TeV collected by the ATLAS detector at the Large Hadron Collider (LHC),

which lasted from 2015 to 2018. A weakly supervised approach, implemented in the Classification Without Labels (CWoLA) paradigm [6], was chosen as it provides sensitivity to anomalous overdensities in the data, even when individual events cannot be identified as anomalous. The analysis is model-agnostic and its primary goal is to highlight regions that might contain a potential BSM signal.

Resonant dijet events are a natural final state for new particle searches because many BSM scenarios feature massive particles that produce a pair of jets [7–9]. These events are also well-suited for weakly supervised AD because data samples with little to no signal contamination can be constructed and used to build the reference data sample. A previous ATLAS search in this final state [4] used weakly supervised AD built on the proposal of Refs. [10, 11] to use the off-resonance sideband of the dijet invariant mass, or simple sideband, as the reference data sample directly. Using the masses of the two jets to train the classifier, competitive limits were set on some signal models where a massive vector boson decays into two other vector bosons; these each decay into pairs of quarks, producing jets with two-prong substructure. The main drawback of this approach is that it requires the classifier features to be nearly independent of the dijet mass. This limits the number of features that can be used by the classifier and thus reduces the breadth of the search.

Several proposals address this challenge. One phenomenologically well-studied technique uses the dijet mass sideband information for the interpolation into the signal region when forming the reference data sample [12–23]. This technique goes beyond the previous search by correcting for differences between the background in the signal region and sideband region that vary smoothly with the dijet mass. The present analysis considers two such strategies: Simulation Assisted Likelihood-free Anomaly Detection (SALAD) [13] and Constructing Unobserved Regions by Transforming Adjacent Intervals Flows for Flows (CURTAINS) [21]. SALAD uses a dijet-mass conditional reweighting function trained in the dijet mass sidebands to correct simulation in the signal region. The reweighted simulation forms the reference data sample. CURTAINS uses a dijet-mass conditional morphing function trained in the dijet mass sidebands to correct the data in the sidebands to look like the data in the signal region. The transformed sideband data forms the reference data sample. Both the approaches correct for correlations between the dijet mass and the classifier features and thus can accommodate more features than were possible in the previous round of the analysis. Accordingly, the substructure features of the two jets in addition to the jet masses are used to train the classifier.

Other classical and AD searches have also probed hadronic final states. Inclusive dijet searches [24, 25] are broadly sensitive while dedicated searches for certain final states have significantly deeper sensitivity to certain types of models, including diboson resonances [26–29]. The CMS Collaboration has performed three-dimensional bump hunts in the dijet and single jet mass spectra, targeting diboson-like decays [30, 31], and a model-agnostic search for dijet resonances with anomalous jet substructure [32]. The ATLAS Collaboration has performed unsupervised AD searches for events with anomalous jets [33] and other resonant activity [34]. The unsupervised AD approaches are complementary to the weakly supervised approach [35].

The paper is organized as follows. Section 2 introduces the ATLAS detector, Section 3 describes the data and simulated event samples used for the search, and Section 4 describes the event reconstruction and selection. The analysis strategy is described in Section 5 and results are presented in Section 6. In addition to using new methods that enable more classifier features, this round of the search also expands on the interpretation of the result in two ways: more signal models are used to probe the sensitive region of BSM models and discovery reach in addition to exclusion is presented. The paper ends with conclusions and outlook in Section 7.

2 ATLAS detector

The ATLAS detector [36] at the LHC covers nearly the entire solid angle around the collision point.¹ It consists of an inner tracking detector surrounded by a thin superconducting solenoid, electromagnetic and hadronic calorimeters, and a muon spectrometer incorporating three large superconducting air-core toroidal magnets.

The inner-detector system (ID) is immersed in a 2 T axial magnetic field and provides charged-particle tracking in the range $|\eta| < 2.5$. The high-granularity silicon pixel detector covers the vertex region and typically provides four measurements per track, the first hit generally being in the insertable B-layer (IBL) installed before Run 2 [37, 38]. It is followed by the SemiConductor Tracker (SCT), which usually provides eight measurements per track. These silicon detectors are complemented by the transition radiation tracker (TRT), which enables radially extended track reconstruction up to $|\eta| = 2.0$. The TRT also provides electron identification information based on the fraction of hits (typically 30 in total) above a higher energy-deposit threshold corresponding to transition radiation.

The calorimeter system covers the pseudorapidity range $|\eta| < 4.9$. Within the region $|\eta| < 3.2$, electromagnetic calorimetry is provided by barrel and endcap high-granularity lead/liquid-argon (LAr) calorimeters, with an additional thin LAr presampler covering $|\eta| < 1.8$ to correct for energy loss in material upstream of the calorimeters. Hadronic calorimetry is provided by the steel/scintillator-tile calorimeter, segmented into three barrel structures within $|\eta| < 1.7$, and two copper/LAr hadronic endcap calorimeters. The solid angle coverage is completed with forward copper/LAr and tungsten/LAr calorimeter modules optimised for electromagnetic and hadronic energy measurements respectively.

The muon spectrometer (MS) comprises separate trigger and high-precision tracking chambers measuring the deflection of muons in a magnetic field generated by the superconducting air-core toroidal magnets. The field integral of the toroids ranges between 2.0 and 6.0 T m across most of the detector. Three layers of precision chambers, each consisting of layers of monitored drift tubes, cover the region $|\eta| < 2.7$, complemented by cathode-strip chambers in the forward region, where the background is highest. The muon trigger system covers the range $|\eta| < 2.4$ with resistive-plate chambers in the barrel, and thin-gap chambers in the endcap regions.

The luminosity is measured mainly by the LUCID-2 [39] detector that records Cherenkov light produced in the quartz windows of photomultipliers located close to the beampipe.

Events are selected by the first-level trigger system implemented in custom hardware, followed by selections made by algorithms implemented in software in the high-level trigger [40]. The first-level trigger accepts events from the 40 MHz bunch crossings at a rate close to 100 kHz, which the high-level trigger further reduces in order to record complete events to disk at about 1.25 kHz.

A software suite [41] is used in data simulation, in the reconstruction and analysis of real and simulated data, in detector operations, and in the trigger and data acquisition systems of the experiment.

¹ ATLAS uses a right-handed coordinate system with its origin at the nominal interaction point (IP) in the center of the detector and the z -axis along the beam pipe. The x -axis points from the IP to the center of the LHC ring, and the y -axis points upwards. Polar coordinates (r, ϕ) are used in the transverse plane, ϕ being the azimuthal angle around the z -axis. The pseudorapidity is defined in terms of the polar angle θ as $\eta = -\ln \tan(\theta/2)$ and is equal to the rapidity $y = \frac{1}{2} \ln \left(\frac{E+p_z}{E-p_z} \right)$ in the relativistic limit. Angular distance is measured in units of $\Delta R \equiv \sqrt{(\Delta y)^2 + (\Delta \phi)^2}$.

3 Data and simulated event samples

The analysis uses data from pp collisions at $\sqrt{s} = 13$ TeV recorded with the ATLAS detector at the LHC during 2015–2018. The total integrated luminosity of this data sample is 139 fb^{-1} [42] after data quality requirements [43]. Events are recorded using the unprescaled single large-radius jet triggers with the lowest p_T -threshold [40]. For the trigger selection to be fully efficient, events are required to have at least one jet with a transverse momentum of $p_T > 500$ GeV, and they are required to satisfy $m_{JJ} > 1.3$ TeV, with m_{JJ} according to the definition in Section 4.

Monte Carlo (MC) simulations [44] are used to: (1) generate a background estimate using SALAD, (2) validate the analysis procedure, and (3) set representative model-dependent limits. PYTHIA 8.2 [45] is used as the nominal MC generator for the event samples. Events are generated at leading order (LO) in QCD using the A14 tune [46] and NNPDF 2.3 LO [47] parton distribution function (PDF) set. The afterburner generator EvtGen [48] is used to model decays of heavy flavor hadrons. Detector effects are simulated using GEANT4 [49]. All simulated events are overlaid with additional minimum-bias events generated with PYTHIA 8.186 [50] using the A3 tune [51] and the NNPDF 2.3 LO [47] PDF set to simulate the effect of multiple pp collisions per bunch crossing (pileup). The distribution of the average number of pileup interactions in simulation is re-weighted during data analysis to match that observed in the Run 2 data.

Samples of MC simulated $2 \rightarrow 2$ dijet events are used to emulate the main Standard Model (SM) background. As the jet production cross-section is $O(100)$ times greater than electroweak processes, the consideration of these samples is sufficient to describe the data and all other processes are negligible. To fully populate a wide range of jet p_T , these samples are generated in slices of the particle-level $R = 0.6$ jet p_T [52].

Samples of MC simulated events are used to emulate twenty different signal models. The samples contain the processes $W' \rightarrow W''Z''$ and $A^0 \rightarrow H''Z''$, for new vector bosons W' [53] and pseudoscalar boson A^0 [54]. Following Ref. [4], the masses of the W' and A^0 are considered to be either 3 TeV or 4.5 TeV, labeled as low-mass and high-mass respectively.

The W'' , Z'' , and H'' particles are altered versions of the SM W , Z , and Higgs bosons. For the $W' \rightarrow W''Z''$ process, following Ref. [4], the masses of the W'' and Z'' bosons are varied to be one of the specific values: 80 GeV, 200 GeV, and 400 GeV. For the $A^0 \rightarrow H''Z''$ process, the mass of the H'' boson is set to 200 GeV and the mass of the Z'' boson is set to 400 GeV. The widths of all altered W'' , Z'' , and H'' particles are set to 0.1 GeV.

In one set of signal samples, as in Ref. [4], the W'' and Z'' bosons decay hadronically with $W''/Z'' \rightarrow q\bar{q}$ for non-top quarks q and \bar{q} , and same-flavor q/\bar{q} for the Z'' decays. An additional set of signals includes $H'' \rightarrow b\bar{b}$ or $H'' \rightarrow \gamma\gamma$ and $W''/Z'' \rightarrow qq$ decays.

The $W' \rightarrow W''Z''$ sample with $m_{W'} = 3$ TeV, $m_{W''} = 200$ GeV, and $m_{Z''} = 400$ GeV is simulated twice, with different m_{JJ} spectra arising from different parton shower settings. This is done to explore the effect of the m_{JJ} spectrum on signal sensitivity. As is shown in Section 6.2, the analysis is more sensitive to the narrower resonance.

Additionally, one set of signal models is simulated from the process $V' \rightarrow WV$, with V' a heavy vector boson from a Heavy Vector Triplet model [7] and $V = W, Z$. The mass of the parent particle ($m_{V'}$) is varied to be one of the specific values 2.6 TeV, 2.8 TeV, and 3.0 TeV, and the daughter particles decay hadronically.

The signal models are named $P_{p,a,b}^{s,d}$, where P is the name of the parent particle and the mass of the parent particle in GeV is denoted by p . If applicable, the masses of the daughter particles in GeV are denoted by the subscripts a, b . If applicable, whether the signal spectrum is narrow (n) or wide (w) is denoted by the superscript s . And, also if applicable, the decay channel is denoted by the superscript d . For example, $W_{3000,80,400}^m$ denotes a 3 TeV W' , which decays into a 80 GeV W'' and a 400 GeV Z'' , with a narrow m_{JJ} spectrum.

4 Event reconstruction and selection

Events are required to contain at least one reconstructed pp collision vertex candidate with at least two associated ID tracks with p_T larger than 0.5 GeV [55]. The primary vertex (PV) for each event is chosen as the reconstructed vertex with the highest sum of the p_T^2 of its associated tracks. Jets are reconstructed from locally calibrated calorimeter cell-clusters [56] using the anti- k_t algorithm [57, 58] with a radius parameter of $R = 1$. These large radius jets are trimmed [59] by reclustering the jet constituents with the k_t algorithm using $R = 0.2$ and removing the constituents with p_T less than 5% of the original jet p_T . The jet four-vectors are then calibrated as detailed in Ref. [60]. The analysis uses a subset of the available kinematic features of the events, which is described in the following. The dijet mass (m_{JJ}) is defined in this study as $m_{JJ}^2 = 2(|\vec{p}_1||\vec{p}_2| - \vec{p}_1 \cdot \vec{p}_2)$, where the momenta are those of the two jets with the highest p_T .² The feature M is defined as the mass of a single jet. The feature $\tau_{21} = \tau_2/\tau_1$ ($\tau_{32} = \tau_3/\tau_2$) is the ratio of the 2- and 1-subjettiness (3- and 2-subjettiness) [61] of each jet, with lower values indicating that the jets are more two- (three-) prong. The features τ_{21} and τ_{32} are selected from a larger set of jet substructure observables for their classification performance across the signal models described in Section 3. Including a specific jet feature in the analysis means incorporating its value for both the jets.

The requirements used to select events are summarized in Table 1. The leading jet p_T selection is based on the trigger, as described in Section 3. A requirement on the p_T of the subleading jet enhances events with a dijet topology. The jets are required to be relatively central without extreme values of jet mass so that their substructures are well reconstructed. The s -channel resonance signals which generate dijet events are targeted, as two jets is the primary decay channel for many new physics processes. Only events where the absolute difference between the rapidity y of the two jets, $|\Delta Y| = |y_1 - y_2|$, is less than 1.2 are considered, as this selection contains a higher proportion of s -channel events.

Table 1: Summary of the event selection used to define the data sample for the analysis based on reconstructed jet properties.

Observable	Selection
leading jet p_T [GeV]	> 500
subleading jet p_T [GeV]	> 200
jet $ \eta $ (both)	< 2.0
jet mass, M [GeV] (both)	$30 < M < 500$
$ \Delta Y = y_1 - y_2 $	< 1.2

² This differs from the typical definition, $m_{JJ}^2 = (p_1^\mu + p_2^\mu)^2$, by setting the individual jet masses to zero. The choice was made to reduce the correlation between m_{JJ} and the training features.

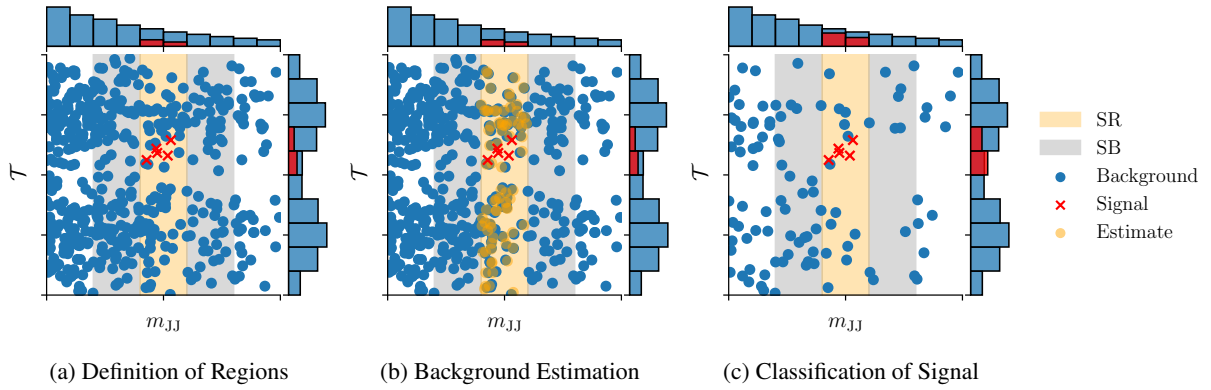


Figure 1: This figure shows a schematic drawing of the analysis strategy with the consecutive steps shown in the different panels. The distribution shows the data which consists of a background and a potential signal which is localized on the m_{JJ} spectrum and (potentially) different from the background in other features, here collectively labeled as \mathcal{T} . The first panel (a) shows how the SR and SB regions are defined on the m_{JJ} spectrum. The second panel (b) shows how the background is estimated in the SR. Then a classifier is trained between the estimated background and the data in the SR. The third panel (c) shows the data after a cut is applied on the classifier output of each event, thereby increasing the relative contribution of a potential signal. After this step, a bump hunt is performed in the m_{JJ} spectrum. The whole process is repeated with shifted regions SR and SB until the entire m_{JJ} spectrum is covered.

5 Analysis method

The analysis employs weakly supervised machine learning to search for resonant signals, which appear as localized peaks in the m_{JJ} spectrum. The primary background arises from non-resonant dijet production via the strong interaction. In addition to being resonant, a potential signal is expected to show distinct properties in other observables, like jet substructure, compared with the background, enabling effective differentiation.

The analysis strategy is structured into four steps, whereas the first three steps are explicitly depicted in Figure 1:

1. Potentially signal-enriched (Signal Region, SR) and signal-depleted regions (Sideband, SB) are defined.
2. Two different methods — SALAD and CURTAINS— use the signal-depleted regions to create estimates of the background process in the signal-enriched region.
3. A weakly supervised machine learning classifier is trained to classify the estimated background from data, and enhances the ratio of a potential signal to the background
4. A statistical inference is performed in the signal-enriched region.

Each step is briefly described in this overview, with more details in the following sections.

The analysis starts with the definition of the SR and SB. As potential signals are localized in the m_{JJ} spectrum, SR and SB are defined as collections of events with m_{JJ} values in ranges on this spectrum. Various mass hypotheses are systematically tested by iteratively shifting the SR and SB over a total of seven combinations of regions, which cover the investigated m_{JJ} spectrum. For each combination of regions the entire analysis chain is independently executed, including the background estimations, the training and

application of the weakly supervised classifier, and the statistical analysis, is employed separately. A more detailed explanation of these definitions and the shifting procedure is provided in Section 5.1.

Different subsets of the event features introduced in Section 4 are used as the outputs of the background estimation and the inputs of the classification. Three subsets \mathcal{T} are used: $\{M\}$, $\{M, \tau_{21}\}$, and $\{M, \tau_{21}, \tau_{32}\}$. Jet mass M is chosen because it is known to be sensitive in anomaly searches [4]; τ_{21} and τ_{32} are included to increase sensitivity to boosted 2- and 3-body decays of BSM particles, reconstructed as single large-radius jets. As the weakly supervised classifier (described below) uses these features to select events, a selection of features is akin to defining a signal region in a traditional analysis. Adding more features may broaden the sensitivity to some signals, but it also makes the model training harder, and thus can weaken the sensitivity to particular signals. The inclusion of uninformative features can generally also degrade the performance of a classifier as shown in Ref. [62]. New strategies for classifier training that scale well with the number of features are being actively developed, as seen in Refs. [63–66].

Because the SB is signal-depleted, it can be used to estimate the background-only distribution in the SR. Two methods use neural networks to explicitly model the high-dimensional background distribution in the SR. The features in \mathcal{T} vary smoothly with m_{JJ} , and the validation methods show that the background distribution in the SR can be estimated from the SB. This explicit modeling is an improvement to the previous weakly supervised analysis in ATLAS [4], as it largely prevents an m_{JJ} dependent bias of the classification of a potential signal. Both the methods are described in greater detail in Section 5.2.

Next, a weakly supervised classification algorithm is trained to distinguish between the data distribution and the estimated background distribution in the SR. Following the CWoLA paradigm [6], this algorithm, implemented as a neural network, approximates an optimal classifier between a potential signal and the background. A cut on the classifier output is then applied to enhance the fraction of signal events in the SR. An ensemble of multiple classifiers ensures more stable results, enables an estimate of the classifier uncertainty, and mitigates the risk of false positives in the absence of a signal. The classification is described in greater detail in Section 5.3.

In the final step of the analysis chain, a parametric function is fitted to the m_{JJ} spectrum in the SB and interpolated into the SR. The inference framework then compares this interpolated prediction with the observed number of data events in the SR. Observed significances of the analyzed data compared with the background estimate are calculated using a profile likelihood fit. Upper limits on the expected number of signal events for various signal models are established at a 95% confidence level (CL) using the CL_s method [67]. The inference strategy is described in greater detail in Section 5.4.

In data-driven weakly supervised AD analyses like this one, the validation of analysis performance is especially critical as the presence of an unknown potential signal changes the method (i.e., the classifier) itself. The validation strategy is explained in greater detail in Section 5.5.

5.1 Definition of signal and background regions

The potential signals are resonant and therefore localized in the m_{JJ} spectrum. Events are considered parts of the SR if their m_{JJ} values fall inside a ± 300 GeV window around the targeted signal mass. The SB consists of events with m_{JJ} values up to 600 GeV below or above the SR edges. Multiple hypotheses are tested by sliding the set of SR and SB over the m_{JJ} spectrum. The analysis investigates the m_{JJ} spectrum between 2.6 TeV and 5.0 TeV in steps of 300 GeV. The SR width was chosen to encompass the experimental

width of narrow resonances at 3 TeV,³ and was tested to ensure that sensitivity is retained at the highest masses considered. The choice of 300 GeV steps ensures that all SR overlap and guarantees a seamless testing of the entire m_{JJ} range.

The tested SRs with values of m_{JJ} in units of TeV are:

$$[2.6, 3.2] \text{ or } [2.9, 3.5] \text{ or } [3.2, 3.8] \text{ or } [3.5, 4.1] \text{ or } [3.8, 4.4] \text{ or } [4.1, 4.7] \text{ or } [4.4, 5.0]. \quad (1)$$

The number of events decreases with increasing m_{JJ} and the highest SR was chosen such that there are more than ten events in data for each bin in the high m_{JJ} SB of this SR at the tightest tested classifier selection explained below. Only the regions which satisfy the validation discussed in Section 5.5 are considered for the final results of the analysis.

5.2 Background estimate

Two different methods are used to generate background templates for training the signal-identification classifier: SALAD and CURTAINS. The techniques are independent and complementary — SALAD uses a simulated prior, whereas CURTAINS is entirely data-driven. As a result, the level of agreement between the SALAD and CURTAINS branches of the analysis provides a consistency check on the results.

In the discussion below, suppose that a data sample is provided with features $\mathcal{T} \cup \{m_{JJ}\}$, where \mathcal{T} is some set of features. The goal is to use the SB to generate an m_{JJ} -parameterised background template which approximates the features \mathcal{T} well in the SR. Then the features \mathcal{T} can be used for training the signal-identification classifier. The specific architectures of all methods are detailed in Appendix A. For the lowest (highest) SR case, a total of 659 059 (6381) SB events are used to train the SALAD and CURTAINS models, and 115 300 (1559) events are in the SR.

The SALAD [13] method generates a background estimate based on a high-fidelity simulation using the following steps:

1. Assign every event in the simulated SB a label of 0, and assign every event in the data SB a label of 1.
2. Train a neural network A to classify simulation and data in the SB using $\mathcal{T} \cup \{m_{JJ}\}$ as training features. The classifier A is parameterized in m_{JJ} [68, 69] to enable an interpolation into the SR.
3. For each simulated event i in the SR, let $A(i)$ be the output of classifier A when it sees the event. Assign event i a weight

$$w_i = \frac{A(i)}{1 - A(i)},$$

which approximated the probability density ratio of data to simulation. The final SALAD background estimation in the SR is the SR simulation with the weight w_i applied to every event.

The CURTAINS method uses the SB data to fit a model and generates a background estimate using the following steps:

1. Train a normalizing flow p_θ with the network parameters θ [70] to estimate the conditional density of the features in the SBs $p(\mathcal{T} | m_{JJ} \in \{\text{SB}\})$.

³ For example, for the signal model $W' \rightarrow W''Z''$ with $m_{W''} = m_{Z''} = 200$ GeV, the standard deviation of m_{JJ} is 400 GeV.

2. Train another normalizing flow to map from $p_\theta(\mathcal{T}|m_{\text{JJ}} = m_1)$ to $p_\theta(\mathcal{T}|m_{\text{JJ}} = m_2)$ for all m_1, m_2 pairs in the joint SBs.
3. Fit the mass distribution in the SBs using the same baseline function used in the previous search [4], $p_1(1-z)^{p_2}z^{p_3}$, where z is the mass divided by the center of mass energy and p_i are free parameters. Interpolate into the SR and sample [71].
4. Use the normalizing flow from Step 2 to map each SB sample to a mass value in the SR sampled using the fit from Step 3.

Long-tailed features in \mathcal{T} are transformed using $f(x) = \log\left(\frac{p}{1-p}\right)$, also known as a logit transform, before being fed into the normalizing flow, as this is shown to improve the modeling performance [16]. The last step can be repeated multiple (m) times, and if there are n events in the combined SBs then CURTAINS will generate $m \times n$ events in the SR. This contrasts with SALAD, which will only generate as many events as there are simulated events in the SR. The oversampling is shown to increase signal sensitivity [16, 19, 21]. Given the seven SRs and three feature sets, a total of 21 CURTAINS models and 21 SALAD models are trained.

5.3 Classification of a potential signal

One fundamental challenge in any weakly supervised application is that both the training and evaluation data are imprecisely labeled. Using the CWoLA paradigm [6] allows training of a classifier even without precise labels. All that is needed to train a binary classifier is two data samples with different frequencies of the two respective classes. As the two example data samples only differ in their signal-to-background composition, the classifier will learn to identify this one difference by separating signal events from background events. Further, a classifier trained this way will converge to an optimal signal vs. background classifier, so long as the initial assumptions about the data samples only differing in composition are correct.

5.3.1 Classifier implementation

In the previous ATLAS weakly supervised search [4], the CWoLA approach was used to search for anomalous signals by discriminating between (1) an SR with a high suspected signal contamination and (2) the SBs with low expected contamination. One major challenge in this approach was the need to ensure decorrelation between the observable used to separate SR and SB and the observables used to train the classifier; otherwise, the classifier could learn the defining distinction between SR and SB and introduce artificial bumps which could form a false excess as a result, a process also known as background sculpting [17].

This analysis improves on the pure CWoLA search by instead training the classifier between (1) the data in a candidate SR and (2) a background template in that region, provided by the approaches described in Section 5.2. Using a direct modeling of the background in that region reduces the need for decorrelation compared with previous approaches. The template is assumed to be signal-depleted, while the data are signal-enriched. Following this assumption, a classifier, which is trained to distinguish the data and the template, will therefore give a higher classifier score to signal-like events. The classifier architecture is defined in Appendix A.

A five-fold cross-validation strategy is applied; this ensures that classifiers are not evaluated on the same data they are trained on. In this setting the CWoLA model is trained to discriminate between a subset of the SR data and a generated template, then evaluated on the unseen portion of the SR data. Two working points are defined for the selection efficiency of the CWoLA classifier — one where the top 10% of events with the highest classifier score are retained $\epsilon = 0.1$, and a tighter selection where the top 2% of events with the highest classifier score are retained $\epsilon = 0.02$. The classifier working points are chosen to enable sensitivity to a wide range of signals while ensuring enough SB events in the high- m_{JJ} region for a viable fit (described in Section 5.4.1). Some signals are more sensitive to tighter cuts, some to looser. For a given signal, the optimal cut is a function of the cross-section and characteristics of the signal, and is not predictable *a priori*.

5.3.2 Ensemble methods

An ensembling method is used to minimize the dependence on the (randomized) classifier-weight initialization. Many classifiers are trained for every SR, whereas each classifier is initialized with a different random seed. Without any signal, the classifiers tend to randomly pick regions of phase-space while with a signal, most of classifiers tend to agree on one region of phase-space [23].

A strategy is developed to combine the classifiers, developed in an idealized setting, where the CWoLA classifier is trained to discriminate between two data samples drawn from the same distribution. This setting is chosen as it removes issues related to template mis-modeling. Using an ensemble of N classifiers, the best strategy is found to be: first make a selection on the classifier output of each of the N classifiers, then fill N histograms in the m_{JJ} distribution, one for each selection, and then average these N histograms using the median. The size of the ensemble in this search is set to $N = 10$.

The averaged histogram is the input to the fit and subsequent statistical analysis. The average bin count is Poisson distributed with an additional uncertainty given by the standard error on the estimate of the median. This strategy can be viewed as a marginalization over randomly placed decision boundaries that removes the bias from the classifier initialization. Ensembling directly based on the output of the classifier was shown to either decrease the sensitivity of the analysis or increase the rate of false positives.

5.4 Inference framework

In the final step of the analysis strategy, a parametric function is fit to the m_{JJ} spectrum in the SB and interpolated to the SR. This interpolation and the recorded data in the SR are used to estimate the statistical significance of potential deviations and to set limits on benchmark models. This section first outlines the fitting strategy and the interpolation, then, it introduces the relevant uncertainties, explains the statistical analysis, and introduces the post-hoc non-closure correction of the significance.

5.4.1 Fitting strategy

The production of dijets in the SM is dominated by QCD processes, and is well-described by a smoothly falling distribution in m_{JJ} . For a given SR, after making a classifier selection as described in Section 5.3 and defining a histogram in bins of m_{JJ} , a fit is made to the SB bins. Thirty bins with a width of 60 GeV evenly span both the SBs and the SR. For the fit, the SR is masked. The bins in the SB are then fit with

an iterative strategy until the p -value from the χ^2 fit is greater than 5%. The same fit strategy is used as in the previous ATLAS weakly supervised search [4]. Upon each iteration, the fit function increases in complexity as follows: (1) a three parameter fit $dn/dx = p_1(1-x)^{p_2}x^{-p_3}$, (2) a four parameter fit $dn/dx = p_1(1-x)^{p_2}x^{-p_3+p_4 \log(x)}$ [72], (3) the UA2 fit function $dn/dx = p_1x^{p_2}e^{-p_3x+p_4x^2}$ [73], where $x = m_{JJ}/\sqrt{s}$ and $\{p_i\}_{i=1}^4$ are the fit parameters. If the fit χ^2 criterion is still not met after cycling through all possible fit functions, then the SB window is reduced by removing the SB-bin furthest from the SR, for each SB. This is repeated until the fit χ^2 criterion is met, or until the SB contains fewer than six bins, in which case the fit is considered to have failed. This kind of fit failure did not occur in practice.

5.4.2 Uncertainties

Both the observed data and the background estimate, which are used in the statistical analysis, contribute a set of uncertainties.

The observed data contributes two different uncertainties: the Poisson statistical uncertainty in the bin count and the uncertainty from the classifier ensemble described in Section 5.3.2. The Poisson statistical uncertainty in the bin count is inferred as \sqrt{n} with the bin count n being the average over the classifier ensemble. The uncertainty from the classifier ensemble is driven by the randomness that results from the different classifier initializations. It is determined for each bin by the spread of the bin counts from the classifiers in the ensemble and includes the correlation between the classifiers.

The uncertainty in the background estimate comes from the fit to the m_{JJ} spectrum. After the fit is performed, the fit uncertainty in the bins in the SR is determined by propagating the uncertainty in the fit parameters to the individual bins. The uncertainty in the fit parameters is driven by the Poisson statistical uncertainty in the bin counts in the SB and the uncertainty from the classifier ensemble in the SB. The uncertainty from the fit and the uncertainty from the classifier ensemble on the data are combined in quadrature in each bin and profiled together in the statistical analysis.

As highlighted above, the primary goal of this weakly supervised search is to look for hints of new physics, not to set limits on particular new physics models. Additionally, the search probes a region of phase-space in which the signal contribution is mostly statistically limited. Therefore, systematic uncertainties in the injected signals are not considered.

The largest uncertainty in all hypothesis tests is the uncertainty in the background estimate from the fit to the m_{JJ} spectrum. The next largest contribution is the Poisson statistical uncertainty in the data which is slightly larger than the uncertainty from the ensembling of the m_{JJ} histograms of the data.

5.4.3 Likelihood fit

To extract a significance on the observed SR counts, a profile likelihood fit is used [11, 74]. The bins of the m_{JJ} histograms that lie in the SR are combined into a single bin. All sources of uncertainties in the likelihood fit are described in Section 5.4.2. The uncertainty from the fit function and ensemble procedure are included as Gaussian distributed constrained uncertainties. All likelihood fits are performed using pyhf [75, 76].

5.4.4 Non-closure correction

Two systematic effects can cause a non-closure of the analysis methodology. The first effect comes from the uncertainty in the function used to fit the m_{JJ} spectrum. The second effect comes from possible deficiencies in the template generation from SALAD or CURTAINS. Such deficiencies could, for example, introduce a systematic bias which could be identified by the classifier. This bias could cause a false excess, which could be caught by the validation described in Section 5.5, but it is more likely to reduce the sensitivity of the search.

In each SR, the possible non-closure is corrected with a post-hoc non-closure correction on the extracted significance, effectively adding a post-evaluation uncertainty. The correction uses the DOWN-UP-SAMPLING test data samples described in Appendix B. The statistical properties of the p -value distribution are assessed on these test data samples and derive a calibration procedure to correct for any biases of the analysis. A linear fit to the mean and standard deviation of the significance across the ten different DOWN-UP-SAMPLING test data samples as a function of m_{JJ} is used to derive a correction to the final significance. The fitted significance is subtracted from the significance as evaluated on the data in the SR. The correction is only used to decrease the significance with the addition that it cannot (further) decrease the significance below zero. The corrections are small everywhere, with no correction to the standard deviation. The largest shift in the mean is of 0.5σ .

5.4.5 Limit setting

Upper limits on the production of various signal models are set at 95% confidence level (CL) using the CL_S method [67]. For each signal model, limits are set by injecting a fixed number of signal events into the data and then running the full analysis, using the injected signal events to calculate the expected number of signal events after a selection is performed. Multiple different signal injections are performed to build curves for the observed, expected, and $\pm 1\sigma$ and $\pm 2\sigma$ bands. The intersection of each of these curves with the horizontal line at 95% CL is used to set the limit.

5.5 Validation

Validating a data-driven, weakly supervised anomaly detection search is inherently challenging because the presence, magnitude, and characteristics of potential signals are unknown; however, the method's performance depends on the input data, which may include these potential signals. The analysis uses three complementary and orthogonal test data samples for validation, referred to as LARGE $|\Delta Y|$, MONTE CARLO, and DOWN-UP-SAMPLING respectively. All three test data samples are described in greater detail in Appendix B. Each of the test data samples is designed to test a different aspect of the analysis and the use of all three provides confidence in the robustness of the analysis.

Each m_{JJ} SR is validated individually using all three test data samples as explained in the following. For each m_{JJ} SR, the significance of the respective data above the background estimate is evaluated with each of the test data samples. An m_{JJ} SR is considered to satisfy the validation for a test data sample if the median significance is less than one and the spread in the significances is less than one on this given test data sample. An m_{JJ} SR has to satisfy the validation for each of the test data samples to satisfy the overall validation and to be considered for further analysis.

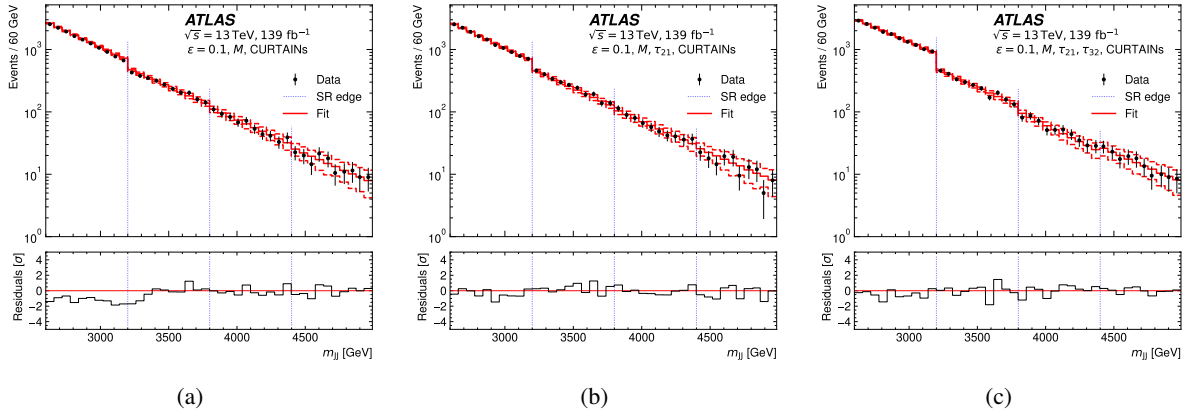


Figure 2: Histograms of m_{JJ} in the first set of non-overlapping m_{JJ} SRs for the CURTAINS method on all feature sets at the $\epsilon = 0.1$ classifier selection using the $|\Delta Y| < 1.2$ data. The figures show the resulting distributions when the analysis is evaluated on the first, third, fifth, and seventh m_{JJ} SRs. Shown are different feature sets: (a) is the result of $\mathcal{T} = M$, (b) is the result of $\mathcal{T} = M, \tau_{21}$ and (c) is the result of $\mathcal{T} = M, \tau_{21}, \tau_{32}$. The fit is derived from the background-only fit interpolated from the SBs. The uncertainties in the observed counts include the Poisson statistical uncertainty of the bin counts. The uncertainties in the fit are represented by the dashed histograms and include the uncertainties in the fit parameters and the uncertainty from the classifier ensemble on the data. The vertical dashed lines mark the edges of each SR in m_{JJ} . The lower panel in each plot shows the Gaussian-equivalent significance of the deviation between the fit and data.

Seven of the original eight m_{JJ} SRs satisfy the validation and are considered for further analysis. The lowest m_{JJ} SR does not satisfy the validation and is excluded from the final results. This validation failure can be attributed to the correlations between m_{JJ} and the masses of the two jets, which are shown to differ between the low and high m_{JJ} regions. These correlations make the background estimates more challenging in the low m_{JJ} region. More details of the validation procedure and the individual results of the validation procedure are shown in Appendix C.

6 Results

This section presents the main results of the analysis. Figure 2 shows the distribution of events over m_{JJ} for different non-overlapping m_{JJ} SRs after the fit when using the CURTAINS method. Between neighboring SRs, sharp discontinuities are observed in the m_{JJ} spectrum. These can appear because the classifier selection is performed in each SR independently. Therefore, there is no guarantee that adjacent SRs will smoothly match each other. A similar feature was observed in the previous ATLAS weakly supervised search [4].

Figure 3 and Figure 4 show the significances of the observed data in the SRs for the SALAD and CURTAINS methods, respectively. The significances are extracted from the likelihood fit described in Section 5.4.3. The largest observed excess for the SALAD (CURTAINS) method has a local significance of 1.24σ (1.26σ). There is a deficit in the first m_{JJ} SR with a local significance of -2.98σ (-2.54σ) when using the SALAD (CURTAINS) method and an efficiency of the CWoLA classifier of $\epsilon = 0.1$. This deficit was not observed on the test data sample as shown in Appendix C. For all other selections and m_{JJ} SRs both the SALAD and CURTAINS behave similarly to the results on the test data samples.

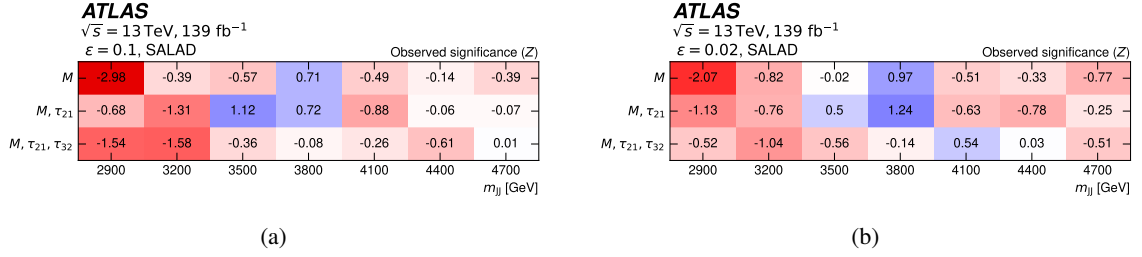


Figure 3: Observed significances (Z) for SALAD at the two different selections, (a) $\epsilon = 0.1$ and (b) $\epsilon = 0.02$. The significances are shown for all feature sets and m_{JJ} SRs.

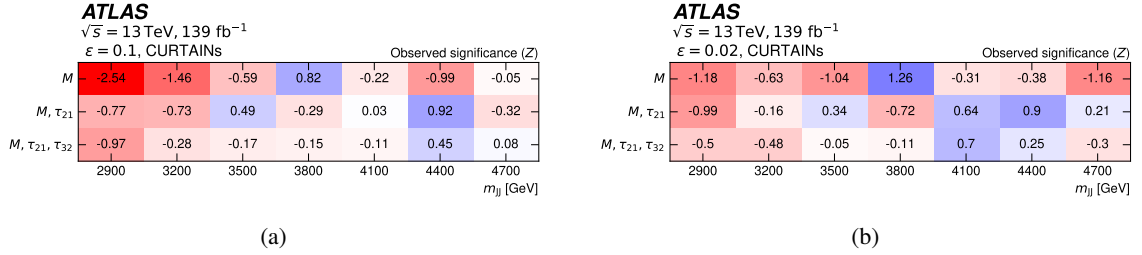


Figure 4: Observed significances (Z) for CURTAINS at the two different selections, (a) $\epsilon = 0.1$ and (b) $\epsilon = 0.02$. The significances are shown for all feature sets and m_{JJ} SRs.

6.1 Signal enhancement

This section shows the ability of the analysis to enhance the potential signals, described in Section 3, when they are injected into the SR. For this test, into each of the regions 2.2 – 3.2 TeV and 4.1 – 4.7 TeV, a count of $S = 3\sqrt{B}$ simulated signal events were injected, with B the number of background events in each region. Thus, the expected significance given perfect knowledge of the data distribution over m_{JJ} in the SR with no systematic uncertainty, would be 3σ . As the analysis incorporates information from more features than just m_{JJ} , this significance can be enhanced for some signals.

In Figure 5, the lower end of the m_{JJ} spectrum SALAD is better able to enhance signals than CURTAINS, whereas the opposite is true at the higher end of the m_{JJ} spectrum. The two methods are therefore complementary. The tighter selection is also observed to better enhance signal across both the methods. Both the methods can be seen to return an observed significance $Z > 3$ for the 3σ signal injection for most of the injected signals. This reflects the significance enhancement ability of both the SALAD and CURTAINS. The analysis may not be sensitive to all possible signal models, and this is what is observed. The M, τ_{21} feature set is seen to have the broadest sensitivity to new physics.

6.2 Exclusion limits

This section shows the ability of the analysis to exclude the potential signals, described in Section 3, using the full CL_S prescription. Tight limits can be placed on a wide range of signal models, which indicates the method's broad sensitivity.

Figure 6 compares the limits set by the analysis to previous dijet [72] and diboson [28] searches. These classical limits are taken from Ref. [4] and were originally obtained by recasting the analysis with the

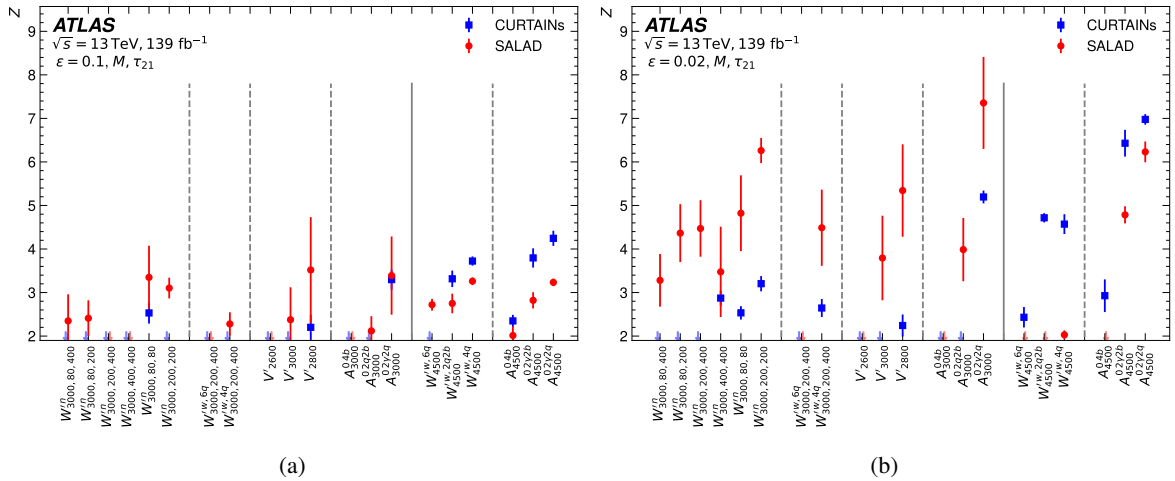


Figure 5: Signal injection tests with $\mathcal{T} = M, \tau_{21}$ at $\epsilon = 0.1$ in (a) and $\epsilon = 0.02$ in (b) for both the SALAD and CURTAINS for all simulated signal models. The signal models are described in detail in Section 3. The local observed significance (Z) is shown as reported by the analysis pipeline after running the analysis with 3σ of signal injected into the data in the m_{JJ} SR centered on the different signals. The errors show one standard deviation on the reported significance as calculated by bootstrapping the signal injection procedure.

new signal cases. The new analysis sets stricter limits than the existing dijet search on signal models with daughter masses high enough such that $\frac{2m}{p_T} > 0.4$ (signal models: $W_{3000,400,400}^m$, $W_{3000,200,400}^m$, $W_{3000,80,400}^m$) and slightly weaker limits on signal cases with daughter masses such that $\frac{2m}{p_T} < 0.4$ (signal models: $W_{3000,200,200}^m$, $W_{3000,80,200}^m$, $W_{3000,80,80}^m$). This is because the dijet search uses $R = 0.4$ jets, and therefore performs worse for cases where $\frac{2m}{p_T} > 0.4$ and the resulting jets are too large to be contained inside the $R = 0.4$ jet radius. The diboson search succeeds for signals with daughter masses close to the SM W mass $W_{3000,80,80}^m$ but fails for other masses.

In Figure 6 both the SALAD and CURTAINS set similar limits on the signal cross-section at both the ends of the m_{JJ} spectrum. The same is true for all selections, feature sets and signals. In Figure 7 the M, τ_{21} feature set is able to set the strictest limits on the signal cross-section across almost all signals and SRs. This is true for both the SALAD and CURTAINS methods. At the $\epsilon = 0.1$ selection in the 2.6 – 3.2 TeV SR, the M, τ_{21} feature set results in the strictest limits on the signal cross-section across almost all signals due to the deficit observed in Figure 2, which only appears in this region for this feature set. Otherwise, the M, τ_{21} feature set most often sets the strictest limits in all regions and selections for both the methods.

It is interesting that the M, τ_{21}, τ_{32} feature set is not significantly better than the other two feature sets for topologies, like the BSM $W''/Z'' \rightarrow qq\bar{q}$ decays, that are expected to have a boosted 3-prong structure. This may indicate that τ_{32} does not add enough information for these topologies to be useful for classification, and would be an interesting area for future study.

The analysis uses the full CL_S method to set limits, and so direct comparisons cannot be made to the limits set by the previous weakly supervised dijet search which used a different approach [4]. However, the previous weakly supervised search used the M feature set and so this should have similar sensitivity to the previous search. Given that the M, τ_{21} feature set generally improves the sensitivity of the analysis, it represents an improvement on the previous weakly supervised search. In a weakly supervised anomaly detection search, it is generally not known beforehand which features are most sensitive to a potential signal.

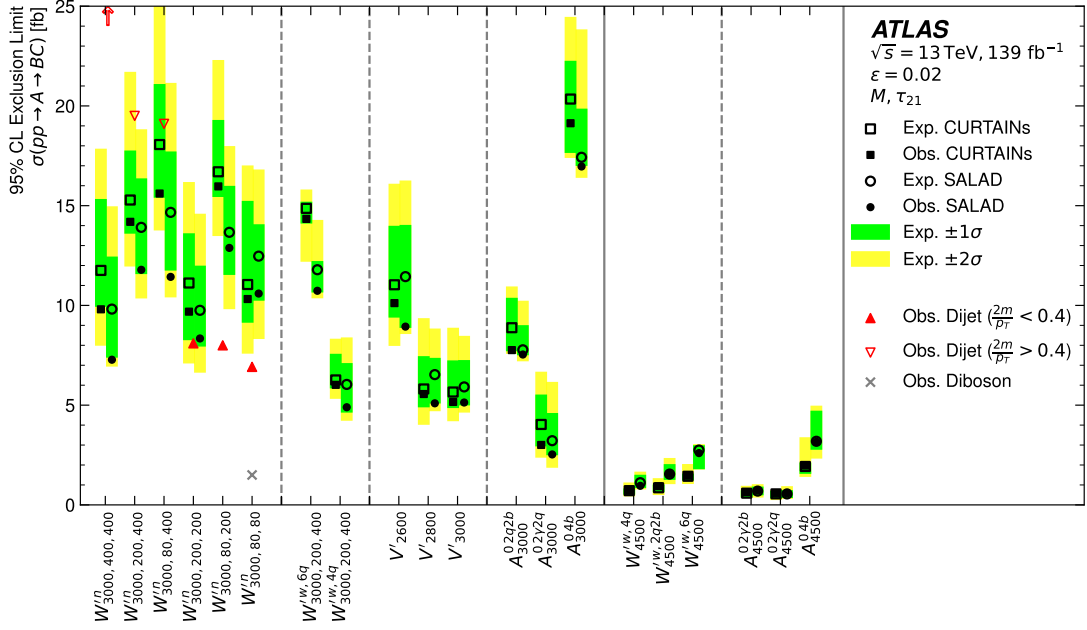


Figure 6: Comparison of the 95% CL upper limits on $\sigma(pp \rightarrow A \rightarrow BC)$ set by SALAD and CURTAINS at $\epsilon = 0.02$ with $\mathcal{T} = M, \tau_{21}$. The one and two sigma variations on the expected limits for both the SALAD and CURTAINS methods are shown as the shaded regions. The signal models are detailed in Section 3. The observed limits from the ATLAS dijet search [72] and the ATLAS all-hadronic diboson search [28] are shown in the red triangles and grey X-symbols respectively, and were derived in the previous weakly supervised ATLAS search [4]. Limits for the inclusive dijet search are calculated using the W' signals from this paper and the analysis of Ref. [72]; the diboson search limits are computed using the Heavy Vector Triplet [7] W' signal from Ref. [28]. The acceptance for the W' in this paper, compared with the W' acceptance in Ref. [28], is 86%. The limit from the inclusive dijet search which exceeds the shown range is marked with a red arrow.

Additionally, as mentioned in Section 5, including uninformative features can degrade the performance of the classifier. The scan over many different feature sets is therefore one of the strengths of the analysis.

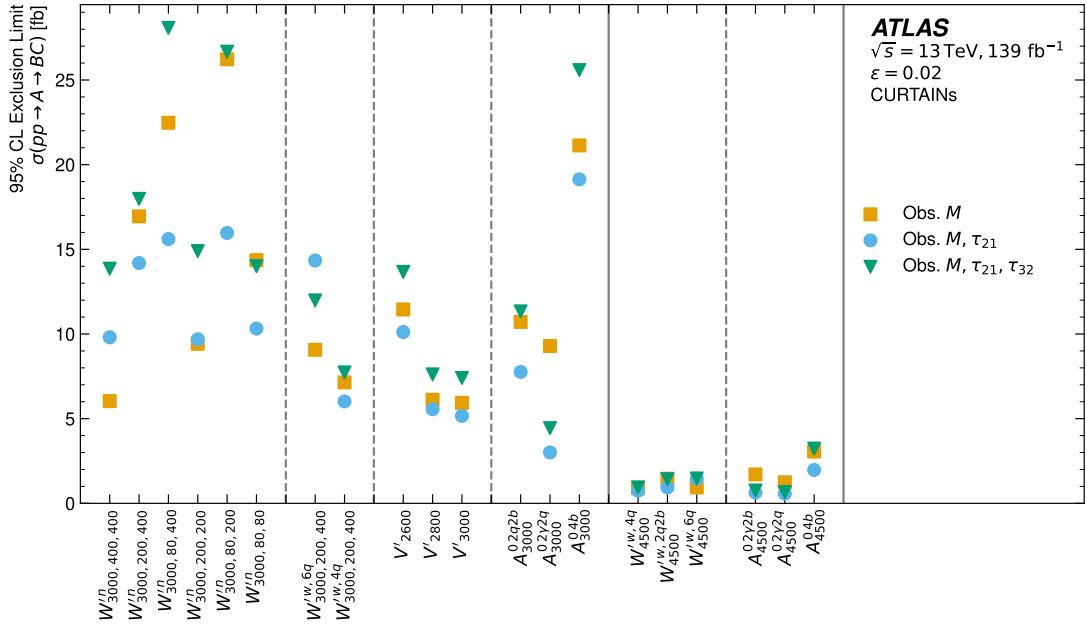


Figure 7: Comparison of the 95% CL upper limits on $\sigma(pp \rightarrow A \rightarrow BC)$ for different feature sets. All limits use the CURTAINS method with the $\epsilon = 0.02$ selection. The signal models are detailed in Section 3.

7 Conclusions

A signal agnostic anomaly detection search is described for narrow-width resonances beyond the SM that produce a pair of jets. The search uses 139 fb^{-1} of pp collisions at $\sqrt{s} = 13 \text{ TeV}$ recorded during 2015—2018 with the ATLAS detector at the LHC. The analysis is designed to be sensitive to a broad range of new physics effects and targets resonances on the m_{JJ} spectrum between 2.6 TeV to 5.0 TeV. After a selection through a weakly supervised classifier, a bump hunt is performed to extract potential local excesses. Two different strategies based on machine learning are used to create background estimates which are utilized in the classifier training.

The search extends the previous weakly supervised search performed by the ATLAS experiment in various ways. The direct background estimate, performed using either the SALAD reweighting technique or the CURTAINS morphing method, allows more features of the events to be used in the search than before. Specifically, this search uses jet substructure features, which are related to the number of prongs in the jets, thereby particularly enhancing the sensitivity to boosted massive particles. Additional benchmark signal models are integrated to probe the sensitivity of the search. New validation methods are developed to address the challenge of developing a blind weakly supervised AD search.

No significant excess is observed in the data, consistent with the validation on the test data samples. To illustrate the sensitivity of the analysis, upper limits at 95% CL are set on the production cross-section for a set of signal benchmark models. These limits are compared between the two background estimation methods and two existing searches. The search is sensitive to many potential signal models which promote resonant dijet final states, such as BSM models including vector bosons W' or pseudoscalar bosons A^0 . Unlike most searches, when a signal is injected into the data, the event selection changes, and so the entire process must be rerun every time a new signal is injected at a new cross-section. The two background

estimation methods, SALAD and CURTAINS, provide comparable yet somewhat complementary sensitivity across the range of signal models considered.

There are various ways that the analysis could be improved in the future. Higher-dimensional feature spaces may broaden the sensitivity. This may require new strategies for training the classifiers that scale well with the number of features. Additional approaches to generate the background estimate, including the combination of approaches, may also improve the sensitivity. A detailed study of differences between data and simulation may also lead to new insight to address challenges that arise in data that are absent from previous phenomenological studies. While the analysis is a significant extension of the previous search, hadronic final states at the LHC present a vast phase-space that may yet reveal signs of new physics with new AD searches in the future.

Acknowledgements

We thank CERN for the very successful operation of the LHC and its injectors, as well as the support staff at CERN and at our institutions worldwide without whom ATLAS could not be operated efficiently.

The crucial computing support from all WLCG partners is acknowledged gratefully, in particular from CERN, the ATLAS Tier-1 facilities at TRIUMF/SFU (Canada), NDGF (Denmark, Norway, Sweden), CC-IN2P3 (France), KIT/GridKA (Germany), INFN-CNAF (Italy), NL-T1 (Netherlands), PIC (Spain), RAL (UK) and BNL (USA), the Tier-2 facilities worldwide and large non-WLCG resource providers. Major contributors of computing resources are listed in Ref. [77].

We gratefully acknowledge the support of ANPCyT, Argentina; YerPhI, Armenia; ARC, Australia; BMWFW and FWF, Austria; ANAS, Azerbaijan; CNPq and FAPESP, Brazil; NSERC, NRC and CFI, Canada; CERN; ANID, Chile; CAS, MOST and NSFC, China; Minciencias, Colombia; MEYS CR, Czech Republic; DNRF and DNSRC, Denmark; IN2P3-CNRS and CEA-DRF/IRFU, France; SRNSFG, Georgia; BMBF, HGF and MPG, Germany; GSRI, Greece; RGC and Hong Kong SAR, China; ICHEP and Academy of Sciences and Humanities, Israel; INFN, Italy; MEXT and JSPS, Japan; CNRST, Morocco; NWO, Netherlands; RCN, Norway; MNiSW, Poland; FCT, Portugal; MNE/IFA, Romania; MSTDI, Serbia; MSSR, Slovakia; ARIS and MVZI, Slovenia; DSI/NRF, South Africa; MICIU/AEI, Spain; SRC and Wallenberg Foundation, Sweden; SERI, SNSF and Cantons of Bern and Geneva, Switzerland; NSTC, Taipei; TENMAK, Türkiye; STFC/UKRI, United Kingdom; DOE and NSF, United States of America.

Individual groups and members have received support from BCKDF, CANARIE, CRC and DRAC, Canada; CERN-CZ, FORTE and PRIMUS, Czech Republic; COST, ERC, ERDF, Horizon 2020, ICSC-NextGenerationEU and Marie Skłodowska-Curie Actions, European Union; Investissements d’Avenir Labex, Investissements d’Avenir Idex and ANR, France; DFG and AvH Foundation, Germany; Herakleitos, Thales and Aristeia programmes co-financed by EU-ESF and the Greek NSRF, Greece; BSF-NSF and MINERVA, Israel; NCN and NAWA, Poland; La Caixa Banking Foundation, CERCA Programme Generalitat de Catalunya and PROMETEO and GenT Programmes Generalitat Valenciana, Spain; Göran Gustafssons Stiftelse, Sweden; The Royal Society and Leverhulme Trust, United Kingdom.

In addition, individual members wish to acknowledge support from Armenia: Yerevan Physics Institute (FAPERJ); CERN: European Organization for Nuclear Research (CERN DOCT); Chile: Agencia Nacional de Investigación y Desarrollo (FONDECYT 1230812, FONDECYT 1230987, FONDECYT 1240864); China: Chinese Ministry of Science and Technology (MOST-2023YFA1605700, MOST-2023YFA1609300), National Natural Science Foundation of China (NSFC - 12175119, NSFC 12275265,

NSFC-12075060); Czech Republic: Czech Science Foundation (GACR - 24-11373S), Ministry of Education Youth and Sports (FORTE CZ.02.01.01/00/22_008/0004632), PRIMUS Research Programme (PRIMUS/21/SCI/017); EU: H2020 European Research Council (ERC - 101002463); European Union: European Research Council (ERC - 948254, ERC 101089007, ERC, BARD, 101116429), European Union, Future Artificial Intelligence Research (FAIR-NextGenerationEU PE00000013), Italian Center for High Performance Computing, Big Data and Quantum Computing (ICSC, NextGenerationEU); France: Agence Nationale de la Recherche (ANR-20-CE31-0013, ANR-21-CE31-0013, ANR-21-CE31-0022, ANR-22-EDIR-0002); Germany: Baden-Württemberg Stiftung (BW Stiftung-Postdoc Eliteprogramme), Deutsche Forschungsgemeinschaft (DFG - 469666862, DFG - CR 312/5-2); Italy: Istituto Nazionale di Fisica Nucleare (ICSC, NextGenerationEU), Ministero dell'Università e della Ricerca (PRIN - 20223N7F8K - PNRR M4.C2.1.1); Japan: Japan Society for the Promotion of Science (JSPS KAKENHI JP22H01227, JSPS KAKENHI JP22H04944, JSPS KAKENHI JP22KK0227, JSPS KAKENHI JP23KK0245); Norway: Research Council of Norway (RCN-314472); Poland: Ministry of Science and Higher Education (IDUB AGH, POB8, D4 no 9722), Polish National Agency for Academic Exchange (PPN/PPO/2020/1/00002/U/00001), Polish National Science Centre (NCN 2021/42/E/ST2/00350, NCN OPUS 2023/51/B/ST2/02507, NCN OPUS nr 2022/47/B/ST2/03059, NCN UMO-2019/34/E/ST2/00393, UMO-2020/37/B/ST2/01043, UMO-2021/40/C/ST2/00187, UMO-2022/47/O/ST2/00148, UMO-2023/49/B/ST2/04085, UMO-2023/51/B/ST2/00920); Spain: Generalitat Valenciana (Artemisa, FEDER, IDIFEDER/2018/048), Ministry of Science and Innovation (MCIN & NextGenEU PCI2022-135018-2, MICIN & FEDER PID2021-125273NB, RYC2019-028510-I, RYC2020-030254-I, RYC2021-031273-I, RYC2022-038164-I); Sweden: Carl Trygger Foundation (Carl Trygger Foundation CTS 22:2312), Swedish Research Council (Swedish Research Council 2023-04654, VR 2018-00482, VR 2022-03845, VR 2022-04683, VR 2023-03403, VR grant 2021-03651), Knut and Alice Wallenberg Foundation (KAW 2018.0458, KAW 2019.0447, KAW 2022.0358); Switzerland: Swiss National Science Foundation (SNSF - PCEFP2_194658); United Kingdom: Leverhulme Trust (Leverhulme Trust RPG-2020-004), Royal Society (NIF-R1-231091); United States of America: U.S. Department of Energy (ECA DE-AC02-76SF00515), Neubauer Family Foundation.

Appendix

A Analysis implementation

All classifiers are sequential neural networks with four layers of size 64, 64, 64, 1 and activation functions ReLU, ReLU, ReLU, sigmoid, respectively. A dropout of 5% was used between each layer to reduce overfitting. These models were implemented in Keras [78] using the Tensorflow [79] backend. The classifiers use binary cross-entropy loss, and training loss is minimized using the Adam [80] optimizer with a learning rate of 0.001 and no scheduling. For the reweighting classifier, half of the data was used for training, and the other half for validation. Training proceeded for 200 epochs with early stopping (with 25-epoch patience) on the validation loss and a batch size of 512.

All CURTAINS models used the same settings as those used in Ref. [19]. All normalizing flows were implemented using the nflows package [81] in pytorch [82]. All flows use rational-quadratic spline layers [83].

For the signal-tagging classifier, the data was split into five tranches. five classifiers were then trained in a five-fold validation scheme — each classifier was trained on 3 tranches of the data, validated on one tranche, and evaluated on the remaining tranche. The classifiers used the same architecture as the reweighting classifier, but with a softmax activation function and binary cross-entropy loss. Training proceeded for 100 epochs with a learning rate of 0.001, no learning rate scheduling, the Adam optimizer, batch sizes of 512, and early stopping with a patience of 10.

No hyperparameter optimization was performed for any of the models used — this would be an interesting area for future study. The optimization problem is nontrivial in the weakly supervised case, as a decision must be made about what to optimize. The optimization is also difficult to do in a way that is signal model agnostic, as the signal model is not known a priori.

All methods used numpy [84], pandas [85], scipy [86], matplotlib [87], scikit-learn [88], scikit-hep [89], and pipeline runs were configured using hydra [90] and omegaconf [91]. The analysis was implemented as a workflow using snakemake [92].

B Test data samples

This section describes the three complementary and orthogonal test data samples that are used in this analysis. Their construction is detailed in this section. Each test data sample models the events in the SR of the analysis in a different way. The DOWN-UP-SAMPLING test data sample is used in the non-closure correction described in Section 5.4.4. All three are used for the validation of the analysis described in Section 5.5.

B.1 LARGE $|\Delta Y|$ test data sample

In the SR, the absolute rapidity difference $|\Delta Y| = |y_1 - y_2|$ between the two jets is required to satisfy $|\Delta Y| < 1.2$. A test data sample can be constructed by inverting this selection requirement to $|\Delta Y| > 1.2$, referred to as LARGE $|\Delta Y|$. This data sample is expected to be dominated by t -channel QCD background

events. Several observables correlate with $|\Delta Y|$, so the correlations in this data sample do not perfectly mimic those of the SR.

B.2 MONTE CARLO test data sample

A QCD dijet MC simulated sample can be used as a signal-free test data sample. Exactly the same selection requirements can be applied to the MC simulated sample as are applied in data. However, mismodeling and undersampling in the MC simulation can limit the validity of this test data sample.

To increase the sample size of the MONTE CARLO test data sample, a generative model is used. First, an m_{JJ} conditional generative model is trained on a subset of the data, second, the samples are simulated using the true m_{JJ} samples as detailed below. This strategy relies on the assumption that any signal, if present, is rare – otherwise it would have been observed by previous model-agnostic searches like the generic dijet search [72, 93]. The performance of the weakly supervised method on this synthetic test data sample is expected to be similar to its performance on the real data, as both data samples cover the same kinematic phase-space.

Conditional diffusion models are used to learn the distribution of $p(x|m_{JJ})$. These diffusion models use continuous flow matching [94] with logitnorm time sampling [95]. The diffusion networks are sequential neural networks with 3 layers of size 32, 32, 32 and activation functions ReLu, ReLu, ReLu, respectively. The output layer has no activation function. The models are trained using the Adam optimizer [80] with a learning rate of 10^{-4} and a batch size of 64 for 100 epochs. The learning rate is linearly ramped up to 10^{-4} over the first 500 steps.

A conditional diffusion model was trained on the full MC simulated sample in the $|\Delta Y| < 1.2$ region. Samples are drawn from this model using m_{JJ} samples from data in the $|\Delta Y| < 1.2$ region. The m_{JJ} samples are not expected to be sensitive to resonances; this was studied by a previous dijet search [72]. When upsampling the background only distribution using m_{JJ} samples from the $|\Delta Y| < 1.2$ data, the resulting distribution is expected to be representative of the background in the $|\Delta Y| < 1.2$ region. Multiple diffusion models with different random seeds were trained on the MC simulated sample to provide some variability in the different upsampled data samples.

B.3 DOWN-UP-SAMPLING test data sample

The fully inclusive $|\Delta Y| < 1.2$ data is not expected to contain any resonant new physics produced at large cross sections; such signals would likely have been seen in prior searches. Thus, any signal present is assumed to be generated with a small cross section. Randomly selecting a small fraction of events will further dilute the significance of any present signal, rendering the sample effectively blinded.

This randomly downsampled data sample does not have the correct statistics to be used as a test data sample, but it can be used to fit a conditional diffusion model $p(x|m_{JJ})$ that can be upsampled using the fully inclusive m_{JJ} samples. The upsampling follows the same strategy as outlined for the MONTE CARLO test data sample above. The use of the m_{JJ} samples in the $|\Delta Y| < 1.2$ region is justified similarly to the MONTE CARLO test data sample. The whole procedure is graphically depicted in Figure 8. The resulting diffusion model can generate samples that are representative of the data in the $|\Delta Y| < 1.2$ region but lack sensitivity to new physics. Conditional diffusion models are also smooth and do not introduce resonance-like artifacts in the conditional distribution.

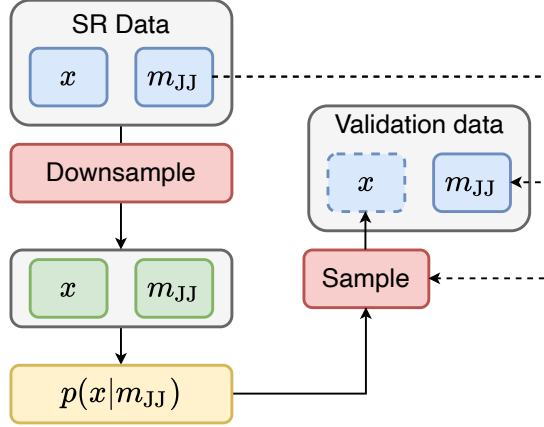


Figure 8: Outline of the procedure used to construct the downsampled $|\Delta Y| < 1.2$ data and upsampled validation sets.

This approach is validated in the $|\Delta Y| > 1.2$ region by injecting a signal into the inclusive data sample such that the analysis produced an excess with a significance of $Z = 3\sigma$ in the 2.6 – 3.2 TeV m_{JJ} SR. Randomly downsampling this data sample, then upsampling resulted in no excess appearing in any SRs. This confirms that the DOWN-UP-SAMPLING procedure eliminates sensitivity to injected signals and does not introduce artifacts that produce a resonance-like effect in m_{JJ} .

C Validation

This section explains the validation strategy and shows the results of the validation of the analysis in greater detail. It uses all three test data samples described in Appendix B. The DOWN-UP-SAMPLING test data sample sets the strictest requirements for the validation.

Figure 9 shows the distribution of events over m_{JJ} for different non-overlapping m_{JJ} SRs after the fit when using the CURTAINS method, in one instance of the DOWN-UP-SAMPLING data sample. It shows that the observations are consistent with the prediction of the background-only fit interpolated from the SBs. The same is true in all SRs for both the methods and all test data samples.

Figure 10 (Figure 11) shows the mean and spread of the significance of the data above the background estimate for CURTAINS and SALAD at the two different selections, $\epsilon = 0.1$ and $\epsilon = 0.02$ as a function of m_{JJ} across ten different instances of the MONTE CARLO (DOWN-UP-SAMPLING) test data sample. These distributions are used to select the m_{JJ} SRs that passed the validation and are used in the final analysis according to the description in Section 5.5.

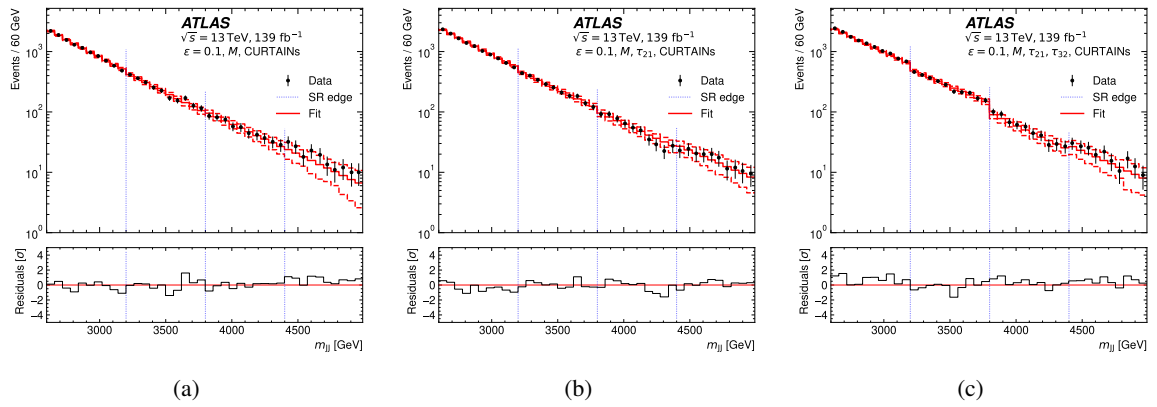


Figure 9: Histograms of m_{JJ} in the first set of non-overlapping m_{JJ} SRs for the CURTAINS method on all feature sets at the $\epsilon = 0.1$ classifier selection on one DOWN-UP-SAMPLING test data sample. The figures show the resulting distributions when the analysis is evaluated on the first, third, fifth, and seventh m_{JJ} SRs. Shown are different feature sets: (a) is the result of $\mathcal{T} = M$, (b) is the result of $\mathcal{T} = M, \tau_{21}$ and (c) is the result of $\mathcal{T} = M, \tau_{21}, \tau_{32}$. The fit is derived from the background-only fit interpolated from the SBs. The uncertainties in the observed counts include the Poisson statistical uncertainty of the bin counts. The uncertainties on the fit are represented by the dashed histograms and include the uncertainties in the fit parameters and the uncertainty from the classifier ensemble on the data. The vertical dashed lines mark the edges of each SR in m_{JJ} . The lower panel in each plot shows the Gaussian-equivalent significance of the deviation between the fit and data.

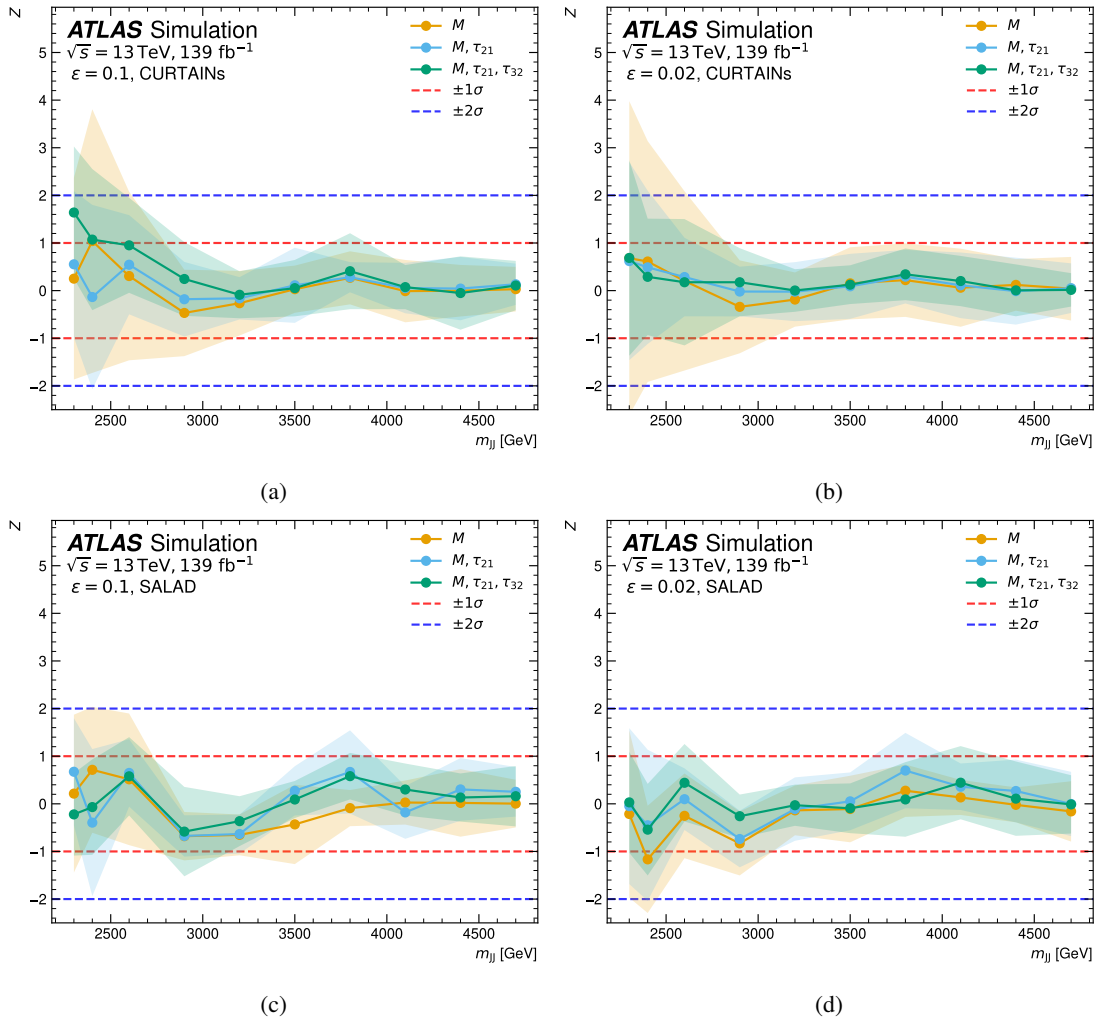


Figure 10: Central values and spread of the local significances (Z) for (a, b) CURTAINS and (c, d) SALAD at the two different selections, (a, c) $\epsilon = 0.1$ and (b, d) $\epsilon = 0.02$. Significances are shown for all feature sets and m_{JJ} SR centers. The bands include the distributions of ten different instances of the MONTE CARLO test data sample.

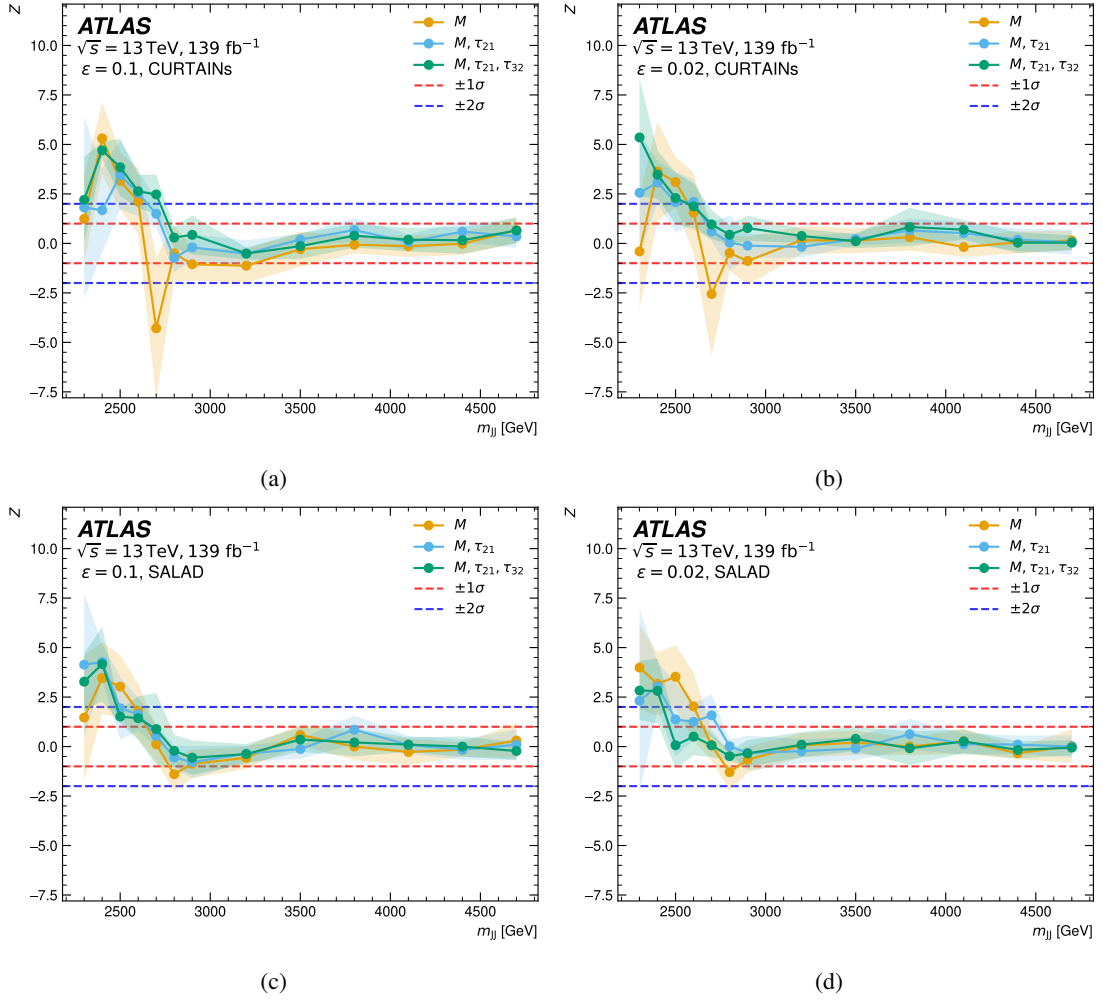


Figure 11: Central values and spread of the local significances (Z) for (a, b) CURTAINS and (c, d) SALAD at the two different selections, (a, c) $\epsilon = 0.1$ and (b, d) $\epsilon = 0.02$. Significances are shown for all feature sets and m_{JJ} SR centers. The bands include the distributions of ten different instances of the DOWN-UP-SAMPLING test data sample.

References

- [1] G. Kasieczka et al., *The LHC Olympics 2020: A Community Challenge for Anomaly Detection in High Energy Physics*, *Rept. Prog. Phys.* **84** (2021) 124201, arXiv: [2101.08320 \[hep-ph\]](#).
- [2] T. Aarrestad et al., *The Dark Machines Anomaly Score Challenge: Benchmark Data and Model Independent Event Classification for the Large Hadron Collider*, *SciPost Phys.* **12** (2022) 043, arXiv: [2105.14027 \[hep-ph\]](#).
- [3] G. Karagiorgi, G. Kasieczka, S. Kravitz, B. Nachman, and D. Shih, *Machine learning in the search for new fundamental physics*, *Nature Rev. Phys.* **4** (2022) 399.
- [4] ATLAS Collaboration, *Dijet Resonance Search with Weak Supervision Using $\sqrt{s} = 13$ TeV pp Collisions in the ATLAS Detector*, *Phys. Rev. Lett.* **125** (2020) 131801, arXiv: [2005.02983 \[hep-ex\]](#).
- [5] G. Kasieczka et al., *Anomaly detection under coordinate transformations*, *Phys. Rev. D* **107** (2023) 015009, arXiv: [2209.06225 \[hep-ph\]](#).
- [6] E. M. Metodiev, B. Nachman, and J. Thaler, *Classification without labels: Learning from mixed samples in high energy physics*, *JHEP* **10** (2017) 174, arXiv: [1708.02949 \[hep-ph\]](#).
- [7] D. Pappadopulo, A. Thamm, R. Torre, and A. Wulzer, *Heavy vector triplets: bridging theory and data*, *JHEP* **09** (2014) 060, arXiv: [1402.4431 \[hep-ph\]](#).
- [8] N. Craig, P. Draper, K. Kong, Y. Ng, and D. Whiteson, *The unexplored landscape of two-body resonances*, (2016), arXiv: [1610.09392 \[hep-ph\]](#).
- [9] J. H. Kim, K. Kong, B. Nachman, and D. Whiteson, *The motivation and status of two-body resonance decays after the LHC Run 2 and beyond*, *JHEP* **04** (2020) 030, arXiv: [1907.06659 \[hep-ph\]](#).
- [10] J. H. Collins, K. Howe, and B. Nachman, *Anomaly Detection for Resonant New Physics with Machine Learning*, *Phys. Rev. Lett.* **121** (2018) 241803, arXiv: [1805.02664 \[hep-ph\]](#).
- [11] J. H. Collins, K. Howe, and B. Nachman, *Extending the search for new resonances with machine learning*, *Phys. Rev. D* **99** (2019) 014038, arXiv: [1902.02634 \[hep-ph\]](#).
- [12] B. Nachman and D. Shih, *Anomaly Detection with Density Estimation*, *Phys. Rev. D* **101** (2020) 075042, arXiv: [2001.04990 \[hep-ph\]](#).
- [13] A. Andreassen, B. Nachman, and D. Shih, *Simulation Assisted Likelihood-free Anomaly Detection*, *Phys. Rev. D* **101** (2020) 095004, arXiv: [2001.05001 \[hep-ph\]](#).
- [14] G. Stein, U. Seljak, and B. Dai, “Unsupervised in-distribution anomaly detection of new physics through conditional density estimation,” *34th Conference on Neural Information Processing Systems*, 2020, arXiv: [2012.11638 \[cs.LG\]](#).
- [15] K. Benkendorfer, L. L. Pottier, and B. Nachman, *Simulation-assisted decorrelation for resonant anomaly detection*, *Phys. Rev. D* **104** (2021) 035003, arXiv: [2009.02205 \[hep-ph\]](#).

- [16] A. Hallin et al., *Classifying anomalies through outer density estimation*, *Phys. Rev. D* **106** (2022) 055006, arXiv: 2109.00546 [hep-ph].
- [17] A. Hallin, G. Kasieczka, T. Quadfasel, D. Shih, and M. Sommerhalder, *Resonant anomaly detection without background sculpting*, *Phys. Rev. D* **107** (2023) 114012, arXiv: 2210.14924 [hep-ph].
- [18] M. F. Chen, B. Nachman, and F. Sala, *Resonant anomaly detection with multiple reference datasets*, *JHEP* **07** (2023) 188, arXiv: 2212.10579 [hep-ph].
- [19] J. A. Raine, S. Klein, D. Sengupta, and T. Golling, *CURTAINS for your sliding window: Constructing unobserved regions by transforming adjacent intervals*, *Front. Big Data* **6** (2023) 899345, arXiv: 2203.09470 [hep-ph].
- [20] T. Golling, S. Klein, R. Mastandrea, and B. Nachman, *Flow-enhanced transportation for anomaly detection*, *Phys. Rev. D* **107** (2023) 096025, arXiv: 2212.11285 [hep-ph].
- [21] D. Sengupta, S. Klein, J. A. Raine, and T. Golling, *CURTAINS flows for flows: Constructing unobserved regions with maximum likelihood estimation*, *SciPost Phys.* **17** (2024) 046, arXiv: 2305.04646 [hep-ph].
- [22] R. Das, G. Kasieczka, and D. Shih, *Residual ANODE*, (2023), arXiv: 2312.11629 [hep-ph].
- [23] T. Golling et al., *The interplay of machine learning-based resonant anomaly detection methods*, *Eur. Phys. J. C* **84** (2024) 241, arXiv: 2307.11157 [hep-ph].
- [24] ATLAS Collaboration, *Search for new phenomena in dijet mass and angular distributions from pp collisions at $\sqrt{s} = 13$ TeV with the ATLAS detector*, *Phys. Lett. B* **754** (2016) 302, arXiv: 1512.01530 [hep-ex].
- [25] CMS Collaboration, *Search for narrow resonances decaying to dijets in proton–proton collisions at $\sqrt{s} = 13$ TeV*, *Phys. Rev. Lett.* **116** (2016) 071801, arXiv: 1512.01224 [hep-ex].
- [26] ATLAS Collaboration, *Search for resonances decaying into a weak vector boson and a Higgs boson in the fully hadronic final state produced in proton–proton collisions at $\sqrt{s} = 13$ TeV with the ATLAS detector*, *Phys. Rev. D* **102** (2020) 112008, arXiv: 2007.05293 [hep-ex].
- [27] ATLAS Collaboration, *Search for resonant WZ production in the fully leptonic final state in proton–proton collisions at $\sqrt{s} = 13$ TeV with the ATLAS detector*, *Eur. Phys. J. C* **83** (2023) 633, arXiv: 2207.03925 [hep-ex].
- [28] ATLAS Collaboration, *Search for diboson resonances in hadronic final states in 139 fb^{-1} of pp collisions at $\sqrt{s} = 13$ TeV with the ATLAS detector*, *JHEP* **09** (2019) 091, arXiv: 1906.08589 [hep-ex].
- [29] ATLAS Collaboration, *Search for heavy resonances decaying into a Z or W boson and a Higgs boson in final states with leptons and b -jets in 139 fb^{-1} of pp collisions at $\sqrt{s} = 13$ TeV with the ATLAS detector*, *JHEP* **06** (2023) 016, arXiv: 2207.00230 [hep-ex].
- [30] CMS Collaboration, *A multi-dimensional search for new heavy resonances decaying to boosted WW , WZ , or ZZ boson pairs in the dijet final state at 13 TeV*, *Eur. Phys. J. C* **80** (2020) 237, arXiv: 1906.05977 [hep-ex].

- [31] CMS Collaboration, *Search for new heavy resonances decaying to WW , WZ , ZZ , WH , or ZH boson pairs in the all-jets final state in proton–proton collisions at $\sqrt{s} = 13$ TeV*, [Phys. Lett. B **844** \(2023\) 137813](#), arXiv: [2210.00043 \[hep-ex\]](#).
- [32] CMS Collaboration, *Model-agnostic search for dijet resonances with anomalous jet substructure in proton–proton collisions at $\sqrt{s} = 13$ TeV*, (2024), arXiv: [2412.03747 \[hep-ex\]](#).
- [33] ATLAS Collaboration, *Anomaly detection search for new resonances decaying into a Higgs boson and a generic new particle X in hadronic final states using $\sqrt{s} = 13$ TeV pp collisions with the ATLAS detector*, [Phys. Rev. D **108** \(2023\) 052009](#), arXiv: [2306.03637 \[hep-ex\]](#).
- [34] ATLAS Collaboration, *Search for New Phenomena in Two-Body Invariant Mass Distributions Using Unsupervised Machine Learning for Anomaly Detection at $\sqrt{s} = 13$ TeV with the ATLAS Detector*, [Phys. Rev. Lett. **132** \(2024\) 081801](#), arXiv: [2307.01612 \[hep-ex\]](#).
- [35] J. H. Collins, P. Martín-Ramiro, B. Nachman, and D. Shih, *Comparing weak- and unsupervised methods for resonant anomaly detection*, [Eur. Phys. J. C **81** \(2021\) 617](#), arXiv: [2104.02092 \[hep-ph\]](#).
- [36] ATLAS Collaboration, *The ATLAS Experiment at the CERN Large Hadron Collider*, [JINST **3** \(2008\) S08003](#).
- [37] ATLAS Collaboration, *ATLAS Insertable B-Layer: Technical Design Report*, ATLAS-TDR-19; CERN-LHCC-2010-013, 2010, URL: <https://cds.cern.ch/record/1291633>, Addendum: ATLAS-TDR-19-ADD-1; CERN-LHCC-2012-009, 2012, URL: <https://cds.cern.ch/record/1451888>.
- [38] B. Abbott et al., *Production and integration of the ATLAS Insertable B-Layer*, [JINST **13** \(2018\) T05008](#), arXiv: [1803.00844 \[physics.ins-det\]](#).
- [39] G. Avoni et al., *The new LUCID-2 detector for luminosity measurement and monitoring in ATLAS*, [JINST **13** \(2018\) P07017](#).
- [40] ATLAS Collaboration, *Performance of the ATLAS trigger system in 2015*, [Eur. Phys. J. C **77** \(2017\) 317](#), arXiv: [1611.09661 \[hep-ex\]](#).
- [41] ATLAS Collaboration, *Software and computing for Run 3 of the ATLAS experiment at the LHC*, (2024), arXiv: [2404.06335 \[hep-ex\]](#).
- [42] ATLAS Collaboration, *Luminosity determination in pp collisions at $\sqrt{s} = 13$ TeV using the ATLAS detector at the LHC*, ATLAS-CONF-2019-021, 2019, URL: <https://cds.cern.ch/record/2677054>.
- [43] ATLAS Collaboration, *ATLAS data quality operations and performance for 2015–2018 data-taking*, [JINST **15** \(2020\) P04003](#), arXiv: [1911.04632 \[physics.ins-det\]](#).
- [44] ATLAS Collaboration, *The ATLAS Simulation Infrastructure*, [Eur. Phys. J. C **70** \(2010\) 823](#), arXiv: [1005.4568 \[physics.ins-det\]](#).
- [45] T. Sjöstrand et al., *An introduction to PYTHIA 8.2*, [Comput. Phys. Commun. **191** \(2015\) 159](#), arXiv: [1410.3012 \[hep-ph\]](#).
- [46] ATLAS Collaboration, *ATLAS Pythia 8 tunes to 7 TeV data*, ATL-PHYS-PUB-2014-021, 2014, URL: <https://cds.cern.ch/record/1966419>.

- [47] NNPDF Collaboration, R. D. Ball, et al., *Parton distributions with LHC data*, *Nucl. Phys. B* **867** (2013) 244, arXiv: [1207.1303 \[hep-ph\]](#).
- [48] D. J. Lange, *The EvtGen particle decay simulation package*, *Nucl. Instrum. Meth. A* **462** (2001) 152.
- [49] S. Agostinelli et al., *GEANT4 – a simulation toolkit*, *Nucl. Instrum. Meth. A* **506** (2003) 250.
- [50] T. Sjöstrand, S. Mrenna, and P. Skands, *A brief introduction to PYTHIA 8.1*, *Comput. Phys. Commun.* **178** (2008) 852, arXiv: [0710.3820 \[hep-ph\]](#).
- [51] ATLAS Collaboration, *The Pythia 8 A3 tune description of ATLAS minimum bias and inelastic measurements incorporating the Donnachie–Landshoff diffractive model*, ATL-PHYS-PUB-2016-017, 2016, URL: <https://cds.cern.ch/record/2206965>.
- [52] ATLAS Collaboration, *Multijet simulation for 13 TeV ATLAS Analyses*, ATL-PHYS-PUB-2019-017, 2019, URL: <https://cds.cern.ch/record/2672252>.
- [53] G. Altarelli, B. Mele, and M. Ruiz-Altaba, *Searching for new heavy vector bosons in $p\bar{p}$ colliders*, *Z. Phys. C* **45** (1989) 109, Erratum: *Z. Phys. C* **47** (1990) 676.
- [54] G. C. Branco et al., *Theory and phenomenology of two-Higgs-doublet models*, *Phys. Rept.* **516** (2012) 1, arXiv: [1106.0034 \[hep-ph\]](#).
- [55] ATLAS Collaboration, *Vertex Reconstruction Performance of the ATLAS Detector at $\sqrt{s} = 13$ TeV*, ATL-PHYS-PUB-2015-026, 2015, URL: <https://cds.cern.ch/record/2037717>.
- [56] ATLAS Collaboration, *Topological cell clustering in the ATLAS calorimeters and its performance in LHC Run 1*, *Eur. Phys. J. C* **77** (2017) 490, arXiv: [1603.02934 \[hep-ex\]](#).
- [57] M. Cacciari, G. P. Salam, and G. Soyez, *The anti- k_t jet clustering algorithm*, *JHEP* **04** (2008) 063, arXiv: [0802.1189 \[hep-ph\]](#).
- [58] M. Cacciari, G. P. Salam, and G. Soyez, *FastJet user manual*, *Eur. Phys. J. C* **72** (2012) 1896, arXiv: [1111.6097 \[hep-ph\]](#).
- [59] D. Krohn, J. Thaler, and L.-T. Wang, *Jet Trimming*, *JHEP* **02** (2010) 084, arXiv: [0912.1342 \[hep-ph\]](#).
- [60] ATLAS Collaboration, *In situ calibration of large-radius jet energy and mass in 13 TeV proton–proton collisions with the ATLAS detector*, *Eur. Phys. J. C* **79** (2019) 135, arXiv: [1807.09477 \[hep-ex\]](#).
- [61] J. Thaler and K. Van Tilburg, *Identifying Boosted Objects with N -subjettiness*, *JHEP* **03** (2011) 015, arXiv: [1011.2268 \[hep-ph\]](#).
- [62] L. Grinsztajn, E. Oyallon, and G. Varoquaux, *Why do tree-based models still outperform deep learning on tabular data?* (2022), arXiv: [2207.08815 \[cs.LG\]](#).
- [63] T. Finke et al., *Tree-based algorithms for weakly supervised anomaly detection*, *Phys. Rev. D* **109** (2024) 034033, arXiv: [2309.13111 \[hep-ph\]](#).
- [64] M. Freytsis, M. Perelstein, and Y. C. San, *Anomaly detection in the presence of irrelevant features*, *JHEP* **02** (2024) 220, arXiv: [2310.13057 \[hep-ph\]](#).
- [65] T. Golling et al., *Masked particle modeling on sets: towards self-supervised high energy physics foundation models*, *Mach. Learn. Sci. Tech.* **5** (2024) 035074, arXiv: [2401.13537 \[hep-ph\]](#).

- [66] V. Mikuni and B. Nachman, *OmniLearn: A Method to Simultaneously Facilitate All Jet Physics Tasks*, (2024), arXiv: [2404.16091 \[hep-ph\]](#).
- [67] A. L. Read, *Presentation of search results: the CL_S technique*, *J. Phys. G* **28** (2002) 2693.
- [68] K. Cranmer, J. Pavez, and G. Louppe, *Approximating Likelihood Ratios with Calibrated Discriminative Classifiers*, (2015), arXiv: [1506.02169 \[stat.AP\]](#).
- [69] P. Baldi, K. Cranmer, T. Faucett, P. Sadowski, and D. Whiteson, *Parameterized neural networks for high-energy physics*, *Eur. Phys. J. C* **76** (2016) 235, arXiv: [1601.07913 \[hep-ex\]](#).
- [70] E. G. Tabak and C. V. Turner, *A Family of Nonparametric Density Estimation Algorithms*, *Commun. Pure Appl. Math.* **66** (2013) 145.
- [71] J. Eschle, A. Puig Navarro, R. Silva Coutinho, and N. Serra, *zfit: scalable pythonic fitting*, *SoftwareX* **11** (2020) 100508, arXiv: [1910.13429 \[physics.data-an\]](#).
- [72] ATLAS Collaboration, *Search for new resonances in mass distributions of jet pairs using 139 fb^{-1} of pp collisions at $\sqrt{s} = 13\text{ TeV}$ with the ATLAS detector*, *JHEP* **03** (2020) 145, arXiv: [1910.08447 \[hep-ex\]](#).
- [73] UA2 Collaboration, *A Measurement of two-jet decays of the W and Z bosons at the CERN $\bar{p}p$ collider*, *Z. Phys. C* **49** (1991) 17.
- [74] G. Cowan, K. Cranmer, E. Gross, and O. Vitells, *Asymptotic formulae for likelihood-based tests of new physics*, *Eur. Phys. J. C* **71** (2011) 1554, arXiv: [1007.1727 \[physics.data-an\]](#), Erratum: *Eur. Phys. J. C* **73** (2013) 2501.
- [75] L. Heinrich, M. Feickert, G. Stark, and K. Cranmer, *pyhf: pure-Python implementation of HistFactory statistical models*, *J. Open Source Softw.* **6** (2021) 2823.
- [76] L. Heinrich, M. Feickert, and G. Stark, *pyhf*, URL: <https://github.com/scikit-hep/pyhf/releases/>.
- [77] ATLAS Collaboration, *ATLAS Computing Acknowledgements*, ATL-SOFT-PUB-2025-001, 2025, URL: <https://cds.cern.ch/record/2922210>.
- [78] F. Chollet et al., *Keras*, 2015, URL: <https://keras.io>.
- [79] M. Abadi et al., *TensorFlow: A system for large-scale machine learning*, (2016), arXiv: [1605.08695 \[cs.DC\]](#).
- [80] D. P. Kingma and J. Ba, *Adam: A Method for Stochastic Optimization*, 2014, arXiv: [1412.6980 \[cs.LG\]](#).
- [81] C. Durkan, A. Bekasov, I. Murray, and G. Papamakarios, *nflows: normalizing flows in PyTorch*, version v0.14, 2020, URL: <https://doi.org/10.5281/zenodo.4296287>.
- [82] A. Paszke et al., *PyTorch: An Imperative Style, High-Performance Deep Learning Library*, (2019), arXiv: [1912.01703 \[cs.LG\]](#).
- [83] C. Durkan, A. Bekasov, I. Murray, and G. Papamakarios, “Neural Spline Flows,” 2019, arXiv: [1906.04032 \[stat.ML\]](#).

- [84] C. R. Harris et al., *Array programming with NumPy*, *Nature* **585** (2020) 357, arXiv: [2006.10256](https://arxiv.org/abs/2006.10256) [[cs.MS](#)].
- [85] The pandas development team, *pandas-dev/pandas: Pandas*, version v2.0.1, 2023, URL: <https://doi.org/10.5281/zenodo.7857418>.
- [86] P. Virtanen et al., *SciPy 1.0: fundamental algorithms for scientific computing in Python*, *Nature Meth.* **17** (2020) 261, arXiv: [1907.10121](https://arxiv.org/abs/1907.10121) [[cs.MS](#)].
- [87] J. D. Hunter, *Matplotlib: A 2D Graphics Environment*, *Comput. Sci. Eng.* **9** (2007) 90.
- [88] F. Pedregosa et al., *Scikit-learn: Machine Learning in Python*, *J. Mach. Learn. Res.* **12** (2011) 2825, URL: <https://dl.acm.org/doi/10.5555/1953048.2078195>.
- [89] E. Rodrigues et al., *The Scikit HEP Project overview and prospects*, *EPJ Web Conf.* **245** (2020) 06028, ed. by C. Doglioni et al., arXiv: [2007.03577](https://arxiv.org/abs/2007.03577) [[physics.comp-ph](#)].
- [90] O. Yadan, *Hydra - A framework for elegantly configuring complex applications*, Github, 2019, URL: <https://github.com/facebookresearch/hydra>.
- [91] O. Yadan, J. Sommer-Simpson, and O. Delalleau, *omegaconf*, 2019, URL: <https://github.com/omry/omegaconf>.
- [92] F. Mölder et al., *Sustainable data analysis with Snakemake*, *F1000Research* **10** (2021) 33.
- [93] CMS Collaboration, *Search for high mass dijet resonances with a new background prediction method in proton–proton collisions at $\sqrt{s} = 13$ TeV*, *JHEP* **05** (2020) 033, arXiv: [1911.03947](https://arxiv.org/abs/1911.03947) [[hep-ex](#)].
- [94] Y. Lipman, R. T. Q. Chen, H. Ben-Hamu, M. Nickel, and M. Le, *Flow Matching for Generative Modeling*, 2023, arXiv: [2210.02747](https://arxiv.org/abs/2210.02747) [[cs.LG](#)].
- [95] P. Esser et al., *Scaling Rectified Flow Transformers for High-Resolution Image Synthesis*, 2024, arXiv: [2403.03206](https://arxiv.org/abs/2403.03206) [[cs.CV](#)].

The ATLAS Collaboration

G. Aad ¹⁰⁵, E. Aakvaag ¹⁷, B. Abbott ¹²⁴, S. Abdelhameed ^{120a}, K. Abeling ⁵⁶, N.J. Abicht ⁵⁰, S.H. Abidi ³⁰, M. Aboeela ⁴⁶, A. Aboulhorma ^{36e}, H. Abramowicz ¹⁵⁸, Y. Abulaiti ¹²¹, B.S. Acharya ^{70a,70b,n}, A. Ackermann ^{64a}, C. Adam Bourdarios ⁴, L. Adamczyk ^{87a}, S.V. Addepalli ¹⁵⁰, M.J. Addison ¹⁰⁴, J. Adelman ¹¹⁹, A. Adiguzel ^{22c}, T. Adye ¹³⁸, A.A. Affolder ¹⁴⁰, Y. Afik ⁴¹, M.N. Agaras ¹³, A. Aggarwal ¹⁰³, C. Agheorghiesei ^{28c}, F. Ahmadov ^{40,ad}, S. Ahuja ⁹⁸, X. Ai ^{144b}, G. Aielli ^{77a,77b}, A. Aikot ¹⁷⁰, M. Ait Tamlihat ^{36e}, B. Aitbenkikh ^{36a}, M. Akbiyik ¹⁰³, T.P.A. Åkesson ¹⁰¹, A.V. Akimov ¹⁵², D. Akiyama ¹⁷⁵, N.N. Akolkar ²⁵, S. Aktas ^{22a}, G.L. Alberghi ^{24b}, J. Albert ¹⁷², P. Albicocco ⁵⁴, G.L. Albouy ⁶¹, S. Alderweireldt ⁵³, Z.L. Alegria ¹²⁵, M. Aleksa ³⁷, I.N. Aleksandrov ⁴⁰, C. Alexa ^{28b}, T. Alexopoulos ¹⁰, F. Alfonsi ^{24b}, M. Algren ⁵⁷, M. Alhroob ¹⁷⁴, B. Ali ¹³⁶, H.M.J. Ali ^{94,w}, S. Ali ³², S.W. Alibocus ⁹⁵, M. Aliev ^{34c}, G. Alimonti ^{72a}, W. Alkahi ⁵⁶, C. Allaire ⁶⁷, B.M.M. Allbrooke ¹⁵³, J.S. Allen ¹⁰⁴, J.F. Allen ⁵³, P.P. Allport ²¹, A. Aloisio ^{73a,73b}, F. Alonso ⁹³, C. Alpigiani ¹⁴³, Z.M.K. Alsolami ⁹⁴, A. Alvarez Fernandez ¹⁰³, M. Alves Cardoso ⁵⁷, M.G. Alviggi ^{73a,73b}, M. Aly ¹⁰⁴, Y. Amaral Coutinho ^{84b}, A. Ambler ¹⁰⁷, C. Amelung ³⁷, M. Amerl ¹⁰⁴, C.G. Ames ¹¹², D. Amidei ¹⁰⁹, B. Amini ⁵⁵, K. Amirie ¹⁶², A. Amirkhanov ⁴⁰, S.P. Amor Dos Santos ^{134a}, K.R. Amos ¹⁷⁰, D. Amperiadou ¹⁵⁹, S. An ⁸⁵, V. Ananiev ¹²⁹, C. Anastopoulos ¹⁴⁶, T. Andeen ¹¹, J.K. Anders ⁹⁵, A.C. Anderson ⁶⁰, A. Andreazza ^{72a,72b}, S. Angelidakis ⁹, A. Angerami ⁴³, A.V. Anisenkov ⁴⁰, A. Annovi ^{75a}, C. Antel ⁵⁷, E. Antipov ¹⁵², M. Antonelli ⁵⁴, F. Anulli ^{76a}, M. Aoki ⁸⁵, T. Aoki ¹⁶⁰, M.A. Aparo ¹⁵³, L. Aperio Bella ⁴⁹, C. Appelt ¹⁵⁸, A. Apyan ²⁷, S.J. Arbiol Val ⁸⁸, C. Arcangeletti ⁵⁴, A.T.H. Arce ⁵², J-F. Arguin ¹¹¹, S. Argyropoulos ¹⁵⁹, J.-H. Arling ⁴⁹, O. Arnaez ⁴, H. Arnold ¹⁵², G. Artoni ^{76a,76b}, H. Asada ¹¹⁴, K. Asai ¹²², S. Asai ¹⁶⁰, N.A. Asbah ³⁷, R.A. Ashby Pickering ¹⁷⁴, A.M. Aslam ⁹⁸, K. Assamagan ³⁰, R. Astalos ^{29a}, K.S.V. Astrand ¹⁰¹, S. Atashi ¹⁶⁶, R.J. Atkin ^{34a}, H. Atmani ^{36f}, P.A. Atmasiddha ¹³², K. Augsten ¹³⁶, A.D. Auriol ⁴², V.A. Austrup ¹⁰⁴, G. Avolio ³⁷, K. Axiotis ⁵⁷, G. Azuelos ^{111,ah}, D. Babal ^{29b}, H. Bachacou ¹³⁹, K. Bachas ^{159,r}, A. Bachiu ³⁵, E. Bachmann ⁵¹, M.J. Backes ^{64a}, A. Badea ⁴¹, T.M. Baer ¹⁰⁹, P. Bagnaia ^{76a,76b}, M. Bahmani ¹⁹, D. Bahner ⁵⁵, K. Bai ¹²⁷, J.T. Baines ¹³⁸, L. Baines ⁹⁷, O.K. Baker ¹⁷⁹, E. Bakos ¹⁶, D. Bakshi Gupta ⁸, L.E. Balabram Filho ^{84b}, V. Balakrishnan ¹²⁴, R. Balasubramanian ⁴, E.M. Baldin ³⁹, P. Balek ^{87a}, E. Ballabene ^{24b,24a}, F. Balli ¹³⁹, L.M. Baltes ^{64a}, W.K. Balunas ³³, J. Balz ¹⁰³, I. Bamwidhi ^{120b}, E. Banas ⁸⁸, M. Bandieramonte ¹³³, A. Bandyopadhyay ²⁵, S. Bansal ²⁵, L. Barak ¹⁵⁸, M. Barakat ⁴⁹, E.L. Barberio ¹⁰⁸, D. Barberis ^{58b,58a}, M. Barbero ¹⁰⁵, M.Z. Barel ¹¹⁸, T. Barillari ¹¹³, M-S. Barisits ³⁷, T. Barklow ¹⁵⁰, P. Baron ¹²⁶, D.A. Baron Moreno ¹⁰⁴, A. Baroncelli ⁶³, A.J. Barr ¹³⁰, J.D. Barr ⁹⁹, F. Barreiro ¹⁰², J. Barreiro Guimarães da Costa ¹⁴, M.G. Barros Teixeira ^{134a}, S. Barsov ³⁹, F. Bartels ^{64a}, R. Bartoldus ¹⁵⁰, A.E. Barton ⁹⁴, P. Bartos ^{29a}, A. Basan ¹⁰³, M. Baselga ⁵⁰, S. Bashiri ⁸⁸, A. Bassalat ^{67,b}, M.J. Basso ^{163a}, S. Bataju ⁴⁶, R. Bate ¹⁷¹, R.L. Bates ⁶⁰, S. Batlamous ¹⁰², M. Battaglia ¹⁴⁰, D. Battulga ¹⁹, M. Bauce ^{76a,76b}, M. Bauer ⁸⁰, P. Bauer ²⁵, L.T. Bayer ⁴⁹, L.T. Bazzano Hurrell ³¹, J.B. Beacham ¹¹³, T. Beau ¹³¹, J.Y. Beaucamp ⁹³, P.H. Beauchemin ¹⁶⁵, P. Bechtel ²⁵, H.P. Beck ^{20,q}, K. Becker ¹⁷⁴, A.J. Beddall ⁸³, V.A. Bednyakov ⁴⁰, C.P. Bee ¹⁵², L.J. Beemster ¹⁶, M. Begalli ^{84d}, M. Begel ³⁰, J.K. Behr ⁴⁹, J.F. Beirer ³⁷, F. Beisiegel ²⁵, M. Belfkir ^{120b}, G. Bella ¹⁵⁸, L. Bellagamba ^{24b}, A. Bellerive ³⁵, P. Bellos ²¹, K. Beloborodov ³⁹, D. Benchebroun ^{36a}, F. Bendebba ^{36a}, Y. Benhammou ¹⁵⁸, K.C. Benkendorfer ⁶², L. Beresford ⁴⁹, M. Beretta ⁵⁴, E. Bergeas Kuutmann ¹⁶⁸, N. Berger ⁴,

B. Bergmann [ID136](#), J. Beringer [ID18a](#), G. Bernardi [ID5](#), C. Bernius [ID150](#), F.U. Bernlochner [ID25](#),
 F. Bernon [ID37](#), A. Berrocal Guardia [ID13](#), T. Berry [ID98](#), P. Berta [ID137](#), A. Berthold [ID51](#), R. Bertrand [ID105](#),
 S. Bethke [ID113](#), A. Betti [ID76a,76b](#), A.J. Bevan [ID97](#), L. Bezio [ID57](#), N.K. Bhalla [ID55](#), S. Bharthuar [ID113](#),
 S. Bhatta [ID152](#), D.S. Bhattacharya [ID173](#), P. Bhattarai [ID150](#), Z.M. Bhatti [ID121](#), K.D. Bhide [ID55](#),
 V.S. Bhopatkar [ID125](#), R.M. Bianchi [ID133](#), G. Bianco [ID24b,24a](#), O. Biebel [ID112](#), M. Biglietti [ID78a](#),
 C.S. Billingsley [ID46](#), Y. Bimngdi [ID36f](#), M. Bindi [ID56](#), A. Bingham [ID178](#), A. Bingul [ID22b](#), C. Bini [ID76a,76b](#),
 G.A. Bird [ID33](#), M. Birman [ID176](#), M. Biroš [ID137](#), S. Biryukov [ID153](#), T. Bisanz [ID50](#), E. Bisceglie [ID24b,24a](#),
 J.P. Biswal [ID138](#), D. Biswas [ID148](#), I. Bloch [ID49](#), A. Blue [ID60](#), U. Blumenschein [ID97](#), J. Blumenthal [ID103](#),
 V.S. Bobrovnikov [ID40](#), M. Boehler [ID55](#), B. Boehm [ID173](#), D. Bogavac [ID37](#), A.G. Bogdanchikov [ID39](#),
 L.S. Boggia [ID131](#), V. Boisvert [ID98](#), P. Bokan [ID37](#), T. Bold [ID87a](#), M. Bomben [ID5](#), M. Bona [ID97](#),
 M. Boonekamp [ID139](#), A.G. Borbély [ID60](#), I.S. Bordulev [ID39](#), G. Borissov [ID94](#), D. Bortoletto [ID130](#),
 D. Boscherini [ID24b](#), M. Bosman [ID13](#), K. Bouaouda [ID36a](#), N. Bouchhar [ID170](#), L. Boudet [ID4](#),
 J. Boudreau [ID133](#), E.V. Bouhova-Thacker [ID94](#), D. Boumediene [ID42](#), R. Bouquet [ID58b,58a](#), A. Boveia [ID123](#),
 J. Boyd [ID37](#), D. Boye [ID30](#), I.R. Boyko [ID40](#), L. Bozianu [ID57](#), J. Bracinek [ID21](#), N. Brahimi [ID4](#),
 G. Brandt [ID178](#), O. Brandt [ID33](#), B. Brau [ID106](#), J.E. Brau [ID127](#), R. Brener [ID176](#), L. Brenner [ID118](#),
 R. Brenner [ID168](#), S. Bressler [ID176](#), G. Brianti [ID79a,79b](#), D. Britton [ID60](#), D. Britzger [ID113](#), I. Brock [ID25](#),
 R. Brock [ID110](#), G. Brooijmans [ID43](#), A.J. Brooks [ID69](#), E.M. Brooks [ID163b](#), E. Brost [ID30](#), L.M. Brown [ID172](#),
 L.E. Bruce [ID62](#), T.L. Bruckler [ID130](#), P.A. Bruckman de Renstrom [ID88](#), B. Brüers [ID49](#), A. Bruni [ID24b](#),
 G. Bruni [ID24b](#), D. Brunner [ID48a,48b](#), M. Bruschi [ID24b](#), N. Bruscinò [ID76a,76b](#), T. Buanes [ID17](#), Q. Buat [ID143](#),
 D. Buchin [ID113](#), A.G. Buckley [ID60](#), O. Bulekov [ID39](#), B.A. Bullard [ID150](#), S. Burdin [ID95](#), C.D. Burgard [ID50](#),
 A.M. Burger [ID37](#), B. Burghgrave [ID8](#), O. Burlayenko [ID55](#), J. Burleson [ID169](#), J.T.P. Burr [ID33](#),
 J.C. Burzynski [ID149](#), E.L. Busch [ID43](#), V. Büscher [ID103](#), P.J. Bussey [ID60](#), J.M. Butler [ID26](#), C.M. Buttar [ID60](#),
 J.M. Butterworth [ID99](#), W. Buttinger [ID138](#), C.J. Buxo Vazquez [ID110](#), A.R. Buzykaev [ID40](#),
 S. Cabrera Urbán [ID170](#), L. Cadamuro [ID67](#), D. Caforio [ID59](#), H. Cai [ID133](#), Y. Cai [ID24b,115c,24a](#), Y. Cai [ID115a](#),
 V.M.M. Cairo [ID37](#), O. Cakir [ID3a](#), N. Calace [ID37](#), P. Calafiura [ID18a](#), G. Calderini [ID131](#), P. Calfayan [ID35](#),
 G. Callea [ID60](#), L.P. Caloba [ID84b](#), D. Calvet [ID42](#), S. Calvet [ID42](#), R. Camacho Toro [ID131](#), S. Camarda [ID37](#),
 D. Camarero Munoz [ID27](#), P. Camarri [ID77a,77b](#), M.T. Camerlingo [ID73a,73b](#), C. Camincher [ID172](#),
 M. Campanelli [ID99](#), A. Camplani [ID44](#), V. Canale [ID73a,73b](#), A.C. Canbay [ID3a](#), E. Canonero [ID98](#),
 J. Cantero [ID170](#), Y. Cao [ID169](#), F. Capocasa [ID27](#), M. Capua [ID45b,45a](#), A. Carbone [ID72a,72b](#),
 R. Cardarelli [ID77a](#), J.C.J. Cardenas [ID8](#), M.P. Cardiff [ID27](#), G. Carducci [ID45b,45a](#), T. Carli [ID37](#),
 G. Carlino [ID73a](#), J.I. Carlotto [ID13](#), B.T. Carlson [ID133,s](#), E.M. Carlson [ID172](#), J. Carmignani [ID95](#),
 L. Carminati [ID72a,72b](#), A. Carnelli [ID4](#), M. Carnesale [ID37](#), S. Caron [ID117](#), E. Carquin [ID141f](#), I.B. Carr [ID108](#),
 S. Carrá [ID72a](#), G. Carratta [ID24b,24a](#), A.M. Carroll [ID127](#), M.P. Casado [ID13,i](#), M. Caspar [ID49](#),
 F.L. Castillo [ID4](#), L. Castillo Garcia [ID13](#), V. Castillo Gimenez [ID170](#), N.F. Castro [ID134a,134e](#),
 A. Catinaccio [ID37](#), J.R. Catmore [ID129](#), T. Cavaliere [ID4](#), V. Cavaliere [ID30](#), L.J. Caviedes Betancourt [ID23b](#),
 Y.C. Cekmecelioglu [ID49](#), E. Celebi [ID83](#), S. Cella [ID37](#), V. Cepaitis [ID57](#), K. Cerny [ID126](#),
 A.S. Cerqueira [ID84a](#), A. Cerri [ID75a,75b](#), L. Cerrito [ID77a,77b](#), F. Cerutti [ID18a](#), B. Cervato [ID72a,72b](#),
 A. Cervelli [ID24b](#), G. Cesarini [ID54](#), S.A. Cetin [ID83](#), P.M. Chabrilat [ID131](#), J. Chan [ID18a](#), W.Y. Chan [ID160](#),
 J.D. Chapman [ID33](#), E. Chapon [ID139](#), B. Chargeishvili [ID156b](#), D.G. Charlton [ID21](#), C. Chauhan [ID137](#),
 Y. Che [ID115a](#), S. Chekanov [ID6](#), S.V. Chekulaev [ID163a](#), G.A. Chelkov [ID40,a](#), B. Chen [ID158](#), B. Chen [ID172](#),
 H. Chen [ID115a](#), H. Chen [ID30](#), J. Chen [ID145a](#), J. Chen [ID149](#), M. Chen [ID130](#), S. Chen [ID90](#), S.J. Chen [ID115a](#),
 X. Chen [ID145a](#), X. Chen [ID15,ag](#), C.L. Cheng [ID177](#), H.C. Cheng [ID65a](#), S. Cheong [ID150](#), A. Cheplakov [ID40](#),
 E. Cheremushkina [ID49](#), E. Cherepanova [ID118](#), R. Cherkaoui El Moursli [ID36e](#), E. Cheu [ID7](#), K. Cheung [ID66](#),
 L. Chevalier [ID139](#), V. Chiarella [ID54](#), G. Chiarelli [ID75a](#), N. Chiedde [ID105](#), G. Chiodini [ID71a](#),
 A.S. Chisholm [ID21](#), A. Chitan [ID28b](#), M. Chitishvili [ID170](#), M.V. Chizhov [ID40,t](#), K. Choi [ID11](#), Y. Chou [ID143](#),
 E.Y.S. Chow [ID117](#), K.L. Chu [ID176](#), M.C. Chu [ID65a](#), X. Chu [ID14,115c](#), Z. Chubinidze [ID54](#), J. Chudoba [ID135](#),
 J.J. Chwastowski [ID88](#), D. Cieri [ID113](#), K.M. Ciesla [ID87a](#), V. Cindro [ID96](#), A. Ciocio [ID18a](#), F. Ciroto [ID73a,73b](#),

Z.H. Citron ¹⁷⁶, M. Citterio ^{72a}, D.A. Ciubotaru ^{28b}, A. Clark ⁵⁷, P.J. Clark ⁵³, N. Clarke Hall ⁹⁹, C. Clarry ¹⁶², S.E. Clawson ⁴⁹, C. Clement ^{48a,48b}, Y. Coadou ¹⁰⁵, M. Cobal ^{70a,70c}, A. Coccaro ^{58b}, R.F. Coelho Barrue ^{134a}, R. Coelho Lopes De Sa ¹⁰⁶, S. Coelli ^{72a}, L.S. Colangeli ¹⁶², B. Cole ⁴³, P. Collado Soto ¹⁰², J. Collot ⁶¹, P. Conde Muiño ^{134a,134g}, M.P. Connell ^{34c}, S.H. Connell ^{34c}, E.I. Conroy ¹³⁰, F. Conventi ^{73a,ai}, H.G. Cooke ²¹, A.M. Cooper-Sarkar ¹³⁰, F.A. Corchia ^{24b,24a}, A. Cordeiro Oudot Choi ¹³¹, L.D. Corpe ⁴², M. Corradi ^{76a,76b}, F. Corriveau ^{107,ab}, A. Cortes-Gonzalez ¹⁹, M.J. Costa ¹⁷⁰, F. Costanza ⁴, D. Costanzo ¹⁴⁶, B.M. Cote ¹²³, J. Couthures ⁴, G. Cowan ⁹⁸, K. Cranmer ¹⁷⁷, L. Cremer ⁵⁰, D. Cremonini ^{24b,24a}, S. Crépe-Renaudin ⁶¹, F. Crescioli ¹³¹, M. Cristinziani ¹⁴⁸, M. Cristoforetti ^{79a,79b}, V. Croft ¹¹⁸, J.E. Crosby ¹²⁵, G. Crosetti ^{45b,45a}, A. Cueto ¹⁰², H. Cui ⁹⁹, Z. Cui ⁷, W.R. Cunningham ⁶⁰, F. Curcio ¹⁷⁰, J.R. Curran ⁵³, P. Czodrowski ³⁷, M.J. Da Cunha Sargedas De Sousa ^{58b,58a}, J.V. Da Fonseca Pinto ^{84b}, C. Da Via ¹⁰⁴, W. Dabrowski ^{87a}, T. Dado ³⁷, S. Dahbi ¹⁵⁵, T. Dai ¹⁰⁹, D. Dal Santo ²⁰, C. Dallapiccola ¹⁰⁶, M. Dam ⁴⁴, G. D'amen ³⁰, V. D'Amico ¹¹², J. Damp ¹⁰³, J.R. Dandoy ³⁵, D. Dannheim ³⁷, M. Danninger ¹⁴⁹, V. Dao ¹⁵², G. Darbo ^{58b}, S.J. Das ³⁰, F. Dattola ⁴⁹, S. D'Auria ^{72a,72b}, A. D'Avanzo ^{73a,73b}, T. Davidek ¹³⁷, I. Dawson ⁹⁷, H.A. Day-hall ¹³⁶, K. De ⁸, C. De Almeida Rossi ¹⁶², R. De Asmundis ^{73a}, N. De Biase ⁴⁹, S. De Castro ^{24b,24a}, N. De Groot ¹¹⁷, P. de Jong ¹¹⁸, H. De la Torre ¹¹⁹, A. De Maria ^{115a}, A. De Salvo ^{76a}, U. De Sanctis ^{77a,77b}, F. De Santis ^{71a,71b}, A. De Santo ¹⁵³, J.B. De Vivie De Regie ⁶¹, J. Debevc ⁹⁶, D.V. Dedovich ⁴⁰, J. Degens ⁹⁵, A.M. Deiana ⁴⁶, J. Del Peso ¹⁰², L. Delagrangé ¹³¹, F. Deliot ¹³⁹, C.M. Delitzsch ⁵⁰, M. Della Pietra ^{73a,73b}, D. Della Volpe ⁵⁷, A. Dell'Acqua ³⁷, L. Dell'Asta ^{72a,72b}, M. Delmastro ⁴, C.C. Delogu ¹⁰³, P.A. Delsart ⁶¹, S. Demers ¹⁷⁹, M. Demichev ⁴⁰, S.P. Denisov ³⁹, H. Denizli ^{22a,1}, L. D'Eramo ⁴², D. Derendarz ⁸⁸, F. Derue ¹³¹, P. Dervan ⁹⁵, K. Desch ²⁵, C. Deutsch ²⁵, F.A. Di Bello ^{58b,58a}, A. Di Ciaccio ^{77a,77b}, L. Di Ciaccio ⁴, A. Di Domenico ^{76a,76b}, C. Di Donato ^{73a,73b}, A. Di Girolamo ³⁷, G. Di Gregorio ³⁷, A. Di Luca ^{79a,79b}, B. Di Micco ^{78a,78b}, R. Di Nardo ^{78a,78b}, K.F. Di Petrillo ⁴¹, M. Diamantopoulou ³⁵, F.A. Dias ¹¹⁸, T. Dias Do Vale ¹⁴⁹, M.A. Diaz ^{141a,141b}, A.R. Didenko ⁴⁰, M. Didenko ¹⁷⁰, S.D. Diefenbacher ^{18a}, E.B. Diehl ¹⁰⁹, S. Díez Cornell ⁴⁹, C. Diez Pardos ¹⁴⁸, C. Dimitriadi ¹⁵¹, A. Dimitrievska ²¹, A. Dimri ¹⁵², J. Dingfelder ²⁵, T. Dingley ¹³⁰, I-M. Dinu ^{28b}, S.J. Dittmeier ^{64b}, F. Dittus ³⁷, M. Divisek ¹³⁷, B. Dixit ⁹⁵, F. Djama ¹⁰⁵, T. Djobava ^{156b}, C. Doglioni ^{104,101}, A. Dohnalova ^{29a}, Z. Dolezal ¹³⁷, K. Domijan ^{87a}, K.M. Dona ⁴¹, M. Donadelli ^{84d}, B. Dong ¹¹⁰, J. Donini ⁴², A. D'Onofrio ^{73a,73b}, M. D'Onofrio ⁹⁵, J. Dopke ¹³⁸, A. Doria ^{73a}, N. Dos Santos Fernandes ^{134a}, P. Dougan ¹⁰⁴, M.T. Dova ⁹³, A.T. Doyle ⁶⁰, M.A. Draguet ¹³⁰, M.P. Drescher ⁵⁶, E. Dreyer ¹⁷⁶, I. Drivas-koulouris ¹⁰, M. Drnevich ¹²¹, M. Drozdova ⁵⁷, D. Du ⁶³, T.A. du Pree ¹¹⁸, F. Dubinin ⁴⁰, M. Dubovsky ^{29a}, E. Duchovni ¹⁷⁶, G. Duckeck ¹¹², P.K. Duckett ⁹⁹, O.A. Ducu ^{28b}, D. Duda ⁵³, A. Dudarev ³⁷, E.R. Duden ²⁷, M. D'uffizi ¹⁰⁴, L. Duflost ⁶⁷, M. Dührssen ³⁷, I. Duminica ^{28g}, A.E. Dumitriu ^{28b}, M. Dunford ^{64a}, S. Dungs ⁵⁰, K. Dunne ^{48a,48b}, A. Duperrin ¹⁰⁵, H. Duran Yildiz ^{3a}, M. Düren ⁵⁹, A. Durglishvili ^{156b}, D. Duvnjak ³⁵, B.L. Dwyer ¹¹⁹, G.I. Dyckes ^{18a}, M. Dyndal ^{87a}, B.S. Dziedzic ³⁷, Z.O. Earnshaw ¹⁵³, G.H. Eberwein ¹³⁰, B. Eckerova ^{29a}, S. Eggebrecht ⁵⁶, E. Egidio Purcino De Souza ^{84e}, G. Eigen ¹⁷, K. Einsweiler ^{18a}, T. Ekelof ¹⁶⁸, P.A. Ekman ¹⁰¹, S. El Farkh ^{36b}, Y. El Ghazali ⁶³, H. El Jarrari ³⁷, A. El Moussaouy ^{36a}, V. Ellajosyula ¹⁶⁸, M. Ellert ¹⁶⁸, F. Ellinghaus ¹⁷⁸, N. Ellis ³⁷, J. Elmsheuser ³⁰, M. Elsayy ^{120a}, M. Elsing ³⁷, D. Emelianov ¹³⁸, Y. Enari ⁸⁵, I. Ene ^{18a}, S. Epari ¹³, D. Ernani Martins Neto ⁸⁸, M. Errenst ¹⁷⁸, M. Escalier ⁶⁷, C. Escobar ¹⁷⁰, E. Etzion ¹⁵⁸, G. Evans ^{134a,134b}, H. Evans ⁶⁹, L.S. Evans ⁹⁸, A. Ezhilov ³⁹, S. Ezzarqtouni ^{36a}, F. Fabbri ^{24b,24a}, L. Fabbri ^{24b,24a}, G. Facini ⁹⁹, V. Fadeyev ¹⁴⁰, R.M. Fakhruddinov ³⁹,

D. Fakoudis [ID103](#), S. Falciano [ID76a](#), L.F. Falda Ulhoa Coelho [ID134a](#), F. Fallavollita [ID113](#),
 G. Falsetti [ID45b,45a](#), J. Faltova [ID137](#), C. Fan [ID169](#), K.Y. Fan [ID65b](#), Y. Fan [ID14](#), Y. Fang [ID14,115c](#),
 M. Fanti [ID72a,72b](#), M. Faraj [ID70a,70b](#), Z. Farazpay [ID100](#), A. Farbin [ID8](#), A. Farilla [ID78a](#), T. Farooque [ID110](#),
 J.N. Farr [ID179](#), S.M. Farrington [ID138,53](#), F. Fassi [ID36e](#), D. Fassouliotis [ID9](#), L. Fayard [ID67](#), P. Federic [ID137](#),
 P. Federicova [ID135](#), O.L. Fedin [ID39,a](#), M. Feickert [ID177](#), L. Feligioni [ID105](#), D.E. Fellers [ID18a](#),
 C. Feng [ID144a](#), Z. Feng [ID118](#), M.J. Fenton [ID166](#), L. Ferencz [ID49](#), P. Fernandez Martinez [ID68](#),
 M.J.V. Fernoux [ID105](#), J. Ferrando [ID94](#), A. Ferrari [ID168](#), P. Ferrari [ID118,117](#), R. Ferrari [ID74a](#), D. Ferrere [ID57](#),
 C. Ferretti [ID109](#), M.P. Fewell [ID1](#), D. Fiacco [ID76a,76b](#), F. Fiedler [ID103](#), P. Fiedler [ID136](#), S. Filimonov [ID39](#),
 A. Filipčić [ID96](#), E.K. Filmer [ID163a](#), F. Filthaut [ID117](#), M.C.N. Fiolhais [ID134a,134c,c](#), L. Fiorini [ID170](#),
 W.C. Fisher [ID110](#), T. Fitschen [ID104](#), P.M. Fitzhugh [ID139](#), I. Fleck [ID148](#), P. Fleischmann [ID109](#), T. Flick [ID178](#),
 M. Flores [ID34d,ae](#), L.R. Flores Castillo [ID65a](#), L. Flores Sanz De Acedo [ID37](#), F.M. Follega [ID79a,79b](#),
 N. Fomin [ID33](#), J.H. Foo [ID162](#), A. Formica [ID139](#), A.C. Forti [ID104](#), E. Fortin [ID37](#), A.W. Fortman [ID18a](#),
 L. Fountas [ID9j](#), D. Fournier [ID67](#), H. Fox [ID94](#), P. Francavilla [ID75a,75b](#), S. Francescato [ID62](#),
 S. Franchellucci [ID57](#), M. Franchini [ID24b,24a](#), S. Franchino [ID64a](#), D. Francis [ID37](#), L. Franco [ID117](#),
 V. Franco Lima [ID37](#), L. Franconi [ID49](#), M. Franklin [ID62](#), G. Frattari [ID27](#), Y.Y. Frid [ID158](#), J. Friend [ID60](#),
 N. Fritzsche [ID37](#), A. Froch [ID57](#), D. Froidevaux [ID37](#), J.A. Frost [ID130](#), Y. Fu [ID110](#),
 S. Fuenzalida Garrido [ID141f](#), M. Fujimoto [ID105](#), K.Y. Fung [ID65a](#), E. Furtado De Simas Filho [ID84e](#),
 M. Furukawa [ID160](#), J. Fuster [ID170](#), A. Gaa [ID56](#), A. Gabrielli [ID24b,24a](#), A. Gabrielli [ID162](#), P. Gadow [ID37](#),
 G. Gagliardi [ID58b,58a](#), L.G. Gagnon [ID18a](#), S. Gaid [ID89b](#), S. Galantzan [ID158](#), J. Gallagher [ID1](#),
 E.J. Gallas [ID130](#), A.L. Gallen [ID168](#), B.J. Gallop [ID138](#), K.K. Gan [ID123](#), S. Ganguly [ID160](#), Y. Gao [ID53](#),
 A. Garabaglu [ID143](#), F.M. Garay Walls [ID141a,141b](#), B. Garcia [ID30](#), C. García [ID170](#), A. Garcia Alonso [ID118](#),
 A.G. Garcia Caffaro [ID179](#), J.E. García Navarro [ID170](#), M. Garcia-Sciveres [ID18a](#), G.L. Gardner [ID132](#),
 R.W. Gardner [ID41](#), N. Garelli [ID165](#), R.B. Garg [ID150](#), J.M. Gargan [ID53](#), C.A. Garner [ID162](#), C.M. Garvey [ID34a](#),
 V.K. Gassmann [ID165](#), G. Gaudio [ID74a](#), V. Gautam [ID13](#), P. Gauzzi [ID76a,76b](#), J. Gavranovic [ID96](#),
 I.L. Gavrilenko [ID134a](#), A. Gavriluk [ID39](#), C. Gay [ID171](#), G. Gaycken [ID127](#), E.N. Gazis [ID10](#), A. Gekow [ID123](#),
 C. Gemme [ID58b](#), M.H. Genest [ID61](#), A.D. Gentry [ID116](#), S. George [ID98](#), W.F. George [ID21](#), T. Gerialis [ID47](#),
 A.A. Gerwin [ID124](#), P. Gessinger-Befurt [ID37](#), M.E. Geyik [ID178](#), M. Ghani [ID174](#), K. Ghorbanian [ID97](#),
 A. Ghosal [ID148](#), A. Ghosh [ID166](#), A. Ghosh [ID7](#), B. Giacobbe [ID24b](#), S. Giagu [ID76a,76b](#), T. Giani [ID118](#),
 A. Giannini [ID63](#), S.M. Gibson [ID98](#), M. Gignac [ID140](#), D.T. Gil [ID87b](#), A.K. Gilbert [ID87a](#), B.J. Gilbert [ID43](#),
 D. Gillberg [ID35](#), G. Gilles [ID118](#), L. Ginabat [ID131](#), D.M. Gingrich [ID2,ah](#), M.P. Giordani [ID70a,70c](#),
 P.F. Giraud [ID139](#), G. Giugliarelli [ID70a,70c](#), D. Giugni [ID72a](#), F. Giuli [ID77a,77b](#), I. Gkialas [ID9j](#),
 L.K. Gladilin [ID39](#), C. Glasman [ID102](#), G. Glemža [ID49](#), M. Glisic [ID127](#), I. Gnesi [ID45b](#), Y. Go [ID30](#),
 M. Goblirsch-Kolb [ID37](#), B. Gocke [ID50](#), D. Godin [ID111](#), B. Gokturk [ID22a](#), S. Goldfarb [ID108](#), T. Golling [ID57](#),
 M.G.D. Gololo [ID34c](#), D. Golubkov [ID39](#), J.P. Gombas [ID110](#), A. Gomes [ID134a,134b](#), G. Gomes Da Silva [ID148](#),
 A.J. Gomez Delegido [ID170](#), R. Gonçalo [ID134a](#), L. Gonella [ID21](#), A. Gongadze [ID156c](#), F. Gonnella [ID21](#),
 J.L. Gonski [ID150](#), R.Y. González Andana [ID53](#), S. González de la Hoz [ID170](#), C. Gonzalez Renteria [ID18a](#),
 M.V. Gonzalez Rodrigues [ID49](#), R. Gonzalez Suarez [ID168](#), S. Gonzalez-Sevilla [ID57](#), L. Goossens [ID37](#),
 B. Gorini [ID37](#), E. Gorini [ID71a,71b](#), A. Gorišek [ID96](#), T.C. Gosart [ID132](#), A.T. Goshaw [ID52](#), M.I. Gostkin [ID40](#),
 S. Goswami [ID125](#), C.A. Gottardo [ID37](#), S.A. Gotz [ID112](#), M. Gouighri [ID36b](#), A.G. Goussiou [ID143](#),
 N. Govender [ID34c](#), R.P. Grabarczyk [ID130](#), I. Grabowska-Bold [ID87a](#), K. Graham [ID35](#), E. Gramstad [ID129](#),
 S. Grancagnolo [ID71a,71b](#), C.M. Grant [ID1,139](#), P.M. Gravila [ID28f](#), F.G. Gravili [ID71a,71b](#), H.M. Gray [ID18a](#),
 M. Greco [ID113](#), M.J. Green [ID1](#), C. Grefe [ID25](#), A.S. Grefsrud [ID17](#), I.M. Gregor [ID49](#), K.T. Greif [ID166](#),
 P. Grenier [ID150](#), S.G. Grewe [ID113](#), A.A. Grillo [ID140](#), K. Grimm [ID32](#), S. Grinstein [ID13,x](#), J.-F. Grivaz [ID67](#),
 E. Gross [ID176](#), J. Grosse-Knetter [ID56](#), L. Guan [ID109](#), G. Guerrieri [ID37](#), R. Gugel [ID103](#), J.A.M. Guhit [ID109](#),
 A. Guida [ID19](#), E. Guilloton [ID174](#), S. Guindon [ID37](#), F. Guo [ID14,115c](#), J. Guo [ID145a](#), L. Guo [ID49](#),
 L. Guo [ID115b,v](#), Y. Guo [ID109](#), A. Gupta [ID50](#), R. Gupta [ID133](#), S. Gurbuz [ID25](#), S.S. Gurdasani [ID49](#),
 G. Gustavino [ID76a,76b](#), P. Gutierrez [ID124](#), L.F. Gutierrez Zagazeta [ID132](#), M. Gutsche [ID51](#), C. Gutschow [ID99](#),

C. Gwenlan [id](#)¹³⁰, C.B. Gwilliam [id](#)⁹⁵, E.S. Haaland [id](#)¹²⁹, A. Haas [id](#)¹²¹, M. Habedank [id](#)⁶⁰,
 C. Haber [id](#)^{18a}, H.K. Hadavand [id](#)⁸, A. Haddad [id](#)⁴², A. Hadeef [id](#)⁵¹, A.I. Hagan [id](#)⁹⁴, J.J. Hahn [id](#)¹⁴⁸,
 E.H. Haines [id](#)⁹⁹, M. Haleem [id](#)¹⁷³, J. Haley [id](#)¹²⁵, G.D. Hallowell [id](#)¹⁰⁵, L. Halser [id](#)²⁰, K. Hamano [id](#)¹⁷²,
 M. Hamer [id](#)²⁵, S.E.D. Hammoud [id](#)⁶⁷, E.J. Hampshire [id](#)⁹⁸, J. Han [id](#)^{144a}, L. Han [id](#)^{115a}, L. Han [id](#)⁶³,
 S. Han [id](#)^{18a}, K. Hanagaki [id](#)⁸⁵, M. Hance [id](#)¹⁴⁰, D.A. Hangal [id](#)⁴³, H. Hanif [id](#)¹⁴⁹, M.D. Hank [id](#)¹³²,
 J.B. Hansen [id](#)⁴⁴, P.H. Hansen [id](#)⁴⁴, D. Harada [id](#)⁵⁷, T. Harenberg [id](#)¹⁷⁸, S. Harkusha [id](#)¹⁸⁰,
 M.L. Harris [id](#)¹⁰⁶, Y.T. Harris [id](#)²⁵, J. Harrison [id](#)¹³, N.M. Harrison [id](#)¹²³, P.F. Harrison [id](#)¹⁷⁴,
 N.M. Hartman [id](#)¹¹³, N.M. Hartmann [id](#)¹¹², R.Z. Hasan [id](#)^{98,138}, Y. Hasegawa [id](#)¹⁴⁷, F. Haslbeck [id](#)¹³⁰,
 S. Hassan [id](#)¹⁷, R. Hauser [id](#)¹¹⁰, C.M. Hawkes [id](#)²¹, R.J. Hawkings [id](#)³⁷, Y. Hayashi [id](#)¹⁶⁰, D. Hayden [id](#)¹¹⁰,
 C. Hayes [id](#)¹⁰⁹, R.L. Hayes [id](#)¹¹⁸, C.P. Hays [id](#)¹³⁰, J.M. Hays [id](#)⁹⁷, H.S. Hayward [id](#)⁹⁵, F. He [id](#)⁶³,
 M. He [id](#)^{14,115c}, Y. He [id](#)⁴⁹, Y. He [id](#)⁹⁹, N.B. Heatley [id](#)⁹⁷, V. Hedberg [id](#)¹⁰¹, A.L. Heggelund [id](#)¹²⁹,
 C. Heidegger [id](#)⁵⁵, K.K. Heidegger [id](#)⁵⁵, J. Heilman [id](#)³⁵, S. Heim [id](#)⁴⁹, T. Heim [id](#)^{18a}, J.G. Heinlein [id](#)¹³²,
 J.J. Heinrich [id](#)¹²⁷, L. Heinrich [id](#)^{113,af}, J. Hejbal [id](#)¹³⁵, A. Held [id](#)¹⁷⁷, S. Hellesund [id](#)¹⁷,
 C.M. Helling [id](#)¹⁷¹, S. Hellman [id](#)^{48a,48b}, L. Henkelmann [id](#)³³, A.M. Henriques Correia [id](#)³⁷, H. Herde [id](#)¹⁰¹,
 Y. Hernández Jiménez [id](#)¹⁵², L.M. Herrmann [id](#)²⁵, T. Herrmann [id](#)⁵¹, G. Herten [id](#)⁵⁵, R. Hertenberger [id](#)¹¹²,
 L. Hervas [id](#)³⁷, M.E. Hesping [id](#)¹⁰³, N.P. Hessey [id](#)^{163a}, J. Hessler [id](#)¹¹³, M. Hidaoui [id](#)^{36b}, N. Hidic [id](#)¹³⁷,
 E. Hill [id](#)¹⁶², S.J. Hillier [id](#)²¹, J.R. Hinds [id](#)¹¹⁰, F. Hinterkeuser [id](#)²⁵, M. Hirose [id](#)¹²⁸, S. Hirose [id](#)¹⁶⁴,
 D. Hirschbuehl [id](#)¹⁷⁸, T.G. Hitchings [id](#)¹⁰⁴, B. Hiti [id](#)⁹⁶, J. Hobbs [id](#)¹⁵², R. Hobincu [id](#)^{28e}, N. Hod [id](#)¹⁷⁶,
 M.C. Hodgkinson [id](#)¹⁴⁶, B.H. Hodgkinson [id](#)¹³⁰, A. Hoecker [id](#)³⁷, D.D. Hofer [id](#)¹⁰⁹, J. Hofer [id](#)¹⁷⁰,
 M. Holzbock [id](#)³⁷, L.B.A.H. Hommels [id](#)³³, B.P. Honan [id](#)¹⁰⁴, J.J. Hong [id](#)⁶⁹, J. Hong [id](#)^{145a},
 T.M. Hong [id](#)¹³³, B.H. Hooberman [id](#)¹⁶⁹, W.H. Hopkins [id](#)⁶, M.C. Hoppesch [id](#)¹⁶⁹, Y. Horii [id](#)¹¹⁴,
 M.E. Horstmann [id](#)¹¹³, S. Hou [id](#)¹⁵⁵, M.R. Housenga [id](#)¹⁶⁹, A.S. Howard [id](#)⁹⁶, J. Howarth [id](#)⁶⁰, J. Hoya [id](#)⁶,
 M. Hrabovsky [id](#)¹²⁶, T. Hryn'ova [id](#)⁴, P.J. Hsu [id](#)⁶⁶, S.-C. Hsu [id](#)¹⁴³, T. Hsu [id](#)⁶⁷, M. Hu [id](#)^{18a}, Q. Hu [id](#)⁶³,
 S. Huang [id](#)³³, X. Huang [id](#)^{14,115c}, Y. Huang [id](#)¹³⁷, Y. Huang [id](#)^{115b}, Y. Huang [id](#)¹⁰³, Y. Huang [id](#)¹⁴,
 Z. Huang [id](#)¹⁰⁴, Z. Hubacek [id](#)¹³⁶, M. Huebner [id](#)²⁵, F. Huegging [id](#)²⁵, T.B. Huffman [id](#)¹³⁰,
 M. Hufnagel Maranha De Faria [id](#)^{84a}, C.A. Hugli [id](#)⁴⁹, M. Huhtinen [id](#)³⁷, S.K. Huiberts [id](#)¹⁷,
 R. Hulsken [id](#)¹⁰⁷, C.E. Hultquist [id](#)^{18a}, N. Huseynov [id](#)^{12,g}, J. Huston [id](#)¹¹⁰, J. Huth [id](#)⁶², R. Hyneman [id](#)⁷,
 G. Iacobucci [id](#)⁵⁷, G. Iakovidis [id](#)³⁰, L. Iconomidou-Fayard [id](#)⁶⁷, J.P. Iddon [id](#)³⁷, P. Iengo [id](#)^{73a,73b},
 R. Iguchi [id](#)¹⁶⁰, Y. Iiyama [id](#)¹⁶⁰, T. Iizawa [id](#)¹³⁰, Y. Ikegami [id](#)⁸⁵, D. Iliadis [id](#)¹⁵⁹, N. Ilic [id](#)¹⁶²,
 H. Imam [id](#)^{84c}, G. Inacio Goncalves [id](#)^{84d}, S.A. Infante Cabanas [id](#)^{141c}, T. Ingebretsen Carlson [id](#)^{48a,48b},
 J.M. Inglis [id](#)⁹⁷, G. Introzzi [id](#)^{74a,74b}, M. Iodice [id](#)^{78a}, V. Ippolito [id](#)^{76a,76b}, R.K. Irwin [id](#)⁹⁵, M. Ishino [id](#)¹⁶⁰,
 W. Islam [id](#)¹⁷⁷, C. Issever [id](#)¹⁹, S. Istin [id](#)^{22a,am}, H. Ito [id](#)¹⁷⁵, R. Iuppa [id](#)^{79a,79b}, A. Ivina [id](#)¹⁷⁶, V. Izzo [id](#)^{73a},
 P. Jacka [id](#)¹³⁵, P. Jackson [id](#)¹, P. Jain [id](#)⁴⁹, K. Jakobs [id](#)⁵⁵, T. Jakoubek [id](#)¹⁷⁶, J. Jamieson [id](#)⁶⁰, W. Jang [id](#)¹⁶⁰,
 S. Jankovych [id](#)¹³⁷, M. Javurkova [id](#)¹⁰⁶, P. Jawahar [id](#)¹⁰⁴, L. Jeanty [id](#)¹²⁷, J. Jejelava [id](#)^{156a}, P. Jenni [id](#)^{55,f},
 C.E. Jessiman [id](#)³⁵, C. Jia [id](#)^{144a}, H. Jia [id](#)¹⁷¹, J. Jia [id](#)¹⁵², X. Jia [id](#)^{14,115c}, Z. Jia [id](#)^{115a}, C. Jiang [id](#)⁵³,
 Q. Jiang [id](#)^{65b}, S. Jiggins [id](#)⁴⁹, J. Jimenez Pena [id](#)¹³, S. Jin [id](#)^{115a}, A. Jinaru [id](#)^{28b}, O. Jinnouchi [id](#)¹⁴²,
 P. Johansson [id](#)¹⁴⁶, K.A. Johns [id](#)⁷, J.W. Johnson [id](#)¹⁴⁰, F.A. Jolly [id](#)⁴⁹, D.M. Jones [id](#)¹⁵³, E. Jones [id](#)⁴⁹,
 K.S. Jones [id](#)⁸, P. Jones [id](#)³³, R.W.L. Jones [id](#)⁹⁴, T.J. Jones [id](#)⁹⁵, H.L. Joos [id](#)^{56,37}, R. Joshi [id](#)¹²³,
 J. Jovicevic [id](#)¹⁶, X. Ju [id](#)^{18a}, J.J. Junggeburth [id](#)³⁷, T. Junkermann [id](#)^{64a}, A. Juste Rozas [id](#)^{13,x},
 M.K. Juzek [id](#)⁸⁸, S. Kabana [id](#)^{141e}, A. Kaczmarzka [id](#)⁸⁸, M. Kado [id](#)¹¹³, H. Kagan [id](#)¹²³, M. Kagan [id](#)¹⁵⁰,
 A. Kahn [id](#)¹³², C. Kahra [id](#)¹⁰³, T. Kaji [id](#)¹⁶⁰, E. Kajomovitz [id](#)¹⁵⁷, N. Kakati [id](#)¹⁷⁶, I. Kalaitzidou [id](#)⁵⁵,
 N.J. Kang [id](#)¹⁴⁰, D. Kar [id](#)^{34g}, K. Karava [id](#)¹³⁰, E. Karentzos [id](#)²⁵, O. Karkout [id](#)¹¹⁸, S.N. Karpov [id](#)⁴⁰,
 Z.M. Karpova [id](#)⁴⁰, V. Kartvelishvili [id](#)⁹⁴, A.N. Karyukhin [id](#)³⁹, E. Kasimi [id](#)¹⁵⁹, J. Katzy [id](#)⁴⁹,
 S. Kaur [id](#)³⁵, K. Kawade [id](#)¹⁴⁷, M.P. Kawale [id](#)¹²⁴, C. Kawamoto [id](#)⁹⁰, T. Kawamoto [id](#)⁶³, E.F. Kay [id](#)³⁷,
 F.I. Kaya [id](#)¹⁶⁵, S. Kazakos [id](#)¹¹⁰, V.F. Kazanin [id](#)³⁹, Y. Ke [id](#)¹⁵², J.M. Keaveney [id](#)^{34a}, R. Keeler [id](#)¹⁷²,
 G.V. Kehris [id](#)⁶², J.S. Keller [id](#)³⁵, J.J. Kempster [id](#)¹⁵³, O. Kepka [id](#)¹³⁵, J. Kerr [id](#)^{163b}, B.P. Kerridge [id](#)¹³⁸,
 B.P. Kerševan [id](#)⁹⁶, L. Keszeghova [id](#)^{29a}, R.A. Khan [id](#)¹³³, A. Khanov [id](#)¹²⁵, A.G. Kharlamov [id](#)³⁹,

T. Kharlamova [ID³⁹](#), E.E. Khoda [ID¹⁴³](#), M. Kholodenko [ID^{134a}](#), T.J. Khoo [ID¹⁹](#), G. Khoriauli [ID¹⁷³](#), J. Khubua [ID^{156b,*}](#), Y.A.R. Khwaira [ID¹³¹](#), B. Kibirige^{34g}, D. Kim [ID⁶](#), D.W. Kim [ID^{48a,48b}](#), Y.K. Kim [ID⁴¹](#), N. Kimura [ID⁹⁹](#), M.K. Kingston [ID⁵⁶](#), A. Kirchhoff [ID⁵⁶](#), C. Kirfel [ID²⁵](#), F. Kirfel [ID²⁵](#), J. Kirk [ID¹³⁸](#), A.E. Kiryunin [ID¹¹³](#), S. Kita [ID¹⁶⁴](#), C. Kitsaki [ID¹⁰](#), O. Kivernyk [ID²⁵](#), M. Klassen [ID¹⁶⁵](#), C. Klein [ID³⁵](#), L. Klein [ID¹⁷³](#), M.H. Klein [ID⁴⁶](#), S.B. Klein [ID⁵⁷](#), U. Klein [ID⁹⁵](#), A. Klimentov [ID³⁰](#), T. Klioutchnikova [ID³⁷](#), P. Kluit [ID¹¹⁸](#), S. Kluth [ID¹¹³](#), E. Kneringer [ID⁸⁰](#), T.M. Knight [ID¹⁶²](#), A. Knue [ID⁵⁰](#), M. Kobel [ID⁵¹](#), D. Kobylanskii [ID¹⁷⁶](#), S.F. Koch [ID¹³⁰](#), M. Kocian [ID¹⁵⁰](#), P. Kodyš [ID¹³⁷](#), D.M. Koeck [ID¹²⁷](#), P.T. Koenig [ID²⁵](#), T. Koffas [ID³⁵](#), O. Kolay [ID⁵¹](#), I. Koletsou [ID⁴](#), T. Komarek [ID⁸⁸](#), K. Köneke [ID⁵⁶](#), A.X.Y. Kong [ID¹](#), T. Kono [ID¹²²](#), N. Konstantinidis [ID⁹⁹](#), P. Kontaxakis [ID⁵⁷](#), B. Konya [ID¹⁰¹](#), R. Kopeliansky [ID⁴³](#), S. Koperny [ID^{87a}](#), K. Korcyl [ID⁸⁸](#), K. Kordas [ID^{159,e}](#), A. Korn [ID⁹⁹](#), S. Korn [ID⁵⁶](#), I. Korolkov [ID¹³](#), N. Korotkova [ID³⁹](#), B. Kortman [ID¹¹⁸](#), O. Kortner [ID¹¹³](#), S. Kortner [ID¹¹³](#), W.H. Kostecka [ID¹¹⁹](#), V.V. Kostyukhin [ID¹⁴⁸](#), A. Kotsokechagia [ID³⁷](#), A. Kotwal [ID⁵²](#), A. Koulouris [ID³⁷](#), A. Kourkoumeli-Charalampidi [ID^{74a,74b}](#), C. Kourkoumelis [ID⁹](#), E. Kourlitis [ID¹¹³](#), O. Kovanda [ID¹²⁷](#), R. Kowalewski [ID¹⁷²](#), W. Kozanecki [ID¹²⁷](#), A.S. Kozhin [ID³⁹](#), V.A. Kramarenko [ID³⁹](#), G. Kramberger [ID⁹⁶](#), P. Kramer [ID²⁵](#), M.W. Krasny [ID¹³¹](#), A. Krasznahorkay [ID¹⁰⁶](#), A.C. Kraus [ID¹¹⁹](#), J.W. Kraus [ID¹⁷⁸](#), J.A. Kremer [ID⁴⁹](#), N.B. Krengel [ID¹⁴⁸](#), T. Kresse [ID⁵¹](#), L. Kretschmann [ID¹⁷⁸](#), J. Kretzschmar [ID⁹⁵](#), K. Kreul [ID¹⁹](#), P. Krieger [ID¹⁶²](#), K. Krizka [ID²¹](#), K. Kroeninger [ID⁵⁰](#), H. Kroha [ID¹¹³](#), J. Kroll [ID¹³⁵](#), J. Kroll [ID¹³²](#), K.S. Krowpman [ID¹¹⁰](#), U. Kruchonak [ID⁴⁰](#), H. Krüger [ID²⁵](#), N. Krumnack⁸², M.C. Kruse [ID⁵²](#), O. Kuchinskaia [ID³⁹](#), S. Kuday [ID^{3a}](#), S. Kuehn [ID³⁷](#), R. Kuesters [ID⁵⁵](#), T. Kuhl [ID⁴⁹](#), V. Kukhtin [ID⁴⁰](#), Y. Kulchitsky [ID⁴⁰](#), S. Kuleshov [ID^{141d,141b}](#), M. Kumar [ID^{34g}](#), N. Kumari [ID⁴⁹](#), P. Kumari [ID^{163b}](#), A. Kupco [ID¹³⁵](#), T. Kupfer⁵⁰, A. Kupich [ID³⁹](#), O. Kuprash [ID⁵⁵](#), H. Kurashige [ID⁸⁶](#), L.L. Kurchaninov [ID^{163a}](#), O. Kurdysh [ID⁴](#), Y.A. Kurochkin [ID³⁸](#), A. Kurova [ID³⁹](#), M. Kuze [ID¹⁴²](#), A.K. Kvam [ID¹⁰⁶](#), J. Kvita [ID¹²⁶](#), N.G. Kyriacou [ID¹⁰⁹](#), L.A.O. Laatu [ID¹⁰⁵](#), C. Lacasta [ID¹⁷⁰](#), F. Lacava [ID^{76a,76b}](#), H. Lacker [ID¹⁹](#), D. Lacour [ID¹³¹](#), N.N. Lad [ID⁹⁹](#), E. Ladygin [ID⁴⁰](#), A. Lafarge [ID⁴²](#), B. Laforge [ID¹³¹](#), T. Lagouri [ID¹⁷⁹](#), F.Z. Lahbabi [ID^{36a}](#), S. Lai [ID⁵⁶](#), J.E. Lambert [ID¹⁷²](#), S. Lammers [ID⁶⁹](#), W. Lampl [ID⁷](#), C. Lampoudis [ID^{159,e}](#), G. Lamprinoudis [ID¹⁰³](#), A.N. Lancaster [ID¹¹⁹](#), E. Lançon [ID³⁰](#), U. Landgraf [ID⁵⁵](#), M.P.J. Landon [ID⁹⁷](#), V.S. Lang [ID⁵⁵](#), O.K.B. Langrekken [ID¹²⁹](#), A.J. Lankford [ID¹⁶⁶](#), F. Lanni [ID³⁷](#), K. Lantzsich [ID²⁵](#), A. Lanza [ID^{74a}](#), M. Lanzac Berrocal [ID¹⁷⁰](#), J.F. Laporte [ID¹³⁹](#), T. Lari [ID^{72a}](#), D. Larsen [ID¹⁷](#), F. Lasagni Manghi [ID^{24b}](#), M. Lassnig [ID³⁷](#), V. Latonova [ID¹³⁵](#), S.D. Lawlor [ID¹⁴⁶](#), Z. Lawrence [ID¹⁰⁴](#), R. Lazaridou¹⁷⁴, M. Lazzaroni [ID^{72a,72b}](#), H.D.M. Le [ID¹¹⁰](#), E.M. Le Boulicaut [ID¹⁷⁹](#), L.T. Le Pottier [ID^{18a}](#), B. Leban [ID^{24b,24a}](#), M. LeBlanc [ID¹⁰⁴](#), F. Ledroit-Guillon [ID⁶¹](#), S.C. Lee [ID¹⁵⁵](#), T.F. Lee [ID⁹⁵](#), L.L. Leeuw [ID^{34c,ak}](#), M. Lefebvre [ID¹⁷²](#), C. Leggett [ID^{18a}](#), G. Lehmann Miotto [ID³⁷](#), M. Leigh [ID⁵⁷](#), W.A. Leight [ID¹⁰⁶](#), W. Leinonen [ID¹¹⁷](#), A. Leisos [ID^{159,u}](#), M.A.L. Leite [ID^{84c}](#), C.E. Leitgeb [ID¹⁹](#), R. Leitner [ID¹³⁷](#), K.J.C. Leney [ID⁴⁶](#), T. Lenz [ID²⁵](#), S. Leone [ID^{75a}](#), C. Leonidopoulos [ID⁵³](#), A. Leopold [ID¹⁵¹](#), J.H. Lepage Bourbonnais [ID³⁵](#), R. Les [ID¹¹⁰](#), C.G. Lester [ID³³](#), M. Levchenko [ID³⁹](#), J. Levêque [ID⁴](#), L.J. Levinson [ID¹⁷⁶](#), G. Levrini [ID^{24b,24a}](#), M.P. Lewicki [ID⁸⁸](#), C. Lewis [ID¹⁴³](#), D.J. Lewis [ID⁴](#), L. Lewitt [ID¹⁴⁶](#), A. Li [ID³⁰](#), B. Li [ID^{144a}](#), C. Li¹⁰⁹, C-Q. Li [ID¹¹³](#), H. Li [ID⁶³](#), H. Li [ID^{144a}](#), H. Li [ID¹⁰⁴](#), H. Li [ID¹⁵](#), H. Li⁶³, H. Li [ID^{144a}](#), J. Li [ID^{145a}](#), K. Li [ID¹⁴](#), L. Li [ID^{145a}](#), R. Li [ID¹⁷⁹](#), S. Li [ID^{14,115c}](#), S. Li [ID^{145b,145a,d}](#), T. Li [ID⁵](#), X. Li [ID¹⁰⁷](#), Z. Li [ID¹⁶⁰](#), Z. Li [ID^{14,115c}](#), Z. Li [ID⁶³](#), S. Liang [ID^{14,115c}](#), Z. Liang [ID¹⁴](#), M. Liberatore [ID¹³⁹](#), B. Liberti [ID^{77a}](#), K. Lie [ID^{65c}](#), J. Lieber Marin [ID^{84e}](#), H. Lien [ID⁶⁹](#), H. Lin [ID¹⁰⁹](#), L. Linden [ID¹¹²](#), R.E. Lindley [ID⁷](#), J.H. Lindon [ID²](#), J. Ling [ID⁶²](#), E. Lipeles [ID¹³²](#), A. Lipniacka [ID¹⁷](#), A. Lister [ID¹⁷¹](#), J.D. Little [ID⁶⁹](#), B. Liu [ID¹⁴](#), B.X. Liu [ID^{115b}](#), D. Liu [ID^{145b,145a}](#), E.H.L. Liu [ID²¹](#), J.K.K. Liu [ID³³](#), K. Liu [ID^{145b}](#), K. Liu [ID^{145b,145a}](#), M. Liu [ID⁶³](#), M.Y. Liu [ID⁶³](#), P. Liu [ID¹⁴](#), Q. Liu [ID^{145b,143,145a}](#), X. Liu [ID⁶³](#), X. Liu [ID^{144a}](#), Y. Liu [ID^{115b,115c}](#), Y.L. Liu [ID^{144a}](#), Y.W. Liu [ID⁶³](#), S.L. Lloyd [ID⁹⁷](#), E.M. Lobodzinska [ID⁴⁹](#), P. Loch [ID⁷](#), E. Lodhi [ID¹⁶²](#), T. Lohse [ID¹⁹](#), K. Lohwasser [ID¹⁴⁶](#), E. Loiacono [ID⁴⁹](#), J.D. Lomas [ID²¹](#), J.D. Long [ID⁴³](#), I. Longarini [ID¹⁶⁶](#), R. Longo [ID¹⁶⁹](#), A. Lopez Solis [ID⁴⁹](#), N.A. Lopez-canelas [ID⁷](#), N. Lorenzo Martinez [ID⁴](#), A.M. Lory [ID¹¹²](#), M. Losada [ID^{120a}](#), G. Lösckke Centeno [ID¹⁵³](#), O. Loseva [ID³⁹](#),

X. Lou ^{48a,48b}, X. Lou ^{14,115c}, A. Lounis ⁶⁷, P.A. Love ⁹⁴, G. Lu ^{14,115c}, M. Lu ⁶⁷, S. Lu ¹³², Y.J. Lu ¹⁵⁵, H.J. Lubatti ¹⁴³, C. Luci ^{76a,76b}, F.L. Lucio Alves ^{115a}, F. Luehring ⁶⁹, B.S. Lunday ¹³², O. Lundberg ¹⁵¹, B. Lund-Jensen ^{151,*}, N.A. Luongo ⁶, M.S. Lutz ³⁷, A.B. Lux ²⁶, D. Lynn ³⁰, R. Lysak ¹³⁵, V. Lysenko ¹³⁶, E. Lytken ¹⁰¹, V. Lyubushkin ⁴⁰, T. Lyubushkina ⁴⁰, M.M. Lyukova ¹⁵², M.Firdaus M. Soberi ⁵³, H. Ma ³⁰, K. Ma ⁶³, L.L. Ma ^{144a}, W. Ma ⁶³, Y. Ma ¹²⁵, J.C. MacDonald ¹⁰³, P.C. Machado De Abreu Farias ^{84e}, R. Madar ⁴², T. Madula ⁹⁹, J. Maeda ⁸⁶, T. Maeno ³⁰, P.T. Mafa ^{34c,k}, H. Maguire ¹⁴⁶, V. Maiboroda ⁶⁷, A. Maio ^{134a,134b,134d}, K. Maj ^{87a}, O. Majersky ⁴⁹, S. Majewski ¹²⁷, R. Makhmanazarov ³⁹, N. Makovec ⁶⁷, V. Maksimovic ¹⁶, B. Malaescu ¹³¹, Pa. Malecki ⁸⁸, V.P. Maleev ³⁹, F. Malek ^{61,p}, M. Mali ⁹⁶, D. Malito ⁹⁸, U. Mallik ^{81,*}, S. Maltezos ¹⁰, S. Malyukov ⁴⁰, J. Mamuzic ¹³, G. Mancini ⁵⁴, M.N. Mancini ²⁷, G. Manco ^{74a,74b}, J.P. Mandalia ⁹⁷, S.S. Mandarray ¹⁵³, I. Mandić ⁹⁶, L. Manhaes de Andrade Filho ^{84a}, I.M. Maniatis ¹⁷⁶, J. Manjarres Ramos ⁹², D.C. Mankad ¹⁷⁶, A. Mann ¹¹², S. Manzoni ³⁷, L. Mao ^{145a}, X. Mapekula ^{34c}, A. Marantis ^{159,u}, G. Marchiori ⁵, M. Marcisovsky ¹³⁵, C. Marcon ^{72a}, M. Marinescu ²¹, S. Marium ⁴⁹, M. Marjanovic ¹²⁴, A. Markhoos ⁵⁵, M. Markovitch ⁶⁷, M.K. Maroun ¹⁰⁶, E.J. Marshall ⁹⁴, Z. Marshall ^{18a}, S. Marti-Garcia ¹⁷⁰, J. Martin ⁹⁹, T.A. Martin ¹³⁸, V.J. Martin ⁵³, B. Martin dit Latour ¹⁷, L. Martinelli ^{76a,76b}, M. Martinez ^{13,x}, P. Martinez Agullo ¹⁷⁰, V.I. Martinez Outschoorn ¹⁰⁶, P. Martinez Suarez ¹³, S. Martin-Haugh ¹³⁸, G. Martinovicova ¹³⁷, V.S. Martoiu ^{28b}, A.C. Martyniuk ⁹⁹, A. Marzin ³⁷, D. Mascione ^{79a,79b}, L. Masetti ¹⁰³, J. Masik ¹⁰⁴, A.L. Maslennikov ⁴⁰, S.L. Mason ⁴³, P. Massarotti ^{73a,73b}, P. Mastrandrea ^{75a,75b}, A. Mastroberardino ^{45b,45a}, T. Masubuchi ¹²⁸, T.T. Mathew ¹²⁷, J. Matousek ¹³⁷, D.M. Mattern ⁵⁰, J. Maurer ^{28b}, T. Maurin ⁶⁰, A.J. Maury ⁶⁷, B. Maček ⁹⁶, D.A. Maximov ³⁹, A.E. May ¹⁰⁴, E. Mayer ⁴², R. Mazini ^{34g}, I. Maznas ¹¹⁹, M. Mazza ¹¹⁰, S.M. Mazza ¹⁴⁰, E. Mazzeo ^{72a,72b}, J.P. Mc Gowan ¹⁷², S.P. Mc Kee ¹⁰⁹, C.A. Mc Lean ⁶, C.C. McCracken ¹⁷¹, E.F. McDonald ¹⁰⁸, A.E. McDougall ¹¹⁸, L.F. Mcelhinney ⁹⁴, J.A. Mcfayden ¹⁵³, R.P. McGovern ¹³², R.P. Mckenzie ^{34g}, T.C. McLachlan ⁴⁹, D.J. McLaughlin ⁹⁹, S.J. McMahon ¹³⁸, C.M. Mcpartland ⁹⁵, R.A. McPherson ^{172,ab}, S. Mehlhase ¹¹², A. Mehta ⁹⁵, D. Melini ¹⁷⁰, B.R. Mellado Garcia ^{34g}, A.H. Melo ⁵⁶, F. Meloni ⁴⁹, A.M. Mendes Jacques Da Costa ¹⁰⁴, H.Y. Meng ¹⁶², L. Meng ⁹⁴, S. Menke ¹¹³, M. Mentink ³⁷, E. Meoni ^{45b,45a}, G. Mercado ¹¹⁹, S. Merianos ¹⁵⁹, C. Merlassino ^{70a,70c}, C. Meroni ^{72a,72b}, J. Metcalfe ⁶, A.S. Mete ⁶, E. Meuser ¹⁰³, C. Meyer ⁶⁹, J-P. Meyer ¹³⁹, R.P. Middleton ¹³⁸, L. Mijović ⁵³, G. Mikenberg ¹⁷⁶, M. Mikestikova ¹³⁵, M. Mikuž ⁹⁶, H. Mildner ¹⁰³, A. Milic ³⁷, D.W. Miller ⁴¹, E.H. Miller ¹⁵⁰, L.S. Miller ³⁵, A. Milov ¹⁷⁶, D.A. Milstead ^{48a,48b}, T. Min ^{115a}, A.A. Minaenko ³⁹, I.A. Minashvili ^{156b}, A.I. Mincer ¹²¹, B. Mindur ^{87a}, M. Mineev ⁴⁰, Y. Mino ⁹⁰, L.M. Mir ¹³, M. Miralles Lopez ⁶⁰, M. Mironova ^{18a}, M.C. Missio ¹¹⁷, A. Mitra ¹⁷⁴, V.A. Mitsou ¹⁷⁰, Y. Mitsumori ¹¹⁴, O. Miu ¹⁶², P.S. Miyagawa ⁹⁷, T. Mkrtychyan ^{64a}, M. Mlinarevic ⁹⁹, T. Mlinarevic ⁹⁹, M. Mlynarikova ³⁷, S. Mobius ²⁰, P. Mogg ¹¹², M.H. Mohamed Farook ¹¹⁶, A.F. Mohammed ^{14,115c}, S. Mohapatra ⁴³, S. Mohiuddin ¹²⁵, G. Mokgatitswane ^{34g}, L. Moleri ¹⁷⁶, B. Mondal ¹⁴⁸, S. Mondal ¹³⁶, K. Mönig ⁴⁹, E. Monnier ¹⁰⁵, L. Monsonis Romero ¹⁷⁰, J. Montejo Berlingen ¹³, A. Montella ^{48a,48b}, M. Montella ¹²³, F. Montekali ^{78a,78b}, F. Monticelli ⁹³, S. Monzani ^{70a,70c}, A. Morancho Tarda ⁴⁴, N. Morange ⁶⁷, A.L. Moreira De Carvalho ⁴⁹, M. Moreno Llácer ¹⁷⁰, C. Moreno Martinez ⁵⁷, J.M. Moreno Perez ^{23b}, P. Morettini ^{58b}, S. Morgenstern ³⁷, M. Morii ⁶², M. Morinaga ¹⁶⁰, M. Moritsu ⁹¹, F. Morodei ^{76a,76b}, P. Moschovakos ³⁷, B. Moser ¹³⁰, M. Mosidze ^{156b}, T. Moskalets ⁴⁶, P. Moskvitina ¹¹⁷, J. Moss ^{32,m}, P. Moszkowicz ^{87a}, A. Moussa ^{36d}, Y. Moyal ¹⁷⁶, E.J.W. Moyse ¹⁰⁶, O. Mtintsilana ^{34g}, S. Muanza ¹⁰⁵, J. Mueller ¹³³, R. Müller ³⁷, G.A. Mullier ¹⁶⁸, A.J. Mullin ³³, J.J. Mullin ⁵², A.E. Mulski ⁶², D.P. Mungo ¹⁶², D. Munoz Perez ¹⁷⁰,

F.J. Munoz Sanchez [id104](#), M. Murin [id104](#), W.J. Murray [id174,138](#), M. Muškinja [id96](#), C. Mwewa [id30](#), A.G. Myagkov [id39,a](#), A.J. Myers [id8](#), G. Myers [id109](#), M. Myska [id136](#), B.P. Nachman [id18a](#), K. Nagai [id130](#), K. Nagano [id85](#), R. Nagasaka [id160](#), J.L. Nagle [id30,aj](#), E. Nagy [id105](#), A.M. Nairz [id37](#), Y. Nakahama [id85](#), K. Nakamura [id85](#), K. Nakkalil [id5](#), H. Nanjo [id128](#), E.A. Narayanan [id46](#), Y. Narukawa [id160](#), I. Naryshkin [id39](#), L. Nasella [id72a,72b](#), S. Nasri [id120b](#), C. Nass [id25](#), G. Navarro [id23a](#), J. Navarro-Gonzalez [id170](#), A. Nayaz [id19](#), P.Y. Nechaeva [id39](#), S. Nechaeva [id24b,24a](#), F. Nechansky [id135](#), L. Nedic [id130](#), T.J. Neep [id21](#), A. Negri [id74a,74b](#), M. Negrini [id24b](#), C. Nellist [id118](#), C. Nelson [id107](#), K. Nelson [id109](#), S. Nemecek [id135](#), M. Nessi [id37,h](#), M.S. Neubauer [id169](#), J. Newell [id95](#), P.R. Newman [id21](#), Y.W.Y. Ng [id169](#), B. Ngair [id120a](#), H.D.N. Nguyen [id111](#), R.B. Nickerson [id130](#), R. Nicolaidou [id139](#), J. Nielsen [id140](#), M. Niemeyer [id56](#), J. Niermann [id37](#), N. Nikiforou [id37](#), V. Nikolaenko [id39,a](#), I. Nikolic-Audit [id131](#), P. Nilsson [id30](#), I. Ninca [id49](#), G. Ninio [id158](#), A. Nisati [id76a](#), N. Nishu [id2](#), R. Nisius [id113](#), N. Nitika [id70a,70c](#), J.-E. Nitschke [id51](#), E.K. Nkadimeng [id34g](#), T. Nobe [id160](#), D. Noll [id18a](#), T. Nommensen [id154](#), M.B. Norfolk [id146](#), B.J. Norman [id35](#), M. Noury [id36a](#), J. Novak [id96](#), T. Novak [id96](#), R. Novotny [id116](#), L. Nozka [id126](#), K. Ntekas [id166](#), N.M.J. Nunes De Moura Junior [id84b](#), J. Ocariz [id131](#), A. Ochi [id86](#), I. Ochoa [id134a](#), S. Oerdek [id49,y](#), J.T. Offermann [id41](#), A. Ogrodnik [id137](#), A. Oh [id104](#), C.C. Ohm [id151](#), H. Oide [id85](#), R. Oishi [id160](#), M.L. Ojeda [id37](#), Y. Okumura [id160](#), L.F. Oleiro Seabra [id134a](#), I. Oleksiyuk [id57](#), S.A. Olivares Pino [id141d](#), G. Oliveira Correa [id13](#), D. Oliveira Damazio [id30](#), J.L. Oliver [id166](#), Ö.O. Öncel [id55](#), A.P. O'Neill [id20](#), A. Onofre [id134a,134e](#), P.U.E. Onyisi [id11](#), M.J. Oreglia [id41](#), D. Orestano [id78a,78b](#), R.S. Orr [id162](#), L.M. Osojnak [id132](#), Y. Osumi [id114](#), G. Otero y Garzon [id31](#), H. Otono [id91](#), G.J. Ottino [id18a](#), M. Ouchrif [id36d](#), F. Ould-Saada [id129](#), T. Ovsiannikova [id143](#), M. Owen [id60](#), R.E. Owen [id138](#), V.E. Ozcan [id22a](#), F. Ozturk [id88](#), N. Ozturk [id8](#), S. Ozturk [id83](#), H.A. Pacey [id130](#), K. Pachal [id163a](#), A. Pacheco Pages [id13](#), C. Padilla Aranda [id13](#), G. Padovano [id76a,76b](#), S. Pagan Griso [id18a](#), G. Palacino [id69](#), A. Palazzo [id71a,71b](#), J. Pampel [id25](#), J. Pan [id179](#), T. Pan [id65a](#), D.K. Panchal [id11](#), C.E. Pandini [id118](#), J.G. Panduro Vazquez [id138](#), H.D. Pandya [id1](#), H. Pang [id139](#), P. Pani [id49](#), G. Panizzo [id70a,70c](#), L. Panwar [id131](#), L. Paolozzi [id57](#), S. Parajuli [id169](#), A. Paramonov [id6](#), C. Paraskevopoulos [id54](#), D. Paredes Hernandez [id65b](#), A. Pareti [id74a,74b](#), K.R. Park [id43](#), T.H. Park [id113](#), F. Parodi [id58b,58a](#), J.A. Parsons [id43](#), U. Parzefall [id55](#), B. Pascual Dias [id42](#), L. Pascual Dominguez [id102](#), E. Pasqualucci [id76a](#), S. Passaggio [id58b](#), F. Pastore [id98](#), P. Patel [id88](#), U.M. Patel [id52](#), J.R. Pater [id104](#), T. Pauly [id37](#), F. Pauwels [id137](#), C.I. Pazos [id165](#), M. Pedersen [id129](#), R. Pedro [id134a](#), S.V. Peleganchuk [id39](#), O. Penc [id37](#), E.A. Pender [id53](#), S. Peng [id15](#), G.D. Penn [id179](#), K.E. Penski [id112](#), M. Penzin [id39](#), B.S. Peralva [id84d](#), A.P. Pereira Peixoto [id143](#), L. Pereira Sanchez [id150](#), D.V. Perepelitsa [id30,aj](#), G. Perera [id106](#), E. Perez Codina [id163a](#), M. Perganti [id10](#), H. Pernegger [id37](#), S. Perrella [id76a,76b](#), O. Perrin [id42](#), K. Peters [id49](#), R.F.Y. Peters [id104](#), B.A. Petersen [id37](#), T.C. Petersen [id44](#), E. Petit [id105](#), V. Petousis [id136](#), A.R. Petri [id72a,72b](#), C. Petridou [id159,e](#), T. Petru [id137](#), A. Petrukhin [id148](#), M. Pettee [id18a](#), A. Petukhov [id83](#), K. Petukhova [id37](#), R. Pezoa [id141f](#), L. Pezzotti [id24b,24a](#), G. Pezzullo [id179](#), L. Pfaffenbichler [id37](#), A.J. Pflieger [id37](#), T.M. Pham [id177](#), T. Pham [id108](#), P.W. Phillips [id138](#), G. Piacquadio [id152](#), E. Pianori [id18a](#), F. Piazza [id127](#), R. Piegai [id31](#), D. Pietreanu [id28b](#), A.D. Pilkington [id104](#), M. Pinamonti [id70a,70c](#), J.L. Pinfeld [id2](#), B.C. Pinheiro Pereira [id134a](#), J. Pinol Bel [id13](#), A.E. Pinto Pinoargote [id131](#), L. Pintucci [id70a,70c](#), K.M. Piper [id153](#), A. Pirttikoski [id57](#), D.A. Pizzi [id35](#), L. Pizzimento [id65b](#), M.-A. Pleier [id30](#), V. Pleskot [id137](#), E. Plotnikova [id40](#), G. Poddar [id97](#), R. Poettgen [id101](#), L. Poggioli [id131](#), S. Polacek [id137](#), G. Polesello [id74a](#), A. Poley [id149,163a](#), A. Polini [id24b](#), C.S. Pollard [id174](#), Z.B. Pollock [id123](#), E. Pompa Pacchi [id124](#), N.I. Pond [id99](#), D. Ponomarenko [id69](#), L. Pontecorvo [id37](#), S. Popa [id28a](#), G.A. Popeneciu [id28d](#), A. Poreba [id37](#), D.M. Portillo Quintero [id163a](#), S. Pospisil [id136](#), M.A. Postill [id146](#), P. Postolache [id28c](#), K. Potamianos [id174](#), P.A. Potepa [id87a](#), I.N. Potrap [id40](#), C.J. Potter [id33](#), H. Potti [id154](#), J. Poveda [id170](#), M.E. Pozo Astigarraga [id37](#), A. Prades Ibanez [id77a,77b](#), J. Pretel [id172](#), D. Price [id104](#), M. Primavera [id71a](#), L. Primomo [id70a,70c](#), M.A. Principe Martin [id102](#),

R. Privara ¹²⁶, T. Procter ⁶⁰, M.L. Proffitt ¹⁴³, N. Proklova ¹³², K. Prokofiev ^{65c}, G. Proto ¹¹³,
 J. Proudfoot ⁶, M. Przybycien ^{87a}, W.W. Przygoda ^{87b}, A. Psallidas ⁴⁷, J.E. Puddefoot ¹⁴⁶,
 D. Pudzha ⁵⁵, D. Pyatiiizbyantseva ¹¹⁷, J. Qian ¹⁰⁹, R. Qian ¹¹⁰, D. Qichen ¹⁰⁴, Y. Qin ¹³,
 T. Qiu ⁵³, A. Quadt ⁵⁶, M. Queitsch-Maitland ¹⁰⁴, G. Quetant ⁵⁷, R.P. Quinn ¹⁷¹,
 G. Rabanal Bolanos ⁶², D. Rafanoharana ⁵⁵, F. Raffaelli ^{77a,77b}, F. Ragusa ^{72a,72b}, J.L. Rainbolt ⁴¹,
 J.A. Raine ⁵⁷, S. Rajagopalan ³⁰, E. Ramakoti ³⁹, L. Rambelli ^{58b,58a}, I.A. Ramirez-Berend ³⁵,
 K. Ran ^{49,115c}, D.S. Rankin ¹³², N.P. Rapheeha ^{34g}, H. Rasheed ^{28b}, V. Raskina ¹³¹,
 D.F. Rassloff ^{64a}, A. Rastogi ^{18a}, S. Rave ¹⁰³, S. Ravera ^{58b,58a}, B. Ravina ³⁷, I. Ravinovich ¹⁷⁶,
 M. Raymond ³⁷, A.L. Read ¹²⁹, N.P. Readioff ¹⁴⁶, D.M. Rebuzzi ^{74a,74b}, A.S. Reed ¹¹³,
 K. Reeves ²⁷, J.A. Reidelsturz ¹⁷⁸, D. Reikher ¹²⁷, A. Rej ⁵⁰, C. Rembser ³⁷, H. Ren ⁶³,
 M. Renda ^{28b}, F. Renner ⁴⁹, A.G. Rennie ¹⁶⁶, A.L. Rescia ⁴⁹, S. Resconi ^{72a},
 M. Ressegotti ^{58b,58a}, S. Rettie ³⁷, W.F. Rettie ³⁵, J.G. Reyes Rivera ¹¹⁰, E. Reynolds ^{18a},
 O.L. Rezanova ⁴⁰, P. Reznicek ¹³⁷, H. Riani ^{36d}, N. Ribaric ⁵², E. Ricci ^{79a,79b}, R. Richter ¹¹³,
 S. Richter ^{48a,48b}, E. Richter-Was ^{87b}, M. Ridel ¹³¹, S. Ridouani ^{36d}, P. Rieck ¹²¹, P. Riedler ³⁷,
 E.M. Riefel ^{48a,48b}, J.O. Rieger ¹¹⁸, M. Rijssenbeek ¹⁵², M. Rimoldi ³⁷, L. Rinaldi ^{24b,24a},
 P. Rincke ⁵⁶, G. Ripellino ¹⁶⁸, I. Riu ¹³, J.C. Rivera Vergara ¹⁷², F. Rizatdinova ¹²⁵, E. Rizvi ⁹⁷,
 B.R. Roberts ^{18a}, S.S. Roberts ¹⁴⁰, D. Robinson ³³, M. Robles Manzano ¹⁰³, A. Robson ⁶⁰,
 A. Rocchi ^{77a,77b}, C. Roda ^{75a,75b}, S. Rodriguez Bosca ³⁷, Y. Rodriguez Garcia ^{23a},
 A.M. Rodríguez Vera ¹¹⁹, S. Roe ³⁷, J.T. Roemer ³⁷, O. Røhne ¹²⁹, R.A. Rojas ³⁷,
 C.P.A. Roland ¹³¹, J. Roloff ³⁰, A. Romaniouk ⁸⁰, E. Romano ^{74a,74b}, M. Romano ^{24b},
 A.C. Romero Hernandez ¹⁶⁹, N. Rompotis ⁹⁵, L. Roos ¹³¹, S. Rosati ^{76a}, B.J. Rosser ⁴¹,
 E. Rossi ¹³⁰, E. Rossi ^{73a,73b}, L.P. Rossi ⁶², L. Rossini ⁵⁵, R. Rosten ¹²³, M. Rotaru ^{28b},
 B. Rottler ⁵⁵, D. Rousseau ⁶⁷, D. Rouso ⁴⁹, S. Roy-Garand ¹⁶², A. Rozanov ¹⁰⁵,
 Z.M.A. Rozario ⁶⁰, Y. Rozen ¹⁵⁷, A. Rubio Jimenez ¹⁷⁰, V.H. Ruelas Rivera ¹⁹, T.A. Ruggeri ¹,
 A. Ruggiero ¹³⁰, A. Ruiz-Martinez ¹⁷⁰, A. Rummler ³⁷, Z. Rurikova ⁵⁵, N.A. Rusakovich ⁴⁰,
 H.L. Russell ¹⁷², G. Russo ^{76a,76b}, J.P. Rutherford ⁷, S. Rutherford Colmenares ³³, M. Rybar ¹³⁷,
 P. Rybczynski ^{87a}, E.B. Rye ¹²⁹, A. Ryzhov ⁴⁶, J.A. Sabater Iglesias ⁵⁷, H.F.W. Sadrozinski ¹⁴⁰,
 F. Safai Tehrani ^{76a}, S. Saha ¹, M. Sahinsoy ⁸³, A. Saibel ¹⁷⁰, B.T. Saifuddin ¹²⁴,
 M. Saimpert ¹³⁹, M. Saito ¹⁶⁰, T. Saito ¹⁶⁰, A. Sala ^{72a,72b}, D. Salamani ³⁷, A. Salnikov ¹⁵⁰,
 J. Salt ¹⁷⁰, A. Salvador Salas ¹⁵⁸, D. Salvatore ^{45b,45a}, F. Salvatore ¹⁵³, A. Salzburger ³⁷,
 D. Sammel ⁵⁵, E. Sampson ⁹⁴, D. Sampsonidis ^{159,e}, D. Sampsonidou ¹²⁷, J. Sánchez ¹⁷⁰,
 V. Sanchez Sebastian ¹⁷⁰, H. Sandaker ¹²⁹, C.O. Sander ⁴⁹, J.A. Sandesara ¹⁰⁶, M. Sandhoff ¹⁷⁸,
 C. Sandoval ^{23b}, L. Sanfilippo ^{64a}, D.P.C. Sankey ¹³⁸, T. Sano ⁹⁰, A. Sansoni ⁵⁴, L. Santi ³⁷,
 C. Santoni ⁴², H. Santos ^{134a,134b}, A. Santra ¹⁷⁶, E. Sanzani ^{24b,24a}, K.A. Saoucha ^{89b},
 J.G. Saraiva ^{134a,134d}, J. Sardain ⁷, O. Sasaki ⁸⁵, K. Sato ¹⁶⁴, C. Sauer ³⁷, E. Sauvan ⁴,
 P. Savard ^{162,ah}, R. Sawada ¹⁶⁰, C. Sawyer ¹³⁸, L. Sawyer ¹⁰⁰, C. Sbarra ^{24b}, A. Sbrizzi ^{24b,24a},
 T. Scanlon ⁹⁹, J. Schaarschmidt ¹⁴³, U. Schäfer ¹⁰³, A.C. Schaffer ^{67,46}, D. Schaile ¹¹²,
 R.D. Schamberger ¹⁵², C. Scharf ¹⁹, M.M. Schefer ²⁰, V.A. Schegelsky ³⁹, D. Scheirich ¹³⁷,
 M. Schernau ^{141e}, C. Scheulen ⁵⁷, C. Schiavi ^{58b,58a}, M. Schioppa ^{45b,45a}, B. Schlag ¹⁵⁰,
 S. Schlenker ³⁷, J. Schmeing ¹⁷⁸, M.A. Schmidt ¹⁷⁸, K. Schmieden ¹⁰³, C. Schmitt ¹⁰³,
 N. Schmitt ¹⁰³, S. Schmitt ⁴⁹, L. Schoeffel ¹³⁹, A. Schoening ^{64b}, P.G. Scholer ³⁵, E. Schopf ¹⁴⁸,
 M. Schott ²⁵, S. Schramm ⁵⁷, T. Schroer ⁵⁷, H-C. Schultz-Coulon ^{64a}, M. Schumacher ⁵⁵,
 B.A. Schumm ¹⁴⁰, Ph. Schune ¹³⁹, H.R. Schwartz ¹⁴⁰, A. Schwartzman ¹⁵⁰, T.A. Schwarz ¹⁰⁹,
 Ph. Schwemling ¹³⁹, R. Schwienhorst ¹¹⁰, F.G. Sciacca ²⁰, A. Sciandra ³⁰, G. Sciolla ²⁷,
 F. Scuri ^{75a}, C.D. Sebastiani ³⁷, K. Sedlaczek ¹¹⁹, S.C. Seidel ¹¹⁶, A. Seiden ¹⁴⁰,
 B.D. Seidlitz ⁴³, C. Seitz ⁴⁹, J.M. Seixas ^{84b}, G. Sekhniadze ^{73a}, L. Selem ⁶¹,
 N. Semprini-Cesari ^{24b,24a}, A. Semushin ^{180,39}, D. Sengupta ⁵⁷, V. Senthilkumar ¹⁷⁰, L. Serin ⁶⁷,

M. Sessa [ID 77a,77b](#), H. Severini [ID 124](#), F. Sforza [ID 58b,58a](#), A. Sfyrla [ID 57](#), Q. Sha [ID 14](#), E. Shabalina [ID 56](#),
H. Shaddix [ID 119](#), A.H. Shah [ID 33](#), R. Shaheen [ID 151](#), J.D. Shahinian [ID 132](#), D. Shaked Renous [ID 176](#),
M. Shamim [ID 37](#), L.Y. Shan [ID 14](#), M. Shapiro [ID 18a](#), A. Sharma [ID 37](#), A.S. Sharma [ID 171](#), P. Sharma [ID 30](#),
P.B. Shatalov [ID 39](#), K. Shaw [ID 153](#), S.M. Shaw [ID 104](#), Q. Shen [ID 145a](#), D.J. Sheppard [ID 149](#), P. Sherwood [ID 99](#),
L. Shi [ID 99](#), X. Shi [ID 14](#), S. Shimizu [ID 85](#), C.O. Shimmin [ID 179](#), I.P.J. Shipsey [ID 130,*](#), S. Shirabe [ID 91](#),
M. Shiyakova [ID 40,z](#), M.J. Shochet [ID 41](#), D.R. Shope [ID 129](#), B. Shrestha [ID 124](#), S. Shrestha [ID 123,al](#),
I. Shreyber [ID 39](#), M.J. Shroff [ID 172](#), P. Sicho [ID 135](#), A.M. Sickles [ID 169](#), E. Sideras Haddad [ID 34g,167](#),
A.C. Sidley [ID 118](#), A. Sidoti [ID 24b](#), F. Siegert [ID 51](#), Dj. Sijacki [ID 16](#), F. Sili [ID 93](#), J.M. Silva [ID 53](#),
I. Silva Ferreira [ID 84b](#), M.V. Silva Oliveira [ID 30](#), S.B. Silverstein [ID 48a](#), S. Simion [ID 67](#), R. Simoniello [ID 37](#),
E.L. Simpson [ID 104](#), H. Simpson [ID 153](#), L.R. Simpson [ID 109](#), S. Simsek [ID 83](#), S. Sindhu [ID 56](#), P. Sinervo [ID 162](#),
S.N. Singh [ID 27](#), S. Singh [ID 30](#), S. Sinha [ID 49](#), S. Sinha [ID 104](#), M. Sioli [ID 24b,24a](#), K. Sioulas [ID 9](#), I. Siral [ID 37](#),
E. Sitnikova [ID 49](#), J. Sjölin [ID 48a,48b](#), A. Skaf [ID 56](#), E. Skorda [ID 21](#), P. Skubic [ID 124](#), M. Slawinska [ID 88](#),
I. Slazyk [ID 17](#), V. Smakhtin [ID 176](#), B.H. Smart [ID 138](#), S.Yu. Smirnov [ID 141b](#), Y. Smirnov [ID 83](#),
L.N. Smirnova [ID 39,a](#), O. Smirnova [ID 101](#), A.C. Smith [ID 43](#), D.R. Smith [ID 166](#), E.A. Smith [ID 41](#), J.L. Smith [ID 104](#),
M.B. Smith [ID 35](#), R. Smith [ID 150](#), H. Smitmanns [ID 103](#), M. Smizanska [ID 94](#), K. Smolek [ID 136](#),
A.A. Snesarev [ID 40](#), H.L. Snoek [ID 118](#), S. Snyder [ID 30](#), R. Sobie [ID 172,ab](#), A. Soffer [ID 158](#),
C.A. Solans Sanchez [ID 37](#), E.Yu. Soldatov [ID 40](#), U. Soldevila [ID 170](#), A.A. Solodkov [ID 34g](#), S. Solomon [ID 27](#),
A. Soloshenko [ID 40](#), K. Solovieva [ID 55](#), O.V. Solovyanov [ID 42](#), P. Sommer [ID 51](#), A. Sonay [ID 13](#),
W.Y. Song [ID 163b](#), A. Sopczak [ID 136](#), A.L. Sopio [ID 53](#), F. Sopkova [ID 29b](#), J.D. Sorenson [ID 116](#),
I.R. Sotarriva Alvarez [ID 142](#), V. Sothilingam [ID 64a](#), O.J. Soto Sandoval [ID 141c,141b](#), S. Sottocornola [ID 69](#),
R. Soualah [ID 89a](#), Z. Soumami [ID 36e](#), D. South [ID 49](#), N. Soybelman [ID 176](#), S. Spagnolo [ID 71a,71b](#),
M. Spalla [ID 113](#), D. Sperlich [ID 55](#), B. Spisso [ID 73a,73b](#), D.P. Spiteri [ID 60](#), L. Splendori [ID 105](#), M. Spousta [ID 137](#),
E.J. Staats [ID 35](#), R. Stamen [ID 64a](#), E. Stanecka [ID 88](#), W. Stanek-Maslouska [ID 49](#), M.V. Stange [ID 51](#),
B. Stanislaus [ID 18a](#), M.M. Stanitzki [ID 49](#), B. Stapf [ID 49](#), E.A. Starchenko [ID 39](#), G.H. Stark [ID 140](#), J. Stark [ID 92](#),
P. Staroba [ID 135](#), P. Starovoitov [ID 89b](#), R. Staszewski [ID 88](#), G. Stavropoulos [ID 47](#), A. Stefl [ID 37](#),
P. Steinberg [ID 30](#), B. Stelzer [ID 149,163a](#), H.J. Stelzer [ID 133](#), O. Stelzer-Chilton [ID 163a](#), H. Stenzel [ID 59](#),
T.J. Stevenson [ID 153](#), G.A. Stewart [ID 37](#), J.R. Stewart [ID 125](#), M.C. Stockton [ID 37](#), G. Stoicea [ID 28b](#),
M. Stolarski [ID 134a](#), S. Stonjek [ID 113](#), A. Straessner [ID 51](#), J. Strandberg [ID 151](#), S. Strandberg [ID 48a,48b](#),
M. Stratmann [ID 178](#), M. Strauss [ID 124](#), T. Strebler [ID 105](#), P. Strizenec [ID 29b](#), R. Ströhmer [ID 173](#),
D.M. Strom [ID 127](#), R. Stroynowski [ID 46](#), A. Strubig [ID 48a,48b](#), S.A. Stucci [ID 30](#), B. Stugu [ID 17](#), J. Stupak [ID 124](#),
N.A. Styles [ID 49](#), D. Su [ID 150](#), S. Su [ID 63](#), W. Su [ID 145b](#), X. Su [ID 63](#), D. Suchy [ID 29a](#), K. Sugizaki [ID 132](#),
V.V. Sulin [ID 39](#), M.J. Sullivan [ID 95](#), D.M.S. Sultan [ID 130](#), L. Sultanaliyeva [ID 39](#), S. Sultansoy [ID 3b](#),
S. Sun [ID 177](#), W. Sun [ID 14](#), O. Sunneborn Gudnadottir [ID 168](#), N. Sur [ID 105](#), M.R. Sutton [ID 153](#),
H. Suzuki [ID 164](#), M. Svatos [ID 135](#), P.N. Swallow [ID 33](#), M. Swiatlowski [ID 163a](#), T. Swirski [ID 173](#),
I. Sykora [ID 29a](#), M. Sykora [ID 137](#), T. Sykora [ID 137](#), D. Ta [ID 103](#), K. Tackmann [ID 49,y](#), A. Taffard [ID 166](#),
R. Tafirout [ID 163a](#), Y. Takubo [ID 85](#), M. Talby [ID 105](#), A.A. Talyshv [ID 39](#), K.C. Tam [ID 65b](#), N.M. Tamir [ID 158](#),
A. Tanaka [ID 160](#), J. Tanaka [ID 160](#), R. Tanaka [ID 67](#), M. Tanasini [ID 152](#), Z. Tao [ID 171](#), S. Tapia Araya [ID 141f](#),
S. Tapprogge [ID 103](#), A. Tarek Abouelfadl Mohamed [ID 110](#), S. Tarem [ID 157](#), K. Tariq [ID 14](#), G. Tarna [ID 28b](#),
G.F. Tartarelli [ID 72a](#), M.J. Tartarin [ID 92](#), P. Tas [ID 137](#), M. Tasevsky [ID 135](#), E. Tassi [ID 45b,45a](#), A.C. Tate [ID 169](#),
G. Tateno [ID 160](#), Y. Tayalati [ID 36e,aa](#), G.N. Taylor [ID 108](#), W. Taylor [ID 163b](#), A.S. Tegetmeier [ID 92](#),
P. Teixeira-Dias [ID 98](#), J.J. Teoh [ID 162](#), K. Terashi [ID 160](#), J. Terron [ID 102](#), S. Terzo [ID 13](#), M. Testa [ID 54](#),
R.J. Teuscher [ID 162,ab](#), A. Thaler [ID 80](#), O. Theiner [ID 57](#), T. Thevenaux-Pelzer [ID 105](#), O. Thielmann [ID 178](#),
D.W. Thomas [ID 98](#), J.P. Thomas [ID 21](#), E.A. Thompson [ID 18a](#), P.D. Thompson [ID 21](#), E. Thomson [ID 132](#),
R.E. Thornberry [ID 46](#), C. Tian [ID 63](#), Y. Tian [ID 57](#), V. Tikhomirov [ID 83](#), Yu.A. Tikhonov [ID 39](#),
S. Timoshenko [ID 39](#), D. Timoshyn [ID 137](#), E.X.L. Ting [ID 1](#), P. Tipton [ID 179](#), A. Tishelman-Charny [ID 30](#),
S.H. Tlou [ID 34g](#), K. Todome [ID 142](#), S. Todorova-Nova [ID 137](#), S. Todt [ID 51](#), L. Toffolin [ID 70a,70c](#), M. Togawa [ID 85](#),
J. Tojo [ID 91](#), S. Tokár [ID 29a](#), O. Toldaiev [ID 69](#), G. Tolkachev [ID 105](#), M. Tomoto [ID 85,114](#), L. Tompkins [ID 150,o](#),

E. Torrence ¹²⁷, H. Torres ⁹², E. Torró Pastor ¹⁷⁰, M. Toscani ³¹, C. Toscirci ⁴¹, M. Tost ¹¹,
 D.R. Tovey ¹⁴⁶, T. Trefzger ¹⁷³, P.M. Tricarico ¹³, A. Tricoli ³⁰, I.M. Trigger ^{163a},
 S. Trincaz-Duvoid ¹³¹, D.A. Trischuk ²⁷, A. Tropina ⁴⁰, L. Truong ^{34c}, M. Trzebinski ⁸⁸,
 A. Trzuppek ⁸⁸, F. Tsai ¹⁵², M. Tsai ¹⁰⁹, A. Tsiamis ¹⁵⁹, P.V. Tsiareshka ⁴⁰, S. Tsigaridas ^{163a},
 A. Tsirigotis ^{159,u}, V. Tsiskaridze ¹⁶², E.G. Tskhadadze ^{156a}, M. Tsopoulou ¹⁵⁹, Y. Tsujikawa ⁹⁰,
 I.I. Tsukerman ³⁹, V. Tsulaia ^{18a}, S. Tsuno ⁸⁵, K. Tsuru ¹²², D. Tsybychev ¹⁵², Y. Tu ^{65b},
 A. Tudorache ^{28b}, V. Tudorache ^{28b}, S. Turchikhin ^{58b,58a}, I. Turk Cakir ^{3a}, R. Turra ^{72a},
 T. Turtuvshin ^{40,ac}, P.M. Tuts ⁴³, S. Tzamarias ^{159,e}, E. Tzovara ¹⁰³, F. Ukegawa ¹⁶⁴,
 P.A. Ulloa Poblete ^{141c,141b}, E.N. Umaka ³⁰, G. Unal ³⁷, A. Undrus ³⁰, G. Unel ¹⁶⁶, J. Urban ^{29b},
 P. Urrejola ^{141a}, G. Usai ⁸, R. Ushioda ¹⁶¹, M. Usman ¹¹¹, F. Ustuner ⁵³, Z. Uysal ⁸³,
 V. Vacek ¹³⁶, B. Vachon ¹⁰⁷, T. Vafeiadis ³⁷, A. Vaitkus ⁹⁹, C. Valderanis ¹¹²,
 E. Valdes Santurio ^{48a,48b}, M. Valente ^{163a}, S. Valentinetti ^{24b,24a}, A. Valero ¹⁷⁰,
 E. Valiente Moreno ¹⁷⁰, A. Vallier ⁹², J.A. Valls Ferrer ¹⁷⁰, D.R. Van Arneeman ¹¹⁸,
 T.R. Van Daalen ¹⁴³, A. Van Der Graaf ⁵⁰, H.Z. Van Der Schyf ^{34g}, P. Van Gemmeren ⁶,
 M. Van Rijnbach ³⁷, S. Van Stroud ⁹⁹, I. Van Vulpen ¹¹⁸, P. Vana ¹³⁷, M. Vanadia ^{77a,77b},
 U.M. Vande Voorde ¹⁵¹, W. Vandelli ³⁷, E.R. Vandewall ¹²⁵, D. Vannicola ¹⁵⁸, L. Vannoli ⁵⁴,
 R. Vari ^{76a}, E.W. Varnes ⁷, C. Varni ^{18b}, D. Varouchas ⁶⁷, L. Varriale ¹⁷⁰, K.E. Varvell ¹⁵⁴,
 M.E. Vasile ^{28b}, L. Vaslin ⁸⁵, M.D. Vassilev ¹⁵⁰, A. Vasyukov ⁴⁰, L.M. Vaughan ¹²⁵, R. Vavricka ¹³⁷,
 T. Vazquez Schroeder ¹³, J. Veatch ³², V. Vecchio ¹⁰⁴, M.J. Veen ¹⁰⁶, I. Veliscek ³⁰,
 L.M. Veloce ¹⁶², F. Veloso ^{134a,134c}, S. Veneziano ^{76a}, A. Ventura ^{71a,71b}, S. Ventura Gonzalez ¹³⁹,
 A. Verbytskyi ¹¹³, M. Verducci ^{75a,75b}, C. Vergis ⁹⁷, M. Verissimo De Araujo ^{84b},
 W. Verkerke ¹¹⁸, J.C. Vermeulen ¹¹⁸, C. Vernieri ¹⁵⁰, M. Vessella ¹⁶⁶, M.C. Vetterli ^{149,ah},
 A. Vgenopoulos ¹⁰³, N. Viaux Maira ^{141f}, T. Vickey ¹⁴⁶, O.E. Vickey Boeriu ¹⁴⁶,
 G.H.A. Viehhauser ¹³⁰, L. Vigani ^{64b}, M. Vigl ¹¹³, M. Villa ^{24b,24a}, M. Villaplana Perez ¹⁷⁰,
 E.M. Villhauer ⁵³, E. Vilucchi ⁵⁴, M.G. Vincter ³⁵, A. Visibile ¹¹⁸, C. Vittori ³⁷, I. Vivarelli ^{24b,24a},
 E. Voevodina ¹¹³, F. Vogel ¹¹², J.C. Voigt ⁵¹, P. Vokac ¹³⁶, Yu. Volkotrub ^{87b}, E. Von Toerne ²⁵,
 B. Vormwald ³⁷, K. Vorobev ³⁹, M. Vos ¹⁷⁰, K. Voss ¹⁴⁸, M. Vozak ³⁷, L. Vozdecky ¹²⁴,
 N. Vranjes ¹⁶, M. Vranjes Milosavljevic ¹⁶, M. Vreeswijk ¹¹⁸, N.K. Vu ^{145b,145a}, R. Vuillermet ³⁷,
 O. Vujinovic ¹⁰³, I. Vukotic ⁴¹, I.K. Vyas ³⁵, S. Wada ¹⁶⁴, C. Wagner ¹⁵⁰, J.M. Wagner ^{18a},
 W. Wagner ¹⁷⁸, S. Wahdan ¹⁷⁸, H. Wahlberg ⁹³, C.H. Waits ¹²⁴, J. Walder ¹³⁸, R. Walker ¹¹²,
 W. Walkowiak ¹⁴⁸, A. Wall ¹³², E.J. Wallin ¹⁰¹, T. Wamorkar ^{18a}, A.Z. Wang ¹⁴⁰, C. Wang ¹⁰³,
 C. Wang ¹¹, H. Wang ^{18a}, J. Wang ^{65c}, P. Wang ¹⁰⁴, P. Wang ⁹⁹, R. Wang ⁶², R. Wang ⁶,
 S.M. Wang ¹⁵⁵, S. Wang ¹⁴, T. Wang ⁶³, T. Wang ⁶³, W.T. Wang ⁸¹, W. Wang ¹⁴, X. Wang ¹⁶⁹,
 X. Wang ^{145a}, X. Wang ⁴⁹, Y. Wang ^{115a}, Y. Wang ⁶³, Z. Wang ¹⁰⁹, Z. Wang ^{145b,52,145a},
 Z. Wang ¹⁰⁹, C. Wanotayaroj ⁸⁵, A. Warburton ¹⁰⁷, R.J. Ward ²¹, A.L. Warnerbring ¹⁴⁸,
 N. Warrack ⁶⁰, S. Waterhouse ⁹⁸, A.T. Watson ²¹, H. Watson ⁵³, M.F. Watson ²¹, E. Watton ⁶⁰,
 G. Watts ¹⁴³, B.M. Waugh ⁹⁹, J.M. Webb ⁵⁵, C. Weber ³⁰, H.A. Weber ¹⁹, M.S. Weber ²⁰,
 S.M. Weber ^{64a}, C. Wei ⁶³, Y. Wei ⁵⁵, A.R. Weidberg ¹³⁰, E.J. Weik ¹²¹, J. Weingarten ⁵⁰,
 C. Weiser ⁵⁵, C.J. Wells ⁴⁹, T. Wenaus ³⁰, B. Wendland ⁵⁰, T. Wengler ³⁷, N.S. Wenke ¹¹³,
 N. Wermes ²⁵, M. Wessels ^{64a}, A.M. Wharton ⁹⁴, A.S. White ⁶², A. White ⁸, M.J. White ¹,
 D. Whiteson ¹⁶⁶, L. Wickremasinghe ¹²⁸, W. Wiedenmann ¹⁷⁷, M. Wielers ¹³⁸,
 C. Wiglesworth ⁴⁴, D.J. Wilbern ¹²⁴, H.G. Wilkens ³⁷, J.J.H. Wilkinson ³³, D.M. Williams ⁴³,
 H.H. Williams ¹³², S. Williams ³³, S. Willocq ¹⁰⁶, B.J. Wilson ¹⁰⁴, D.J. Wilson ¹⁰⁴,
 P.J. Windischhofer ⁴¹, F.I. Winkel ³¹, F. Winklmeier ¹²⁷, B.T. Winter ⁵⁵, M. Wittgen ¹⁵⁰,
 M. Wobisch ¹⁰⁰, T. Wojtkowski ⁶¹, Z. Wolffs ¹¹⁸, J. Wollrath ³⁷, M.W. Wolter ⁸⁸, H. Wolters ^{134a,134c},
 M.C. Wong ¹⁴⁰, E.L. Woodward ⁴³, S.D. Worm ⁴⁹, B.K. Wosiek ⁸⁸, K.W. Woźniak ⁸⁸,
 S. Wozniowski ⁵⁶, K. Wraight ⁶⁰, C. Wu ²¹, M. Wu ^{115b}, M. Wu ¹¹⁷, S.L. Wu ¹⁷⁷, S. Wu ¹⁴,

X. Wu ^{id57}, X. Wu ^{id63}, Y. Wu ^{id63}, Z. Wu ^{id4}, J. Wuerzinger ^{id113,af}, T.R. Wyatt ^{id104}, B.M. Wynne ^{id53}, S. Xella ^{id44}, L. Xia ^{id115a}, M. Xia ^{id15}, M. Xie ^{id63}, A. Xiong ^{id127}, J. Xiong ^{id18a}, D. Xu ^{id14}, H. Xu ^{id63}, L. Xu ^{id63}, R. Xu ^{id132}, T. Xu ^{id109}, Y. Xu ^{id143}, Z. Xu ^{id53}, Z. Xu ^{id115a}, B. Yabsley ^{id154}, S. Yacoob ^{id34a}, Y. Yamaguchi ^{id85}, E. Yamashita ^{id160}, H. Yamauchi ^{id164}, T. Yamazaki ^{id18a}, Y. Yamazaki ^{id86}, S. Yan ^{id60}, Z. Yan ^{id106}, H.J. Yang ^{id145a,145b}, H.T. Yang ^{id63}, S. Yang ^{id63}, T. Yang ^{id65c}, X. Yang ^{id37}, X. Yang ^{id14}, Y. Yang ^{id160}, Y. Yang ^{id63}, W-M. Yao ^{id18a}, C.L. Yardley ^{id153}, H. Ye ^{id56}, J. Ye ^{id14}, S. Ye ^{id30}, X. Ye ^{id63}, Y. Yeh ^{id99}, I. Yeletsikh ^{id40}, B. Yeo ^{id18b}, M.R. Yexley ^{id99}, T.P. Yildirim ^{id130}, P. Yin ^{id43}, K. Yorita ^{id175}, S. Younas ^{id28b}, C.J.S. Young ^{id37}, C. Young ^{id150}, N.D. Young ^{id127}, Y. Yu ^{id63}, J. Yuan ^{id14,115c}, M. Yuan ^{id109}, R. Yuan ^{id145b,145a}, L. Yue ^{id99}, M. Zaazoua ^{id63}, B. Zabinski ^{id88}, I. Zahir ^{id36a}, Z.K. Zak ^{id88}, T. Zakareishvili ^{id170}, S. Zambito ^{id57}, J.A. Zamora Saa ^{id141d,141b}, J. Zang ^{id160}, D. Zanzi ^{id55}, R. Zanzottera ^{id72a,72b}, O. Zaplatilek ^{id136}, C. Zeitnitz ^{id178}, H. Zeng ^{id14}, J.C. Zeng ^{id169}, D.T. Zenger Jr ^{id27}, O. Zenin ^{id39}, T. Ženiš ^{id29a}, S. Zenz ^{id97}, S. Zerradi ^{id36a}, D. Zerwas ^{id67}, M. Zhai ^{id14,115c}, D.F. Zhang ^{id146}, J. Zhang ^{id144a}, J. Zhang ^{id6}, K. Zhang ^{id14,115c}, L. Zhang ^{id63}, L. Zhang ^{id115a}, P. Zhang ^{id14,115c}, R. Zhang ^{id177}, S. Zhang ^{id92}, T. Zhang ^{id160}, X. Zhang ^{id145a}, Y. Zhang ^{id143}, Y. Zhang ^{id99}, Y. Zhang ^{id63}, Y. Zhang ^{id115a}, Z. Zhang ^{id18a}, Z. Zhang ^{id144a}, Z. Zhang ^{id67}, H. Zhao ^{id143}, T. Zhao ^{id144a}, Y. Zhao ^{id35}, Z. Zhao ^{id63}, Z. Zhao ^{id63}, A. Zhemchugov ^{id40}, J. Zheng ^{id115a}, K. Zheng ^{id169}, X. Zheng ^{id63}, Z. Zheng ^{id150}, D. Zhong ^{id169}, B. Zhou ^{id109}, H. Zhou ^{id7}, N. Zhou ^{id145a}, Y. Zhou ^{id15}, Y. Zhou ^{id115a}, Y. Zhou ^{id7}, C.G. Zhu ^{id144a}, J. Zhu ^{id109}, X. Zhu ^{id145b}, Y. Zhu ^{id145a}, Y. Zhu ^{id63}, X. Zhuang ^{id14}, K. Zhukov ^{id69}, N.I. Zimine ^{id40}, J. Zinsser ^{id64b}, M. Ziolkowski ^{id148}, L. Živković ^{id16}, A. Zoccoli ^{id24b,24a}, K. Zoch ^{id62}, T.G. Zorbas ^{id146}, O. Zormpa ^{id47}, W. Zou ^{id43}, L. Zwalinski ^{id37}.

¹Department of Physics, University of Adelaide, Adelaide; Australia.

²Department of Physics, University of Alberta, Edmonton AB; Canada.

³(^a)Department of Physics, Ankara University, Ankara; (^b)Division of Physics, TOBB University of Economics and Technology, Ankara; Türkiye.

⁴LAPP, Université Savoie Mont Blanc, CNRS/IN2P3, Annecy; France.

⁵APC, Université Paris Cité, CNRS/IN2P3, Paris; France.

⁶High Energy Physics Division, Argonne National Laboratory, Argonne IL; United States of America.

⁷Department of Physics, University of Arizona, Tucson AZ; United States of America.

⁸Department of Physics, University of Texas at Arlington, Arlington TX; United States of America.

⁹Physics Department, National and Kapodistrian University of Athens, Athens; Greece.

¹⁰Physics Department, National Technical University of Athens, Zografou; Greece.

¹¹Department of Physics, University of Texas at Austin, Austin TX; United States of America.

¹²Institute of Physics, Azerbaijan Academy of Sciences, Baku; Azerbaijan.

¹³Institut de Física d'Altes Energies (IFAE), Barcelona Institute of Science and Technology, Barcelona; Spain.

¹⁴Institute of High Energy Physics, Chinese Academy of Sciences, Beijing; China.

¹⁵Physics Department, Tsinghua University, Beijing; China.

¹⁶Institute of Physics, University of Belgrade, Belgrade; Serbia.

¹⁷Department for Physics and Technology, University of Bergen, Bergen; Norway.

¹⁸(^a)Physics Division, Lawrence Berkeley National Laboratory, Berkeley CA; (^b)University of California, Berkeley CA; United States of America.

¹⁹Institut für Physik, Humboldt Universität zu Berlin, Berlin; Germany.

²⁰Albert Einstein Center for Fundamental Physics and Laboratory for High Energy Physics, University of Bern, Bern; Switzerland.

²¹School of Physics and Astronomy, University of Birmingham, Birmingham; United Kingdom.

- ^{22(a)}Department of Physics, Bogazici University, Istanbul; ^(b)Department of Physics Engineering, Gaziantep University, Gaziantep; ^(c)Department of Physics, Istanbul University, Istanbul; Türkiye.
- ^{23(a)}Facultad de Ciencias y Centro de Investigaciones, Universidad Antonio Nariño, Bogotá; ^(b)Departamento de Física, Universidad Nacional de Colombia, Bogotá; Colombia.
- ^{24(a)}Dipartimento di Fisica e Astronomia A. Righi, Università di Bologna, Bologna; ^(b)INFN Sezione di Bologna; Italy.
- ²⁵Physikalisches Institut, Universität Bonn, Bonn; Germany.
- ²⁶Department of Physics, Boston University, Boston MA; United States of America.
- ²⁷Department of Physics, Brandeis University, Waltham MA; United States of America.
- ^{28(a)}Transilvania University of Brasov, Brasov; ^(b)Horia Hulubei National Institute of Physics and Nuclear Engineering, Bucharest; ^(c)Department of Physics, Alexandru Ioan Cuza University of Iasi, Iasi; ^(d)National Institute for Research and Development of Isotopic and Molecular Technologies, Physics Department, Cluj-Napoca; ^(e)National University of Science and Technology Politehnica, Bucharest; ^(f)West University in Timisoara, Timisoara; ^(g)Faculty of Physics, University of Bucharest, Bucharest; Romania.
- ^{29(a)}Faculty of Mathematics, Physics and Informatics, Comenius University, Bratislava; ^(b)Department of Subnuclear Physics, Institute of Experimental Physics of the Slovak Academy of Sciences, Kosice; Slovak Republic.
- ³⁰Physics Department, Brookhaven National Laboratory, Upton NY; United States of America.
- ³¹Universidad de Buenos Aires, Facultad de Ciencias Exactas y Naturales, Departamento de Física, y CONICET, Instituto de Física de Buenos Aires (IFIBA), Buenos Aires; Argentina.
- ³²California State University, CA; United States of America.
- ³³Cavendish Laboratory, University of Cambridge, Cambridge; United Kingdom.
- ^{34(a)}Department of Physics, University of Cape Town, Cape Town; ^(b)iThemba Labs, Western Cape; ^(c)Department of Mechanical Engineering Science, University of Johannesburg, Johannesburg; ^(d)National Institute of Physics, University of the Philippines Diliman (Philippines); ^(e)University of South Africa, Department of Physics, Pretoria; ^(f)University of Zululand, KwaDlangezwa; ^(g)School of Physics, University of the Witwatersrand, Johannesburg; South Africa.
- ³⁵Department of Physics, Carleton University, Ottawa ON; Canada.
- ^{36(a)}Faculté des Sciences Ain Chock, Université Hassan II de Casablanca; ^(b)Faculté des Sciences, Université Ibn-Tofail, Kénitra; ^(c)Faculté des Sciences Semailia, Université Cadi Ayyad, LPHEA-Marrakech; ^(d)LPMR, Faculté des Sciences, Université Mohamed Premier, Oujda; ^(e)Faculté des sciences, Université Mohammed V, Rabat; ^(f)Institute of Applied Physics, Mohammed VI Polytechnic University, Ben Guerir; Morocco.
- ³⁷CERN, Geneva; Switzerland.
- ³⁸Affiliated with an institute formerly covered by a cooperation agreement with CERN.
- ³⁹Affiliated with an institute covered by a cooperation agreement with CERN.
- ⁴⁰Affiliated with an international laboratory covered by a cooperation agreement with CERN.
- ⁴¹Enrico Fermi Institute, University of Chicago, Chicago IL; United States of America.
- ⁴²LPC, Université Clermont Auvergne, CNRS/IN2P3, Clermont-Ferrand; France.
- ⁴³Nevis Laboratory, Columbia University, Irvington NY; United States of America.
- ⁴⁴Niels Bohr Institute, University of Copenhagen, Copenhagen; Denmark.
- ^{45(a)}Dipartimento di Fisica, Università della Calabria, Rende; ^(b)INFN Gruppo Collegato di Cosenza, Laboratori Nazionali di Frascati; Italy.
- ⁴⁶Physics Department, Southern Methodist University, Dallas TX; United States of America.
- ⁴⁷National Centre for Scientific Research "Demokritos", Agia Paraskevi; Greece.
- ^{48(a)}Department of Physics, Stockholm University; ^(b)Oskar Klein Centre, Stockholm; Sweden.
- ⁴⁹Deutsches Elektronen-Synchrotron DESY, Hamburg and Zeuthen; Germany.

- ⁵⁰Fakultät Physik , Technische Universität Dortmund, Dortmund; Germany.
- ⁵¹Institut für Kern- und Teilchenphysik, Technische Universität Dresden, Dresden; Germany.
- ⁵²Department of Physics, Duke University, Durham NC; United States of America.
- ⁵³SUPA - School of Physics and Astronomy, University of Edinburgh, Edinburgh; United Kingdom.
- ⁵⁴INFN e Laboratori Nazionali di Frascati, Frascati; Italy.
- ⁵⁵Physikalisches Institut, Albert-Ludwigs-Universität Freiburg, Freiburg; Germany.
- ⁵⁶II. Physikalisches Institut, Georg-August-Universität Göttingen, Göttingen; Germany.
- ⁵⁷Département de Physique Nucléaire et Corpusculaire, Université de Genève, Genève; Switzerland.
- ⁵⁸(^a)Dipartimento di Fisica, Università di Genova, Genova;(^b) INFN Sezione di Genova; Italy.
- ⁵⁹II. Physikalisches Institut, Justus-Liebig-Universität Giessen, Giessen; Germany.
- ⁶⁰SUPA - School of Physics and Astronomy, University of Glasgow, Glasgow; United Kingdom.
- ⁶¹LPSC, Université Grenoble Alpes, CNRS/IN2P3, Grenoble INP, Grenoble; France.
- ⁶²Laboratory for Particle Physics and Cosmology, Harvard University, Cambridge MA; United States of America.
- ⁶³Department of Modern Physics and State Key Laboratory of Particle Detection and Electronics, University of Science and Technology of China, Hefei; China.
- ⁶⁴(^a) Kirchhoff-Institut für Physik, Ruprecht-Karls-Universität Heidelberg, Heidelberg;(^b) Physikalisches Institut, Ruprecht-Karls-Universität Heidelberg, Heidelberg; Germany.
- ⁶⁵(^a) Department of Physics, Chinese University of Hong Kong, Shatin, N.T., Hong Kong;(^b) Department of Physics, University of Hong Kong, Hong Kong;(^c) Department of Physics and Institute for Advanced Study, Hong Kong University of Science and Technology, Clear Water Bay, Kowloon, Hong Kong; China.
- ⁶⁶Department of Physics, National Tsing Hua University, Hsinchu; Taiwan.
- ⁶⁷IJCLab, Université Paris-Saclay, CNRS/IN2P3, 91405, Orsay; France.
- ⁶⁸Centro Nacional de Microelectrónica (IMB-CNM-CSIC), Barcelona; Spain.
- ⁶⁹Department of Physics, Indiana University, Bloomington IN; United States of America.
- ⁷⁰(^a) INFN Gruppo Collegato di Udine, Sezione di Trieste, Udine;(^b) ICTP, Trieste;(^c) Dipartimento Politecnico di Ingegneria e Architettura, Università di Udine, Udine; Italy.
- ⁷¹(^a) INFN Sezione di Lecce;(^b) Dipartimento di Matematica e Fisica, Università del Salento, Lecce; Italy.
- ⁷²(^a) INFN Sezione di Milano;(^b) Dipartimento di Fisica, Università di Milano, Milano; Italy.
- ⁷³(^a) INFN Sezione di Napoli;(^b) Dipartimento di Fisica, Università di Napoli, Napoli; Italy.
- ⁷⁴(^a) INFN Sezione di Pavia;(^b) Dipartimento di Fisica, Università di Pavia, Pavia; Italy.
- ⁷⁵(^a) INFN Sezione di Pisa;(^b) Dipartimento di Fisica E. Fermi, Università di Pisa, Pisa; Italy.
- ⁷⁶(^a) INFN Sezione di Roma;(^b) Dipartimento di Fisica, Sapienza Università di Roma, Roma; Italy.
- ⁷⁷(^a) INFN Sezione di Roma Tor Vergata;(^b) Dipartimento di Fisica, Università di Roma Tor Vergata, Roma; Italy.
- ⁷⁸(^a) INFN Sezione di Roma Tre;(^b) Dipartimento di Matematica e Fisica, Università Roma Tre, Roma; Italy.
- ⁷⁹(^a) INFN-TIFPA;(^b) Università degli Studi di Trento, Trento; Italy.
- ⁸⁰Universität Innsbruck, Department of Astro and Particle Physics, Innsbruck; Austria.
- ⁸¹University of Iowa, Iowa City IA; United States of America.
- ⁸²Department of Physics and Astronomy, Iowa State University, Ames IA; United States of America.
- ⁸³Istinye University, Sariyer, Istanbul; Türkiye.
- ⁸⁴(^a) Departamento de Engenharia Elétrica, Universidade Federal de Juiz de Fora (UFJF), Juiz de Fora;(^b) Universidade Federal do Rio De Janeiro COPPE/EE/IF, Rio de Janeiro;(^c) Instituto de Física, Universidade de São Paulo, São Paulo;(^d) Rio de Janeiro State University, Rio de Janeiro;(^e) Federal University of Bahia, Bahia; Brazil.
- ⁸⁵KEK, High Energy Accelerator Research Organization, Tsukuba; Japan.

- ⁸⁶Graduate School of Science, Kobe University, Kobe; Japan.
- ⁸⁷(^a) AGH University of Krakow, Faculty of Physics and Applied Computer Science, Krakow; (^b) Marian Smoluchowski Institute of Physics, Jagiellonian University, Krakow; Poland.
- ⁸⁸Institute of Nuclear Physics Polish Academy of Sciences, Krakow; Poland.
- ⁸⁹(^a) Khalifa University of Science and Technology, Abu Dhabi; (^b) University of Sharjah, Sharjah; United Arab Emirates.
- ⁹⁰Faculty of Science, Kyoto University, Kyoto; Japan.
- ⁹¹Research Center for Advanced Particle Physics and Department of Physics, Kyushu University, Fukuoka ; Japan.
- ⁹²L2IT, Université de Toulouse, CNRS/IN2P3, UPS, Toulouse; France.
- ⁹³Instituto de Física La Plata, Universidad Nacional de La Plata and CONICET, La Plata; Argentina.
- ⁹⁴Physics Department, Lancaster University, Lancaster; United Kingdom.
- ⁹⁵Oliver Lodge Laboratory, University of Liverpool, Liverpool; United Kingdom.
- ⁹⁶Department of Experimental Particle Physics, Jožef Stefan Institute and Department of Physics, University of Ljubljana, Ljubljana; Slovenia.
- ⁹⁷School of Physics and Astronomy, Queen Mary University of London, London; United Kingdom.
- ⁹⁸Department of Physics, Royal Holloway University of London, Egham; United Kingdom.
- ⁹⁹Department of Physics and Astronomy, University College London, London; United Kingdom.
- ¹⁰⁰Louisiana Tech University, Ruston LA; United States of America.
- ¹⁰¹Fysiska institutionen, Lunds universitet, Lund; Sweden.
- ¹⁰²Departamento de Física Teórica C-15 and CIAFF, Universidad Autónoma de Madrid, Madrid; Spain.
- ¹⁰³Institut für Physik, Universität Mainz, Mainz; Germany.
- ¹⁰⁴School of Physics and Astronomy, University of Manchester, Manchester; United Kingdom.
- ¹⁰⁵CPPM, Aix-Marseille Université, CNRS/IN2P3, Marseille; France.
- ¹⁰⁶Department of Physics, University of Massachusetts, Amherst MA; United States of America.
- ¹⁰⁷Department of Physics, McGill University, Montreal QC; Canada.
- ¹⁰⁸School of Physics, University of Melbourne, Victoria; Australia.
- ¹⁰⁹Department of Physics, University of Michigan, Ann Arbor MI; United States of America.
- ¹¹⁰Department of Physics and Astronomy, Michigan State University, East Lansing MI; United States of America.
- ¹¹¹Group of Particle Physics, University of Montreal, Montreal QC; Canada.
- ¹¹²Fakultät für Physik, Ludwig-Maximilians-Universität München, München; Germany.
- ¹¹³Max-Planck-Institut für Physik (Werner-Heisenberg-Institut), München; Germany.
- ¹¹⁴Graduate School of Science and Kobayashi-Maskawa Institute, Nagoya University, Nagoya; Japan.
- ¹¹⁵(^a) Department of Physics, Nanjing University, Nanjing; (^b) School of Science, Shenzhen Campus of Sun Yat-sen University; (^c) University of Chinese Academy of Science (UCAS), Beijing; China.
- ¹¹⁶Department of Physics and Astronomy, University of New Mexico, Albuquerque NM; United States of America.
- ¹¹⁷Institute for Mathematics, Astrophysics and Particle Physics, Radboud University/Nikhef, Nijmegen; Netherlands.
- ¹¹⁸Nikhef National Institute for Subatomic Physics and University of Amsterdam, Amsterdam; Netherlands.
- ¹¹⁹Department of Physics, Northern Illinois University, DeKalb IL; United States of America.
- ¹²⁰(^a) New York University Abu Dhabi, Abu Dhabi; (^b) United Arab Emirates University, Al Ain; United Arab Emirates.
- ¹²¹Department of Physics, New York University, New York NY; United States of America.
- ¹²²Ochanomizu University, Otsuka, Bunkyo-ku, Tokyo; Japan.

- ¹²³Ohio State University, Columbus OH; United States of America.
- ¹²⁴Homer L. Dodge Department of Physics and Astronomy, University of Oklahoma, Norman OK; United States of America.
- ¹²⁵Department of Physics, Oklahoma State University, Stillwater OK; United States of America.
- ¹²⁶Palacký University, Joint Laboratory of Optics, Olomouc; Czech Republic.
- ¹²⁷Institute for Fundamental Science, University of Oregon, Eugene, OR; United States of America.
- ¹²⁸Graduate School of Science, Osaka University, Osaka; Japan.
- ¹²⁹Department of Physics, University of Oslo, Oslo; Norway.
- ¹³⁰Department of Physics, Oxford University, Oxford; United Kingdom.
- ¹³¹LPNHE, Sorbonne Université, Université Paris Cité, CNRS/IN2P3, Paris; France.
- ¹³²Department of Physics, University of Pennsylvania, Philadelphia PA; United States of America.
- ¹³³Department of Physics and Astronomy, University of Pittsburgh, Pittsburgh PA; United States of America.
- ¹³⁴(^a) Laboratório de Instrumentação e Física Experimental de Partículas - LIP, Lisboa; (^b) Departamento de Física, Faculdade de Ciências, Universidade de Lisboa, Lisboa; (^c) Departamento de Física, Universidade de Coimbra, Coimbra; (^d) Centro de Física Nuclear da Universidade de Lisboa, Lisboa; (^e) Departamento de Física, Escola de Ciências, Universidade do Minho, Braga; (^f) Departamento de Física Teórica y del Cosmos, Universidad de Granada, Granada (Spain); (^g) Departamento de Física, Instituto Superior Técnico, Universidade de Lisboa, Lisboa; Portugal.
- ¹³⁵Institute of Physics of the Czech Academy of Sciences, Prague; Czech Republic.
- ¹³⁶Czech Technical University in Prague, Prague; Czech Republic.
- ¹³⁷Charles University, Faculty of Mathematics and Physics, Prague; Czech Republic.
- ¹³⁸Particle Physics Department, Rutherford Appleton Laboratory, Didcot; United Kingdom.
- ¹³⁹IRFU, CEA, Université Paris-Saclay, Gif-sur-Yvette; France.
- ¹⁴⁰Santa Cruz Institute for Particle Physics, University of California Santa Cruz, Santa Cruz CA; United States of America.
- ¹⁴¹(^a) Departamento de Física, Pontificia Universidad Católica de Chile, Santiago; (^b) Millennium Institute for Subatomic physics at high energy frontier (SAPHIR), Santiago; (^c) Instituto de Investigación Multidisciplinario en Ciencia y Tecnología, y Departamento de Física, Universidad de La Serena; (^d) Universidad Andres Bello, Department of Physics, Santiago; (^e) Instituto de Alta Investigación, Universidad de Tarapacá, Arica; (^f) Departamento de Física, Universidad Técnica Federico Santa María, Valparaíso; Chile.
- ¹⁴²Department of Physics, Institute of Science, Tokyo; Japan.
- ¹⁴³Department of Physics, University of Washington, Seattle WA; United States of America.
- ¹⁴⁴(^a) Institute of Frontier and Interdisciplinary Science and Key Laboratory of Particle Physics and Particle Irradiation (MOE), Shandong University, Qingdao; (^b) School of Physics, Zhengzhou University; China.
- ¹⁴⁵(^a) School of Physics and Astronomy, Shanghai Jiao Tong University, Key Laboratory for Particle Astrophysics and Cosmology (MOE), SKLPPC, Shanghai; (^b) Tsung-Dao Lee Institute, Shanghai; China.
- ¹⁴⁶Department of Physics and Astronomy, University of Sheffield, Sheffield; United Kingdom.
- ¹⁴⁷Department of Physics, Shinshu University, Nagano; Japan.
- ¹⁴⁸Department Physik, Universität Siegen, Siegen; Germany.
- ¹⁴⁹Department of Physics, Simon Fraser University, Burnaby BC; Canada.
- ¹⁵⁰SLAC National Accelerator Laboratory, Stanford CA; United States of America.
- ¹⁵¹Department of Physics, Royal Institute of Technology, Stockholm; Sweden.
- ¹⁵²Departments of Physics and Astronomy, Stony Brook University, Stony Brook NY; United States of America.
- ¹⁵³Department of Physics and Astronomy, University of Sussex, Brighton; United Kingdom.

- ¹⁵⁴School of Physics, University of Sydney, Sydney; Australia.
- ¹⁵⁵Institute of Physics, Academia Sinica, Taipei; Taiwan.
- ¹⁵⁶(^a) E. Andronikashvili Institute of Physics, Iv. Javakhishvili Tbilisi State University, Tbilisi; (^b) High Energy Physics Institute, Tbilisi State University, Tbilisi; (^c) University of Georgia, Tbilisi; Georgia.
- ¹⁵⁷Department of Physics, Technion, Israel Institute of Technology, Haifa; Israel.
- ¹⁵⁸Raymond and Beverly Sackler School of Physics and Astronomy, Tel Aviv University, Tel Aviv; Israel.
- ¹⁵⁹Department of Physics, Aristotle University of Thessaloniki, Thessaloniki; Greece.
- ¹⁶⁰International Center for Elementary Particle Physics and Department of Physics, University of Tokyo, Tokyo; Japan.
- ¹⁶¹Graduate School of Science and Technology, Tokyo Metropolitan University, Tokyo; Japan.
- ¹⁶²Department of Physics, University of Toronto, Toronto ON; Canada.
- ¹⁶³(^a) TRIUMF, Vancouver BC; (^b) Department of Physics and Astronomy, York University, Toronto ON; Canada.
- ¹⁶⁴Division of Physics and Tomonaga Center for the History of the Universe, Faculty of Pure and Applied Sciences, University of Tsukuba, Tsukuba; Japan.
- ¹⁶⁵Department of Physics and Astronomy, Tufts University, Medford MA; United States of America.
- ¹⁶⁶Department of Physics and Astronomy, University of California Irvine, Irvine CA; United States of America.
- ¹⁶⁷University of West Attica, Athens; Greece.
- ¹⁶⁸Department of Physics and Astronomy, University of Uppsala, Uppsala; Sweden.
- ¹⁶⁹Department of Physics, University of Illinois, Urbana IL; United States of America.
- ¹⁷⁰Instituto de Física Corpuscular (IFIC), Centro Mixto Universidad de Valencia - CSIC, Valencia; Spain.
- ¹⁷¹Department of Physics, University of British Columbia, Vancouver BC; Canada.
- ¹⁷²Department of Physics and Astronomy, University of Victoria, Victoria BC; Canada.
- ¹⁷³Fakultät für Physik und Astronomie, Julius-Maximilians-Universität Würzburg, Würzburg; Germany.
- ¹⁷⁴Department of Physics, University of Warwick, Coventry; United Kingdom.
- ¹⁷⁵Waseda University, Tokyo; Japan.
- ¹⁷⁶Department of Particle Physics and Astrophysics, Weizmann Institute of Science, Rehovot; Israel.
- ¹⁷⁷Department of Physics, University of Wisconsin, Madison WI; United States of America.
- ¹⁷⁸Fakultät für Mathematik und Naturwissenschaften, Fachgruppe Physik, Bergische Universität Wuppertal, Wuppertal; Germany.
- ¹⁷⁹Department of Physics, Yale University, New Haven CT; United States of America.
- ¹⁸⁰Yerevan Physics Institute, Yerevan; Armenia.
- ^a Also Affiliated with an institute covered by a cooperation agreement with CERN.
- ^b Also at An-Najah National University, Nablus; Palestine.
- ^c Also at Borough of Manhattan Community College, City University of New York, New York NY; United States of America.
- ^d Also at Center for High Energy Physics, Peking University; China.
- ^e Also at Center for Interdisciplinary Research and Innovation (CIRI-AUTH), Thessaloniki; Greece.
- ^f Also at CERN, Geneva; Switzerland.
- ^g Also at CMD-AC UNEC Research Center, Azerbaijan State University of Economics (UNEC); Azerbaijan.
- ^h Also at Département de Physique Nucléaire et Corpusculaire, Université de Genève, Genève; Switzerland.
- ⁱ Also at Departament de Física de la Universitat Autònoma de Barcelona, Barcelona; Spain.
- ^j Also at Department of Financial and Management Engineering, University of the Aegean, Chios; Greece.
- ^k Also at Department of Mathematical Sciences, University of South Africa, Johannesburg; South Africa.

- ^l Also at Department of Physics, Bolu Abant Izzet Baysal University, Bolu; Türkiye.
- ^m Also at Department of Physics, California State University, Sacramento; United States of America.
- ⁿ Also at Department of Physics, King's College London, London; United Kingdom.
- ^o Also at Department of Physics, Stanford University, Stanford CA; United States of America.
- ^p Also at Department of Physics, Stellenbosch University; South Africa.
- ^q Also at Department of Physics, University of Fribourg, Fribourg; Switzerland.
- ^r Also at Department of Physics, University of Thessaly; Greece.
- ^s Also at Department of Physics, Westmont College, Santa Barbara; United States of America.
- ^t Also at Faculty of Physics, Sofia University, 'St. Kliment Ohridski', Sofia; Bulgaria.
- ^u Also at Hellenic Open University, Patras; Greece.
- ^v Also at Henan University; China.
- ^w Also at Imam Mohammad Ibn Saud Islamic University; Saudi Arabia.
- ^x Also at Institutio Catalana de Recerca i Estudis Avancats, ICREA, Barcelona; Spain.
- ^y Also at Institut für Experimentalphysik, Universität Hamburg, Hamburg; Germany.
- ^z Also at Institute for Nuclear Research and Nuclear Energy (INRNE) of the Bulgarian Academy of Sciences, Sofia; Bulgaria.
- ^{aa} Also at Institute of Applied Physics, Mohammed VI Polytechnic University, Ben Guerir; Morocco.
- ^{ab} Also at Institute of Particle Physics (IPP); Canada.
- ^{ac} Also at Institute of Physics and Technology, Mongolian Academy of Sciences, Ulaanbaatar; Mongolia.
- ^{ad} Also at Institute of Physics, Azerbaijan Academy of Sciences, Baku; Azerbaijan.
- ^{ae} Also at National Institute of Physics, University of the Philippines Diliman (Philippines); Philippines.
- ^{af} Also at Technical University of Munich, Munich; Germany.
- ^{ag} Also at The Collaborative Innovation Center of Quantum Matter (CICQM), Beijing; China.
- ^{ah} Also at TRIUMF, Vancouver BC; Canada.
- ^{ai} Also at Università di Napoli Parthenope, Napoli; Italy.
- ^{aj} Also at University of Colorado Boulder, Department of Physics, Colorado; United States of America.
- ^{ak} Also at University of the Western Cape; South Africa.
- ^{al} Also at Washington College, Chestertown, MD; United States of America.
- ^{am} Also at Yeditepe University, Physics Department, Istanbul; Türkiye.
- * Deceased